QATAR UNIVERSITY

COLLEGE OF ENGINEERING

# FRAMEWORK FOR CONTENT DISTRIBUTION OVER WIRELESS LANS

BY

MUHAMMAD ASIF KHAN

A Dissertation Submitted to

the College of Engineering

in Partial Fulfillment of the Requirements for the Degree of

Doctorate of Philosophy in Electrical Engineering

January 2020

## COMMITTEE PAGE

The members of the Committee approve the Dissertation of Muhammad Asif Khan defended on [Defense Date].

Ridha Hamila
Thesis/Dissertation Supervisor

[Name]
Committee Member

[Name]
Committee Member

[Name]
Committee Member

[Add Member]

Approved:

Abdel Magid Hamouda , Dean, College of Engineering

# ABSTRACT

KHAN, MUHAMMAD ASIF., Doctorate : January : 2020,

Doctorate of Philosophy in Electrical Engineering

Title: Framework for Content Distribution over Wireless LANs

Supervisors of Dissertation: Ridha, Hamila.

Wireless LAN (also called as Wi-Fi) is dominantly considered as the most pervasive technology for Intent access. Due to the low-cost of chipsets and support for high data rates, Wi-Fi has become a universal solution for ever-increasing application space which includes, video streaming, content delivery, emergency communication, vehicular communication and Internet-of-Things (IoT).

Wireless LAN technology is defined by the IEEE 802.11 standard. The 802.11 standard has been amended several times over the last two decades, to incorporate the requirement of future applications. The 802.11 based Wi-Fi networks are infrastructure networks in which devices communicate through an access point. However, in 2010, Wi-Fi Alliance has released a specification to standardize direct communication in Wi-Fi networks. The technology is called Wi-Fi Direct. Wi-Fi Direct after 9 years of its release is still used for very basic services (connectivity, file transfer etc.), despite the potential to support a wide range of applications. The reason behind the limited inception of Wi-Fi Direct is some inherent shortcomings that limit its performance in dense networks. These include the issues related to topology design, such as non-optimal group formation, Group Owner selection problem, clustering in dense networks and coping with device mobility in dynamic networks.

Furthermore, Wi-Fi networks also face challenges to meet the growing number of Wi-Fi users. The next generation of Wi-Fi networks is characterized as ultra-dense networks where the topology changes frequently which directly affects the network performance. The dynamic nature of such networks challenges the operators to design and make optimum planifications.

In this dissertation, we propose solutions to the aforementioned problems. We contributed to the existing Wi-Fi Direct technology by enhancing the group formation process. The proposed group formation scheme is backwards-compatible and incorporates role selection based on the device's capabilities to improve network performance. Optimum clustering scheme using mixed integer programming is proposed to design efficient topologies in fixed dense networks, which improves network throughput and reduces packet loss ratio.  A novel architecture using Unmanned Aeriel Vehicles (UAVs) in Wi-Fi Direct networks is proposed for dynamic networks. In ultra-dense, highly dynamic topologies, we propose cognitive networks using machine-learning algorithms to predict the network changes ahead of time and self-configuring the network.

# DEDICATION

*To my family who supported me throughout the duration of my studies.*

ACKNOWLEDGEMENTS

First and foremost, I wish to thank my advisor, Prof. Ridha Hamila, one of the most prominent faculty members in the Electrical Engineering department. He has been supportive since the days I began working on the research proposal; I remember he always expressed his confidence in me. His words of confidence always motivated me to do my work in the best way. Ever since Prof. Ridha has supported me academically and emotionally through the rough road to finish this dissertation. He helped me to refine the research objectives and guided me over almost 5 years to achieve my aims. During the most difficult times when writing this dissertation, he gave me the moral support and the freedom I needed to move on.

My thesis committee guided me through all these years. Thank you to all those prestigious professors, for their support in my research.

Completing this work would have been all the more difficult without the academic support from people who taught me immensely at QU, especially Prof. Serkan Kiranyaz, and Dr Tamer Khattab.

I owe a deep sense of gratitude to Dr Fethi Filali and Dr Wael Cherif for their kind support and providing me with the opportunity to work at Qatar Mobility Innovation Center (QMIC) and co-authored several research papers. I thank my university colleagues, Khaliqur Rahman, Shoaib Allam Mallick and Lutfi Samara for their support in various PhD courses.

Lastly, thank goes to my family, the most basic source where my life energy resides: I have an amazing family, unique in many ways, and the stereotype of a perfect family in many others. Their support has been unconditional all these years; they have given

up many things for me to complete my studies; they have cherished with me every great moment and supported me whenever I needed it.

TABLE OF CONTENTS

# LIST OF TABLES

LIST OF FIGURES

ABBREVIATIONS

| | |
|---|---|
| ANN | Artificial Neural Network |
| AOA | Angle of Arrival |
| AOD | Average Outage Duration |
| ATG | Air To Ground |
| AP | Access Point |
| BGO | Backup Group Owner |
| BSS | Basic Service Set |
| CN | Cognitive Networks |
| CSI | Channel State Information |
| CSMA | Carrier Sense Multiple Access |
| CTWindow | Client Traffic Window |
| CTS | Clear To Send |
| D2D | Device to Device |
| DHCP | Dynamic Host Configuration Protocol |
| DIFS | Distributed Inter Frame Space |
| DMS | Directed Multicast Group |
| DT | Decision Tree |
| ELBP | Enhanced Leader Based Protocol |
| EM | Expectation Maximization |
| DTN | Delay Tolerant Networks |

| | |
|---|---|
| ESS | Extended Service Set |
| GAS | Generic Advertisement Service |
| GCR | Groupcast with Retries |
| GO | Group Owner |
| GMM | Gaussian Mixture Model |
| HMM | Hidden Markov Model |
| i.i.d | Independently and Identically Distributed |
| IAT | Inter Arrival Time |
| ICA | Independent Component Analysis |
| IE | Information Element |
| IEEE | Institute of Electrical and Electronic Engineers |
| IoT | Internet of Things |
| ITU | International Telecommunication Union |
| KNN | K Nearest Neighbors |
| LBP | Leader Based Protocol |
| LLF | Least Loaded First |
| LOS | Line of Sight |
| LR | Long Range |
| MAC | Medium Access Control |
| MCS | Modulation Coding Index |
| MIFS | Multicast Inter Frame Space |
| MILP | Mixed Integer Linear Program |

| | |
|---|---|
| MIMO | Multi Input Multi Output |
| MINLP | Mixed Integer Non-Linear Program |
| MIP | Mixed Integer Program |
| ML | Machine Learning |
| MLP | Multi-Layer Perceptron |
| MRG | More Reliable Groupcast |
| MUDIV | Multi-User Diversity |
| NS-3 | Network Simulator - 3 |
| NoA | Notice of Absence |
| OppOS | Opportunistic Power Save |
| PAR | Packet Arrival Rate |
| PCA | Principle Component Analysis |
| PLR | Packet Loss Ratio |
| PREQ | Probe Request |
| PRES | Probe Response |
| P2P | Peer to Peer |
| QoS | Quality of Service |
| QoE | Quality of Experience |
| RBF | Radial Basis Function |
| RF | Random Forest |
| RSSI | Received Signal Strength Indicator |
| RTS | Request to Send |

| | |
|---|---|
| SDN | Software-Defined Networks |
| SIFS | Short Inter Frame Space |
| SNR | Signal to Noise Ratio |
| SON | Self-Organizing Networks |
| SR | Short Range |
| SSF | Strongest Signal First |
| STA | Station |
| SVM | Support Vector Machine |
| SVR | Support Vector Regressor |
| UAV | Unmanned Aerial Vehicle |
| VoIP | Voice over IP |
| WEP | Wireless Encryption Protocol |
| WLAN | Wireless Local Area Network |
| WPA | Wireless Protected Access |
| WPS | Wireless Protected Setup |

# CHAPTER 1 : INTRODUCTION

Wireless Local Area Networks (WLANs) also known as Wi-Fi (Wireless Fidelity) has become a choice of communication in homes, offices and public areas due to the cost-effective deployment of Wi-Fi networks, its large-scale implementation and availability of Wi-Fi devices e.g. smartphones, consumer electronics and industrial sensors.

Today almost all digital devices such as laptops, smartphones, personal digital assistants (PDAs), notebook and tablets come with pre-installed Wi-Fi chips. Due to its growing inception in the market, new attractive applications have found Wi-Fi as a potential candidate technology. Hence, Wi-Fi is being used in modern Internet-of-Things (IoT) networks, transportation and medical applications.

## 1.1 Motivation and Background

Wi-Fi has experienced enormous growth in the last two decades. The first standard of Wireless LANs, the IEEE 802.11 [1] was released in 1997 which defines the Physical (PHY) and Medium Access Control (MAC) layers and supported low data rates of up to 2 Mbps. The standard was proceeded by subsequent amendments [2-10] for enhanced supports. These legacy WLAN standards [2, 3, 11] were designed to support best-effort services which were common in that era.

However, there has been an increasing trend in multimedia-based applications causing a dramatic increase in video traffic. According to Cisco VNI (Visual Networking Index) released in February 2019 [12], video traffic will be 79% of total mobile data traffic by 2022, whereas an average smartphone will generate 11GB of mobile data per month with more than 60% of traffic via Wi-Fi networks. There are also staggering predictions about the number of Wi-Fi-enabled mobile devices. It is predicted that mobile data traffic will be growing much faster than traffic over the fixed networks, due to the wide availability of smartphones and ubiquitous wireless networks e.g. 4G or Wi-Fi. The VNI report forecasts 5.7 billion mobile users and 12.3 billion mobile-connected devices by 2022.

The rapid increase in multimedia-based services and applications over wireless devices have brought new challenges to existing wireless networks. These applications require special treatment from the wireless networks in terms of bandwidth and Quality of Service (QoS). In addition to QoS requirements by such applications, there is a new paradigm shift in terms of Wi-Fi usage. Wi-Fi, beyond the traditional home and office networking solution, is now used as a common method of Internet access and content distribution in large geographical areas such as sports stadiums, convention centres, airports, metros, and shopping malls.

Wi-Fi is also enjoying direct connectivity solutions using Wi-Fi Direct [13] for simple applications such as content sharing, however, the direct communication between devices encounters several challenges. Wi-Fi Direct at this stage supports only small networks and simple data sharing applications.

## 1.2 Research Problem

The deployment of dense networks, the growing use of multimedia contents and direct communication between devices, are the new paradigms where existing WLAN standards face severe challenges.

In dense networks, the access point (AP) has insufficient capacity to serve a large number of devices. As wireless is a shared medium, hence the performance degrades with the increasing number of devices. To reduce the congestions on APs, device-to-device (D2D) networking is introduced using Wi-Fi Direct technology. However, the Wi-Fi Direct technology has several shortcomings in terms of scalability and connection establishment delay. The specification of Wi-Fi Direct [13] defines the mechanism of how to form network clusters but leaves the selection of the cluster head ("Group Owner" in Wi-Fi Direct terminology) unaddressed. The cluster head selection is of crucial importance for performance and lifetime of the network. Moreover, the cluster formation ("group formation" in Wi-Fi Direct terminology) mechanism is also very limited and does not support scalability to be deployed in large D2D networks.

In dense WLAN networks, the coverage regions of APs overlap, which causes unnecessarily frequent inter-BSS handovers. These undesired handovers cause connection disruptions which limit the overall performance of the network and affect the quality of service. Secondly, the association of users in overlapping BSS is also a challenge to balance the load on the access points for optimal performance.

### 1.3 Research Objectives

This dissertation aims to investigate the most recent developments in WLAN. The study systematically reviews the legacy and recent standards for WLAN networks, the limitations of these standards in future networks and the state-of-the-art solutions to these problems. The goal of this research project is to design a framework, which addresses the aforementioned issues. The framework covers the physical and link layers of the OSI reference model in addition to novel schemes using cross-layer design.

The following research objectives have been defined for this work.

a) Designing dense Wi-Fi networks using device-to-device (D2D) communication techniques such as Wi-Fi Direct.
b) Choosing efficient relaying schemes to realize multi-hop networks.
c) Proposing optimal clustering schemes in ultra-dense scenarios using Wi-Fi Direct for cluster formation and re-formation.
d) Proposing novel architecture to cope with user mobility in highly dynamic and dense networks. This includes the use of UAVs.
e) Designing self-organizing cognitive networks using machine learning techniques.

## 1.4 Main Contributions

There are several important areas where this research makes an original contribution. The study offers some important insights into the existing WLAN standards (medium access techniques, traffic prioritization), cooperative communication and D2D networking protocols for reliable and efficient multicasting. The issues related to the standard Wi-Fi Direct technology has been addressed. A comprehensive study has been presented to explain these issues and their impact on network performance. These include missing criteria for the selection of Group Owner (GO), the lack of scalability due to inefficient group formation mechanism and group reformation mechanism.

This research has the following specific contribution to the body of knowledge:

- A GO selection scheme has been proposed to select the best GO among a set of devices based on the device's capabilities such as RSS, battery life and the number of neighbours.
- An enhanced group formation scheme is proposed to reduce the group formation delay. The enhanced group formation scheme also incorporates the possibility to select a backup GO for group reformation.
- Group Owner selection and clustering of dense Wi-Fi Direct networks using Mixed Integer Programming (MIP) are proposed termed as "optimal group formation". The optimal group formation also supports multiple groups' formation using multiple GOs and devices' allocation to the selected GOs. The optimal scheme is also used to enhance multicast traffic.
- A novel scheme is proposed to use Unmanned Aerial Vehicles (UAVs) for highly dynamic networks to cope with devices' mobility including both GO and clients' mobility.
- Cognitive network architecture is proposed to solve the handover prediction and access point (AP) selection problem in dense networks involving overlapping BSSs (OBSS). The proposed cognitive network architecture is based on machine learning algorithms to implement complex prediction functions in ultra-dense, highly dynamic systems.
- The aforementioned contributions are validated using realistic simulation approaches and results are validated by comparing with other state-of-the-art schemes.

## 1.5 Thesis Organization

The dissertation has been organized into the following chapters:

CHAPTER 1 gives a brief overview of the dissertation. The chapter begins with the motivation and contextual background, formulates the problems, outlines the research objectives and presents the contribution of this dissertation.

CHAPTER 2 presents a historical overview of WLAN technology and outlines the characteristics of next-generation WLAN (NG-WLAN) networks. It also covers, in details, the device-to-device (D2D) paradigm in WLAN networks.

CHAPTER 3 covers the major portion of this dissertation. It includes three important contributions mainly related to Wi-Fi Direct: the group owner election, enhanced group formation and optimal clustering scheme in ultra-dense networks.

CHAPTER 4 presents a novel UAV-aided network architecture i.e. to deploy UAVs (Unmanned Aerial Vehicles) in highly dynamic dense Wi-Fi networks for efficient network topologies.

CHAPTER 5 outlines the state-of-the-art in machine learning (ML) applied to Wi-Fi networks. It explains how ML techniques can be used to efficiently solve two challenging problems that cannot be efficiently solved using traditional analytical approaches.

CHAPTER 6 draws conclusions, provides a brief summary and critique of the findings. It also discusses the implication of the findings to future research works in this area.

# CHAPTER 2 : LITERATURE REVIEW

Wireless Local Area Networks (WLANs) which are more commonly known as Wi-Fi (Wireless Fidelity) networks are based on IEEE 802.11 family of standards. Since the first draft of the 802.11 standard [1] released in 1997, there has been a huge development to support new applications and services. Besides a series of enhancements in 802.11 standard introduced by IEEE for infrastructure networks, Wi-Fi Alliance has developed an infrastructure-less device-to-device (D2D) architecture for direct communication in Wi-Fi networks.

This chapter covers the following topics:

- Wireless LANs and the IEEE 802.11 standards
- Cooperative Relaying schemes for D2D communication
- Wi-Fi Direct specification for D2D networking
- UAV-Aided communication in Wi-Fi networks
- Self-Organizing Networks (SON) using Machine Learning techniques
- Multicasting in Wi-Fi

## 2.1 Network Architecture

*Figure 2.1* illustrates the network architecture of Wireless LANs. The basic entity of a Wi-Fi network is called "Basic Service Set" (BSS). A BSS consists of an Access Point (AP) and one or more Wi-Fi-enabled devices called stations (STAs). Two or more BSS's connect to a wired network to form an Extended Service Set (ESS).

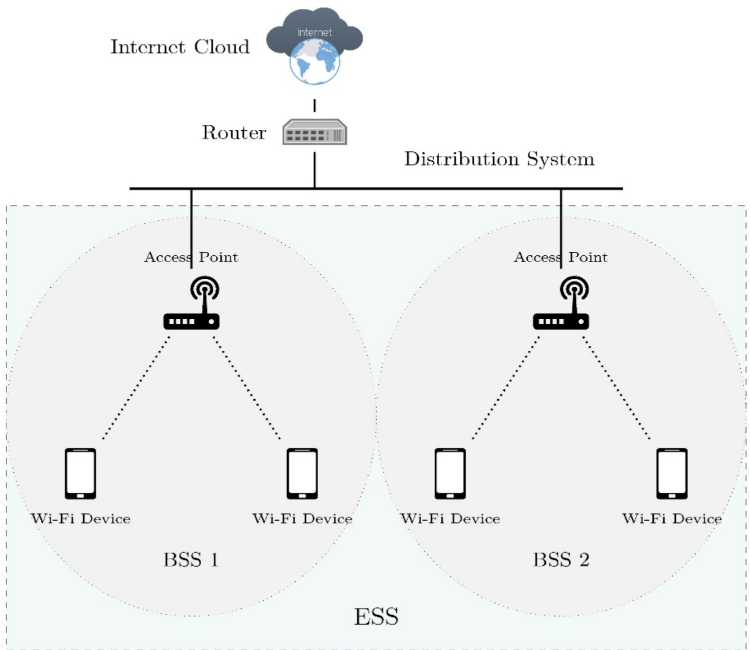


*Figure 2.1* WLAN architecture.

## 2.2 The IEEE 802.11 Standards

The 802.11 standard has been evolved through a series of developments and improvements. The first release of IEEE 802.11 [1] that defines the PHY and MAC layers supports very low data rates of up to 2 Mbps. The legacy WLAN standard does not efficiently support multimedia transmission, because of several reasons: (i) the transmission rates impose bottleneck on the maximum achievable rate regardless of the efficiency of MAC layer protocol, (ii) support for only best-effort services (traffic prioritization is not supported) and (iii) inefficient and unreliable multicast transmissions. These issues were addressed by the subsequent amendments to the 802.11 standard, which mainly focused on the PHY layer. The IEEE 802.11b [3] increased the supported data rates to 11 Mbps. The data rates were further increased to 54 Mbps in 802.11a [2] and 802.11g [3] and finally to 250 Mbps in 802.11n standard.

The legacy WLAN standards IEEE 802.11 use Distributed Coordination Function (DCF) for medium access. DCF was designed for best-effort services and lack support for QoS required by video and voice traffic. Later in 2005, IEEE approved IEEE 802.11e [4] standard that introduced a new channel access technique called Enhanced Distributed Channel Access (EDCA). EDCA divides incoming traffic streams of different priorities into four access categories (AC) with different contention windows assigned at MAC layer. The four access categories are AC_VO, AC_VI, AC_BE and AC_BK representing AC for voice, video, best effort and background traffic respectively. EDCA provides the delay-sensitive voice and video traffic more frequent access to the shared wireless medium to satisfy their performance needs. The traffic classification scheme using EDCA is presented in *Figure 2.2*.

The assignment of different priorities in EDCA is implemented using different contention window size. The contention parameters can be tuned to optimal values for improved performance [14].

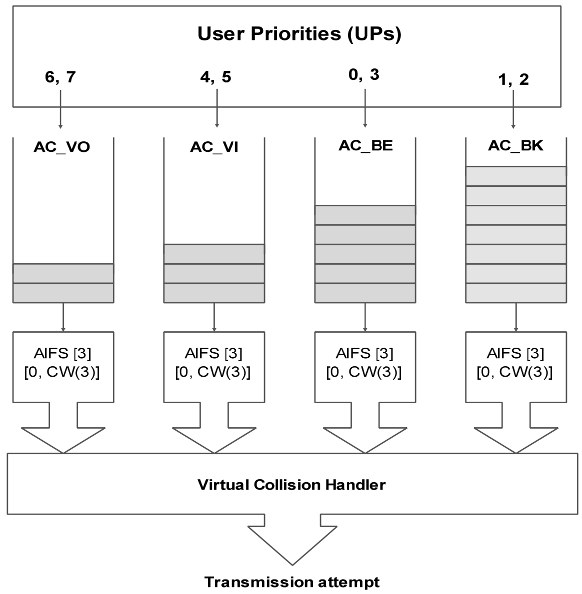


*Figure 2.2* EDCA channel access scheme.

To support higher data rates required by high throughput multimedia applications the IEEE 802.11n [6] standard was proposed. The 802.11n increased data rates tremendously up to 600 Mbps using Multiple Input, Multiple Output (MIMO) technology. The 802.11n also introduced some enhancements at the MAC layer e.g. Aggregate MAC Service Data Units (A-MSDU), MAC Protocol Data Units (MPDU) and Block Acknowledgement (BA). The 802.11n extensively increased data rates, however; the standard has some limitations inherited from its predecessor standards.

The legacy and 802.11n standard support only one-to-one communication in Infrastructure mode at both uplink and downlink. To overcome this limitation, IEEE 802.11ac [9] was developed to allow Access Point (AP) to send multiple independent (eight) streams to multiple devices at the downlink simultaneously using Multi-User MIMO.

In order to allow efficient and robust transmission of multicast flows in Wireless LAN, the IEEE 802.11aa standard [8] is proposed. The 802.11aa standard defines new mechanisms to support robust audio and video transmission: (i) Stream Classification Service (SCS), which provide intra-flow prioritization for graceful degradation of video quality (ii) interworking with IEEE 802.1AVB [15] for end-to-end reservation, (iii) Overlapping Basic Service (OBSS) management for coordination between AP's and (iv) Group Addressed Transmission Service (GATS) for efficient multicasting. The intra-AC stream classification service of 802.11aa standard is illustrated in Figure 2.

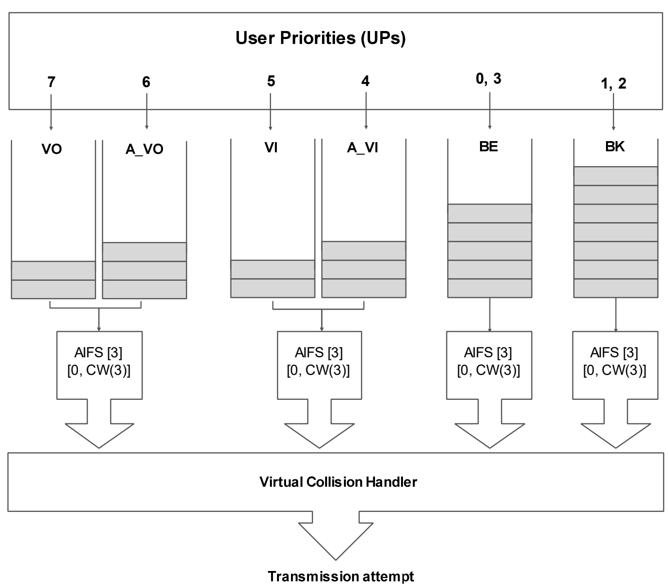


*Figure 2.3* Intra-AC streams classification in IEEE 802.11aa.

The 802.11aa standard defines different mechanisms for link-layer multicast transmission; however, it does not provide any guidelines on which of these mechanisms shall be used in a given scenario. Table 2.1 summarizes a historical overview of developments and improvements in the 802.11 standard.

Table 2.1 *Summary of IEEE WLAN standards.*

| **IEEE Standard** | **Year** | **Purpose** |
|---|---|---|
| 802.11 [1] | 1997 | The first standard that specifies the PHY and MAC layers of the Wireless LAN technology, FHSS and DSSS |
| 802.11a [2] | 1999 | 54Mbps, 5GHz band, OFDM |
| 802.11b [16] | 1999 | 11Mbps, 2.4GHz, DSSS only. |
| 802.11g [3] | 2003 | 54Mbps, 2.4GHz standard. For transmission over short distances |
| 802.11e [4] | 2005 | Quality of Service support for WLANs. |
| 802.11-2007 [5] | 2007 | Include amendments a, b, g, e |
| 802.11n [6] | 2009 | High throughput improvement using MIMO, 250Mbps |
| 802.11aa [8] | 2012 | QoS enhancement |
| 802.11-2012 [7] | 2012 | Include amendments n, aa and others |
| 802.11-ac [9] | 2012 | Very high throughput, MU-MIMO, wider channels, 5GHz, 433Mbps |
| 802.11-2016 [10] | 2016 | Revision of IEEE 802.11-2012 |
| 802.11ax [17] | 2017 | High Efficiency WLANs |

## 2.3 Cooperative Relaying

Cooperative relaying is used to increase reliability; data rates and coverage range by allowing nodes to receive or recover data from surrounding nodes. Cooperation among nodes improves the overall system capacity to meet the Quality of Service (QoS) requirements of the given application or service.

Cooperative relaying can provide several advantages in communication networks:

- Re-transmission of lost packets
- Increased throughput
- Increased coverage augmentation
- Cooperative multicasting

When the feedback channel from the source to the destination is not implemented or suffered from significant fading, the source may send the data packets through a relay node. In the case of Wireless LAN, the channel between the AP and the relay node is shared between the AP and relay nodes and hence the time slots are divided between the AP and relay. In [18, 19], the optimal time allocation between the source and relays is proposed.

When multicasting is used, the multicast group members can be elected as a relay, such as illustrated in *Figure 2.4*. However, such implementations require several considerations. If the nodes with the best links to the source are selected as relays, this will result in higher data rates on source-relay channels. Whereas, if the relay-destinations channels are more faded causing lower rates selection on relay-destination channels. Such a situation will result in bottlenecks at relay nodes. Moreover, authors in [20] stated that QoS can be improved by allowing end nodes to receive data from both relay and source thus exploiting diversity.

Relay selection can be implemented in several ways. In [21], the relay is selected by the nodes by monitoring "Service Request Message (SRM)" packets sent by the relay to AP. The relay is selected based on the highest transmission rates. However, the performance of relay in this scheme can be degraded when the source to relay channel is faded such that it can no longer support high data rates.

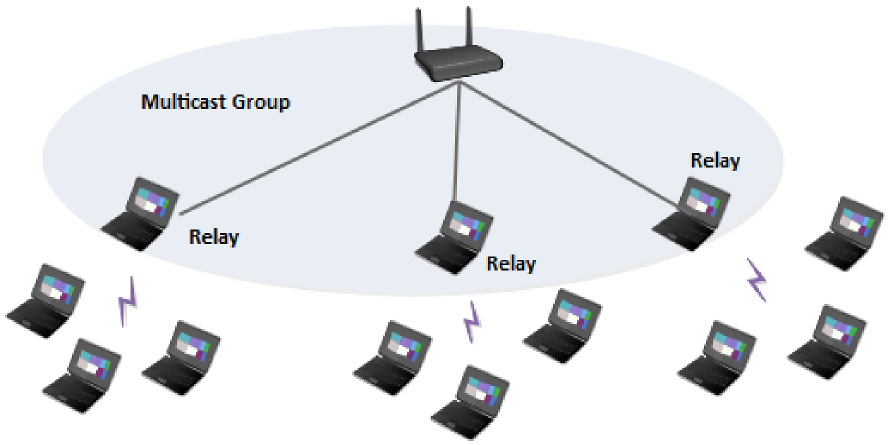


*Figure 2.4* Multicasting with cooperative relaying.

Another problem of using the relay nodes in Wireless LANs is the limit on the number of relays in the same wireless range due to limited wireless channels, the so-called social channels. If the relay uses the same channel as the AP, the channel is shared between the AP and relay on a time basis, which can limit the overall system performance. It is proposed in [21] to assign different channels to each relay in the same interference range. In [22], the authors proposed to assign different sub-carriers to relays in the same interference range to transmit data at the same time. If relay uses Omni-directional radios, then selecting spatially separated relays can be useful to minimize the number of relays [23].

The number of relays required decreases if the transmit power of relays increases [24]. The authors in [24] also showed that decreasing the number of relays resulted in improved video quality because of increased bit rate.

Authors in [25-27] extended the cooperation among nodes such that instead of using selected relays, all nodes receiving data can forward the received data if the nodes experience SNR higher than a specified threshold value. Similarly, each node receives multiple copies of the same data packet. This is analogous to Multiple Input – Multiple Output (MIMO) diversity system. In [28], authors used Maximum Ratio Combining (MRC) at the relay node to combine signal received from the source and another relay, amplify and transmit to the receiver. The receiver then combines the signal from two different relays using the MRC scheme.

The increase in the emergence of multi-home devices that are connected to long-range networks such as 3G/4G and short-range networks such as WLAN, several solutions are proposed. In [29], authors studied the performance of a dual-hop network with fixed gain relay over Nakagami-m fading channel. The authors also consider the mobility of the relay and destination nodes, while the source is considered as a fixed node. The performance was measured using outage probability and bit error rate.

In [30], the authors presented the closed-form expressions for Average Outage Duration (AOD) of multi-hop regenerative systems. Average Outage Duration (AOD) is defined as the time in seconds on average that any of the relays in the multi-hop system remains in outage i.e. the received SNR drops below a pre-defined threshold. The model can be applied to any fading channel including Rayleigh, Rician and Nakagami. The results show that the relayed path has a smaller AOD than the direct path. Moreover, the performance can be further improved if the number of relays increases at a fixed distance. For high values of transmit power, the number of hops becomes less relevant. It is worth noting that such an evaluation of the outage duration should be carefully treated. The increasing number of relay nodes will introduce transmission delay due to regeneration of the transmitted symbols at each relay node [31]. Furthermore, AF relaying can outperform the DF protocol if the relay is close to the destination.

In [32], authors presented the concept of multi-user diversity (MUDiv) and an estimation of the amount of feedback required to share feedback information (Channel States Information - CSI) among users with the solution to reduce feedback. The model used the assumption of i.i.d. Rayleigh fading channels. The authors also proposed a threshold optimizing scheme to attain a certain level of the outage.

In [33], the authors investigated the optimal allocation of power over relay paths for a given power budget assuming Rayleigh fading channels. The authors provided closed-form expressions for outage probability and optimal power allocations to source and relay nodes. The authors also evaluated the relay path using the proposed power allocation and concluded that the AF relaying system can outperform the DF relaying without power optimization. In [34], the authors approximated the ergodic capacity of MIMO Rayleigh fading channels in low SNR regimes. Closed-form expressions for the ergodic capacity assuming full CSI at both transmitter and receiver are derived. The authors also proposed opportunistic transmission in the low SNR region, called ON-OFF Transmission. Further studies of the performance of such relaying networks can be found in [35-40].

### 2.4 D2D Networking using Wi-Fi Direct

In the current deployment of Wi-Fi infrastructure mode, devices connect to a common Access Point (AP) to connect to other Wi-Fi devices.

Wi-Fi Alliance [1] introduced in 2010 the Wi-Fi Direct technology to enable Wi-Fi devices to directly connect to each other without connecting to an AP. Wi-Fi Direct, initially called Wi-Fi Peer-to-Peer (Wi-Fi P2P), is built upon the IEEE 802.11 *Infrastructure* mode and offers a direct, secure and rapid device-to-device communication. The recent Wi-Fi P2P Technical Specification was released in 2016 (version 1.7).

Direct communication between devices i.e. D2D communication can bring several potential benefits. Direct communication between nodes will suffer from reduced delay as compared to relayed path through AP. This also leaves more space for other devices to transmit thus reducing queuing and contention delay for other devices in the network. The Wi-Fi Direct is becoming an interesting and suitable candidate for communication in several application domains including content distribution, resource sharing, emergency communication, alert dissemination, online gaming, proximity-based advertising and social networking. Wi-Fi Direct enables Wi-Fi devices such as smartphones, laptops, smart TVs, printers, cameras and other appliances to inter-connect quickly and conveniently without incorporating an Access Point (AP). Wi-Fi Direct is built on the infrastructure mode of WLAN. Wi-Fi Direct connections are secured with Wireless Protected Access - 2 (WPA2) [41]. Wi-Fi Direct supports the same high data rates as in Wi-Fi (up to 250 Mbps). The range of Wi-Fi Direct connection is 200 meters (this is theoretical range and practical range might be nominal of this). The specifications also require 1:1 connection mandatory

[1] http://www.wi-fi.org/

for Wi-Fi Direct certified devices, whereas keeping 1:N connection optional feature. In the subsequent sections, we provide a detailed overview of Wi-Fi Direct features.

The functional entity of Wi-Fi Direct architecture is called a "P2P Group" that is functionally equivalent to a Basic Service Set (BSS) in *Legacy* Wi-Fi network. A P2P Group consists of a P2P Group Owner (P2P GO) and zero or more P2P Clients. The P2P GO (sometimes referred to as "GO") is also called a *Soft-AP*. AP functions are implemented within Wi-Fi P2P devices. A P2P device can dynamically take the role of an AP or client. The roles of P2P Devices (i.e. P2P GO and P2P Client) are usually negotiated before creating a P2P Group and remain fixed while the P2P Group is active. *Figure 2.5* illustrates the different roles of P2P Devices.

Device Discovery is a mandatory feature to be supported by all P2P Devices. Prior to forming a P2P Group, a P2P Device runs the Device Discovery procedure to detect the presence of other P2P Devices in its wireless range. The procedure consists of two distinct phases: *Scan* and *Find*. In the *Scan* phase, the P2P Device performs traditional Wi-Fi scan (passive scan) through all supported channels in order to collect information about the surrounding devices, P2P Groups and legacy Wi-Fi networks.

Once the *Scan* phase is completed, the device enters into the *Find* phase. In the *Find* phase, the P2P Device alternates between two states: *Search* and *Listen*. In the *Search* state, the P2P Device sends one or more *Probe Request (PREQ)* frames on the social channel namely channels 1, 6 and 11 in the 2.4 GHz band.

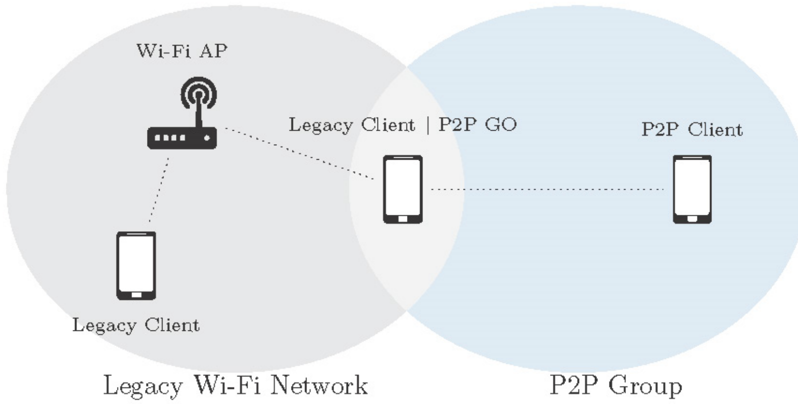


*Figure 2.5* Wi-Fi direct architecture.

In the *Listen* state, the P2P Device dwells on one of the social channels (1, 6 and 11) called the *Listen* channel and waits for *Probe Request (PREQ)* frames from other P2P Devices. Thus, the success of the *Find* phase is that when two devices come to a common channel to communicate. It is noticeable that the P2P Device Discovery process can induce some delay to let a P2P Device discovers all P2P Devices in its vicinity. This delay, termed as "Device Discovery delay", can be relatively high if several P2P Devices are simultaneously performing Device Discovery in the same wireless range. *Figure 2.6* illustrates the P2P Device Discovery procedure in Wi-Fi Direct.

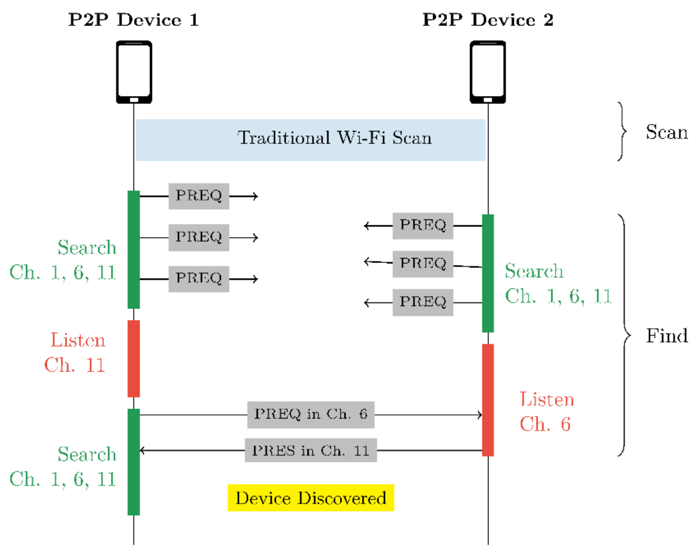


*Figure 2.6* Device discovery procedure in Wi-Fi direct.

Service Discovery is an optional procedure in Wi-Fi Direct. The procedure starts after the Device Discovery and prior to the Group Formation procedure. It allows a P2P Device to connect to other P2P Devices only if the latter offers the intended service. Using the Service Discovery procedure, a P2P Device advertises available services using link-layer Generic Advertisement Service (GAS) protocol. Wi-Fi Alliance has defined a set of standardized services supported by Wi-Fi Direct such as *Play*, *Send* and *Print*.

Following a successful Device Discovery (mandatory procedure) and Service Discovery (optional procedure), P2P Devices can establish the P2P Group. During the Group Formation, the device that will act as GO is determined. As described in Fig. 3, three types of P2P Group Formation schemes are possible in Wi-Fi Direct: (1) Standard Group Formation (2) Autonomous Group Formation and (3) Persistent Group Formation.

In *Standard* Group Formation, presented in Fig. 3(a) two P2P Devices negotiate the role of the P2P GO. The GO Negotiation is a three-way handshake. During the handshake, the two devices send to each other a randomly chosen numeric value called "Intent value". The Intent value ranges from 0 to 15, and it measures the desire of the P2P Device to be the P2P GO. The P2P Device sending the higher Intent value shall become GO. In case both P2P devices send equal GO Intent values, a tie-breaker bit is used for decision and the device with tie-breaker bit set to 1 shall become GO. Fig. 4 illustrates the Intent value comparison between two P2P devices during Standard Group Formation.

The P2P Device selected as P2P GO shall start a P2P Group session. The other P2P Device can then connect to the P2P GO to obtain credentials and exchange data. Similarly, other P2P Devices and legacy Wi-Fi devices can join the P2P Group as clients.

In *Autonomous* Group Formation, depicted in Fig. 3(b) the role of GO is not negotiated. Instead, a P2P Device announces itself as GO and starts sending Beacons. This process is much similar to the legacy Wi-Fi in which an AP directly sends Beacons into the network to become discoverable. The Autonomous Group Formation is simpler and faster than Standard Group Formation.

In *Persistent* Group Formation, depicted in Fig. 3(c), a P2P Device sends an invitation to another P2P Device, which was previously connected to it in a P2P Group, in order to re-instantiate the P2P Group. This is accomplished using the *P2P Invitation Request* and *P2P Invitation Response* frames. The role of each P2P Device shall remain the same as in the previously formed P2P Group. To establish a Persistent group, the P2P Devices must declare the P2P Group as Persistent during the Standard or Autonomous formation of the group. A flag bit inside the P2P Beacons, Probe Response and GO Negotiation frames is used to indicate that the P2P Group is Persistent or not. If the flag is not set during Group Formation procedure, the P2P Devices cannot re-instantiate a Persistent group in future and must start a Standard or Autonomous group.

The Wi-Fi Direct specification defines the Standard and Persistent Group Formation procedures only between two P2P Devices. Other P2P Devices can only join, as clients, an already-formed P2P Group.

Legacy Wi-Fi uses power-saving scheme using *Sleep* and *Active* modes for Wi-Fi STAs (clients). Most of the traditional APs are permanently connected to a regular power source, and thus, they have no need for any power-saving feature. However, in Wi-Fi Direct, the P2P GO, which acts as a Soft-AP, is a battery-powered device and have a limited lifetime. Hence, Wi-Fi Direct introduces two novel schemes for power saving in the P2P Devices. These schemes are (1) *Opportunistic Power Save (OppPS)* and (2) *Notice of Absence (NoA)*.

In *OppPS* scheme, the GO can save power when its clients are in the *Sleep* mode. The GO announces its presence period called "*CTWindow*". At the end of the *CTWindow*, if all nodes are in *Sleep* mode, the GO can also go to *Sleep* mode until the next Beacon.

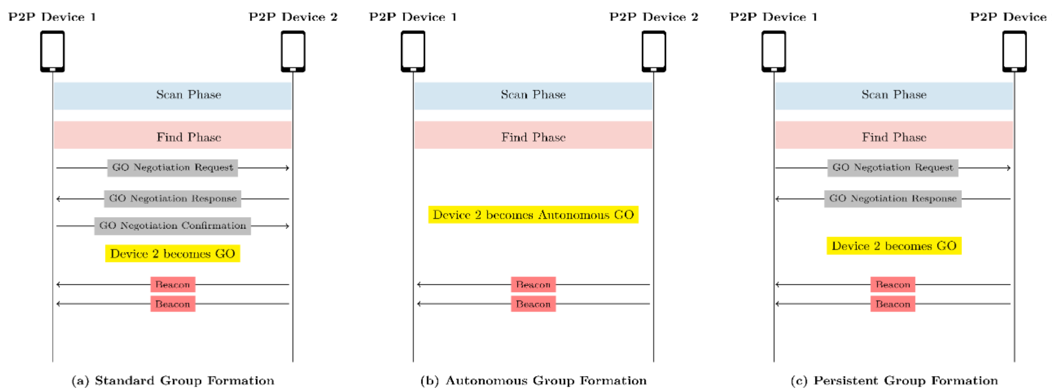


*Figure 2.7* Group formation schemes.

However, at the end of *CTWindow*, if one of the P2P Client nodes is in *Active* mode, then the GO must remain active until the next Beacon.

In the *NoA* scheme, the GO announces via Beacons and *Probe Response* frames, an "*absence period*". During the *absence period*, its clients cannot access the channel, thus the GO shut down its radio to save energy used in transmission or reception. The absence period is announced in Beacons using *NoA* schedule, consisting of four parameters:

1. *Duration* - the length of absence period,
2. *Interval* - the time between two consecutive absence periods,
3. *Start Time* - the start time of the first absence period after the current Beacon, and
4. *Count* - the number of absence periods in the current *NoA* schedule.

The Wi-Fi Direct specification [13] does not define the values of these parameters.

Wi-Fi Direct requires all P2P Devices to implement *Wi-Fi Protected Setup (WPS)* [42] in order to secure the connection establishment process and communication in the P2P Group. In WPS scheme, the P2P GO implements the internal *Registrar* whereas the P2P Client implements *Enrollee*. The WPS scheme works into two phases. In phase 1, the internal *Registrar* generates and issues the network credentials to *Enrollee*. In phase 2, the *Enrollee* (P2P Client) reconnects to the internal *Registrar* (P2P GO) using the new credentials.

Wi-Fi Direct is primarily designed to enable device-to-device communication for short-range (SR) communication without any existing infrastructure. In this section, we discuss several issues and challenges of Wi-Fi Direct implementation and applications. We also highlight the potentials of Wi-Fi Direct and comparison with other SR technologies.

- *Energy Efficiency*

Wi-Fi Direct devices will more likely run on batteries and therefore energy efficiency is an important factor. Although the protocol includes two new power-saving schemes (i.e. OppPS and NoA) for P2P GO as discussed in Section 2.1.5, energy efficiency is still a challenge in Wi-Fi Direct. The OppPS scheme can save energy only in low traffic conditions whereas the NoA scheme can be implemented to save energy in various traffic conditions. However, NoA scheme requires the computation of the optimum length of absence periods. Larger duration of absence periods will save more energy but will result in less throughput and vice versa.

- *GO Selection and Clustering*

Wi-Fi Direct defines the Group Formation procedure to be used between two P2P Devices. The Wi-Fi Direct specification does not define the mechanism when multiple P2P Devices simultaneously start Device Discovery and Group Formation.

As per the current Group Formation procedure, such a situation will result in a formation of several P2P Groups, with most of the groups consisting of two devices. This is not desired in several applications like content-centric networks (CCN).

- *Multi-hop and Scalability*

Wi-Fi Direct currently supports single-hop communication. Using P2P Concurrent mode, a P2P Client in one P2P Group can serve as a P2P GO in another P2P Group. An example of such topology is a laptop being a P2P Client in one P2P Group and simultaneously connected to a printer in another P2P Group. The P2P Concurrent Device can be used as a relay node by becoming a GO for another set of devices to form a multi-hop network. This relay node will be responsible to receive and forward packets between the AP and the P2P Clients. The detailed operation of concurrent P2P device is not specified in the Wi-Fi P2P specification. However, it can increase the scalability of the Wi-Fi Direct network.

- *Load Balancing*

When defining cluster size, the important parameter to consider is how many clients can be better served by the P2P GO. Even if the best GO is selected, the characteristics of the traffic sent by devices cannot be estimated in several applications, hence we need some kind of load balancing mechanism to implement on P2P GO in order to increase the throughput and reduce the end-to-end delay. Examples of load balancing techniques are given in [43-45].

- *Coping User Mobility*

The current applications of Wi-Fi Direct are only limited to static environments, where users have very limited movement. However, the random mobility of users can lead to the formation of very unstable P2P Groups. The connection breaking and Group Formation delays might not be desired in some application. Therefore, the mobility of both P2P GO and P2P Clients is a challenging problem. Mobility parameter can be considered during the GO election, in order to avoid tearing down of the P2P Group when P2P devices move. However, in several multi-hop scenarios, mobility can be opportunistically used to provide services. For instance, the dissemination of local marketing advertisements [46] can be extended to exploit the user's mobility to spread the number of messages sent to the target users. Similar applications can be found in alert dissemination as in [47, 48].

### 2.5 Dynamic Topologies and UAV-Aided Architectures:

UAVs in communication networks are preferred due to their mobility, flexibility, and adaptive altitude [49]. Authors in [50] proposed the 3D placement of UAVs to maximize the total coverage area using circle packing theory. The normalized results obtained in this study exhibits a general coverage performance versus the number of UAVs deployed in the network. Authors in [51] formulated the placement of the base station in 3-dimensional space as a Mixed-Integer Non-Linear Problem (MINLP), with the objective to maximize the coverage of the base station. The proposed scheme considers cellular networks and it uses the Air-to-Ground (ATG) model proposed by ITU in [52] which is a function of the altitude of the UAV and the horizontal distance between UAV and mobile stations. In [53], authors used reinforcement algorithm to find the optimum placement of the UAV in 3D space to increase the coverage and throughput. In the proposed scheme, an aerial base station is deployed to assist a number of ground base-stations. In case, the QoS on a ground base station is not met due to user mobility, it triggers the aerial base station to find and move to the optimum location in the air and take over the respective ground base station to serve users connected to it. In [54], authors studied the optimum placement of UAV-aided relay along the altitude to improve the reliability of dual-hop communication networks. Three performance metrics, bit error rate, outage probability and total power loss are studied, and numerical approximations are provided. However, the study is limited to a single user connected to UAV-aided relay. Moreover, the study considers a numerical approximation of the physical layer metrics, which might not exhibit the actual network performance and the QoS, delivered to the end-user. Authors in [55] showed that the end to end network throughput with UAVs as mobile relays can be significantly improved with optimum trajectory design. The authors performed Monte-Carlo simulations of the physical-layer model only.

Unlike cellular networks, UAVs in SR communication networks such as IoT and Wi-Fi networks are placed at very low altitude due to short communication range (5-10 meters usually). Apart from the range limitation in Wi-Fi networks, the altitude in UAV placement is also considered less significant in Wi-Fi networks. For instance, according to [52], the coverage increases by 1-2% for each meter of altitude increase. Hence, slight changes in UAV altitude poses less impact on the coverage of Wi-Fi networks. The authors in [52] further demonstrated that by decreasing the UAV altitude, the SNR does not improve significantly.

UAV-based communication in SR communication networks has been studied in [50, 56, 57]. Authors in [49] stated that UAVs can be used in SR communication networks such as IoT scenarios [58, 59] where the devices cannot communicate over long distances. Three potential benefits of UAV communication in SR communication networks are discussed in the state-of-the-art, i.e. improved coverage, high throughput and energy efficiency. In [57], the authors propose the use of UAV communication to extend the coverage of Wi-Fi networks. Authors in [56], propose to deploy UAVs as Wi-Fi hotspots to extend the coverage of the cellular networks. The UAVs are placed in 3D space such that it maximizes the aggregated SNR of all nodes. The study claimed up to 44% throughput gain. However, the authors did not consider the mobility of nodes. Authors in [60] investigated the throughput performance of point-to-point aerial links in 802.11n Wireless LANs. The results show that throughput is not improved significantly. However, the authors in [61] further investigated the use of UAVs in infrastructure Wi-Fi networks and evaluated network throughput. The results obtained in [61] show a significant increase in the network throughput of IEEE 802.11n. The results also show that the mobility of users greatly affects the transmission rates and thus the network throughput.

Authors in [62] studied the throughput of UAV-aided wireless networks as an optimization problem. The aim is to maximize the minimum average throughput of all users by jointly optimizing the UAV trajectory and OFDMA resource allocation. A recent study on the UAV positioning in Wi-Fi networks is conducted in [63]. The authors proposed a Tabu search algorithm to determine the optimal position for the UAVs to improve network throughput. The study report 26% improvement in the average network throughput using the proposed scheme for UAV positioning.

One of the benefits of UAVs in Wi-Fi networks is the potential to reduce energy consumption. The first logical reason to reduce energy consumption is UAV networks is the reduction in transmit power of the devices if the distance between them is shortened. Authors in [64] show that the total transmit power of the devices can be minimized by placing the UAVs in the centre of the optimal clusters. Secondly, at short distances, the frame loss can be reduced which decreases the retransmissions, thus resulting in energy efficiency [65]. Authors in [66] further investigated the energy efficiency in an IoT network. The authors showed that the average transmit power of devices can be reduced by the optimal deployment of the UAVs. Authors in [50] studied the UAV-aided Internet-of-Things (IoT) to enable energy-efficient networks. The study considered K-means clustering algorithm to optimally cluster the network devices and find the optimal location of the UAVs. The study shows a reduction in total energy consumption.

### 2.6 Cognitive Networks

The large set of network parameters, the dynamic network topology, and the unpredictable behaviour of the wireless channel offer big challenges in designing optimal WLAN networks. In fact, very accurate and scalable analytical models may not characterize such complex systems. Recently, new cognitive network architectures using sophisticated learning techniques are increasingly being applied to such problems. In this chapter, data-driven machine learning (ML) schemes are proposed that efficiently address well-known problems in WLAN networks, i.e. throughput estimation, handover prediction and access point (AP) selection.

Recently, a new centralized architecture has been proposed in the literature [67-69] based on Software Defined Network (SDN) [70] and Cognitive Networking (CN) [69, 71]. Software-Defined Networks or SDN refers to the type of networks in which the control and data forwarding parts are separated. In such architectures, the network devices such as switches, routers and access points act as non-intelligent data forwarding devices while the intelligent functions such as data routing are implemented in a central controller also called the SDN Controller. On the other hand, cognitive networking [69] refers to the network paradigm in which the networks automatically learns its behaviour and respond to network changes by actively taking decisions and planning network resources to achieve an end to end performance. Cognitive networks can be realized using both distributed and centralized architecture. A novel approach to realize cognitive networks is to adapt data-driven machine learning (ML) algorithms to address state-of-the-art challenges [72-74]. ML algorithms can be used for both network design [75-77] and network performance evaluation [78-81].

Several studies have been carried out to demonstrate the significance of machine learning in wireless communication in a range of applications [72-78, 80-84]. Supervised learning algorithms such as regression models [85], K-Nearest Neighbors (KNN) [86], and Support Vector Machines (SVM) [87, 88] can be applied in channel estimation, user localization [89] and energy learning [90]. Similarly, Bayesian learning [91] can be applied in multiple-input, multiple-output (MIMO) for channel learning [92] and spectrum sensing using Gaussian Mixture Models (GMM) [93], Expectation-Maximization (EM) [94] and Hidden Markov Model (HMM) [95]. Unsupervised learning algorithms such as K-means [96, 97] clustering can be used to build optimal topologies in Device-to-Device (D2D) networks for energy efficiency and overall network efficiency [98]. Principal Component Analysis (PCA) [99] and (ICA) [100] can be efficiently utilized in applications of anomaly detection, fault isolation, and intrusion detection. Multi-Layer Perceptron's (MLPs) [101, 102] as a sub-class of Artificial Neural Networks have been applied to several problems in next-generation wired and wireless networks in several applications [72, 73].

The literature review presented in this chapter provides a deep understanding of the state-of-the-art in the respective areas. The following chapters present the original research conducted.

# CHAPTER 3 : ENHANCED GROUP FORMATION IN WI-FI DIRECT

In this chapter, we identify the issues related to the standard group formation procedure in the Wi-Fi Direct protocol that limit the performance of the protocol in several applications. Following the identification of these issues, we present our proposed modifications to improve network performance.

## 3.1 Group Owner Election

The P2P GO negotiation procedure starts between two devices where one becomes a GO. The criterion for GO is a single byte numeric number called Intent Value that ranges from 0 to 15. Each P2P device sends an Intent Value to other devices in its range through GO negotiation frames. The device that sends a higher Intent Value becomes GO. The Wi-Fi Direct specification does not define any mechanism to select Intent Value, which leaves a room for developers to implement their own schemes to compute Intent Value. In the following section, different approaches are discussed to compute Intent Value.

### 3.1.1 Intent Value Computation:

The Intent Value shows the willingness of a P2P device to become a GO in the P2P group. The device sending a higher Intent Value shall become GO. While forming a P2P group, a P2P device must send the Intent Value attribute in the GO Negotiation Request and GO Negotiation Response frames. The Intent Value attribute contains a 1-byte Intent Value that corresponds to decimal values of 0 to 15. The first bit is a Tiebreaker which is used when both P2P devices send the same Intent Value in the GO Negotiation. The Intent Value is a useful parameter and shall be carefully chosen.

The more useful approach to choose Intent Value is based on the device capabilities to serve as GO because once a device becomes GO, it shall serve all associated P2P client devices for communication. All data distend to P2P clients in a given P2P group must be routed through the GO. For example, in the case of video content distribution, all the data is first received by the AP and then forwarded to the GO, which forward to the destination P2P client in the group. Similarly, devices in the same P2P Group also communicate with each other via GO. Thus, the GO shall be responsible for all data forwarding and works as Soft-AP. The capabilities of a P2P device depend on the application. In this section, various parameters to compute Intent Value are discussed:

- Battery life – P2P devices, including the GO, are battery-powered devices. If the battery life is not considered in electing a GO, there is a probability that a P2P device having a low value of the remaining battery is elected as GO. The GO being the most active device in the P2P group would exhaust soon and the P2P group will be broken.
- Processing capability – The device that becomes GO shall be equipped with enough processing power and large memory to better serve the connected clients. The processing power and memory requirements for GO might become more significant when the P2P group consists of a large number of nodes and the group is intended for multimedia application. In simpler applications, e.g., data transfer between two mobile devices, or connecting a laptop to the printer, the processing requirement becomes less significant.
- RSSI – The Received Signal Strength Indicator (RSSI) indicates the quality of the connection between two devices. The data rate of the wireless link is badly

affected by low RSSI. If the P2P group is used for content distribution, the strong connection between the AP and the GO is more crucial. With multimedia traffic e.g. video streaming applications, it would be almost impossible to stream live video if the GO receives a very weak signal from the access point. The RSSI of GO to the AP and GO to group clients both have a significant impact on the P2P group performance.

- The number of connected devices – If the P2P group is intended to connect a large number of devices, then it is important to elect as GO the P2P device that has more devices in its range to connect as clients. There should also be a limit on the maximum number of nodes in a P2P Group. The GO is a battery-powered mobile device with limited processing capabilities and memory. It may not be capable to serve a large number of devices. Using such constraints, this becomes a problem to identify the optimum size of the P2P group and the optimum number of P2P groups from a given pool of P2P devices. This becomes a classical cluster optimization problem. Several clustering algorithms exist to cope with such a problem [97, 103-105]. However, in this work, we are interested in considering one or more of these parameters to compute Intent Value based on the application. Node's degree is a commonly used parameter instead of the number of neighbours. Node's degree is computed in different ways i.e. the number of neighbours, mean value of distances to all neighbouring nodes.

The battery life parameter becomes more significant when the group is intended for longer duration e.g. a group of people connecting to Internet AP through a P2P device as GO. If the device with a low battery is elected as GO, the GO will soon be exhausted, and the group will be eliminated. A new group formation would be required.

The device with longer battery life in the aforementioned scenario guarantees a longer life of the P2P group. However, what if the P2P device with longer battery life is having a weak internet connection with the access point or this device has very low processing capabilities? Electing such device would lead to poor services for all group clients. If the RSSI value indicates a very poor connection, it may lead to connection tear down between GO and AP. The P2P group might be intended to serve a large number of nodes. In this case, the battery power, good processing capability and reliable radio connection are not enough. There is a possibility that a device with a more remaining battery and better connection to AP becomes a GO, but this GO has only one device in its radio range. Furthermore, the number of such small P2P group might be less significant than forming larger P2P groups having a greater number of nodes.

On the contrary, there is another case when a single large P2P group is formed, and the elected GO might suffer from network overhead. From the above discussion, it is concluded that the Intent Value that defines the desire or the capability of a P2P device to become a GO shall be computed by considering the combined effect of all these parameters (each parameter is scaled on the range 0 to 5). A simple approach to compute Intent Value is shown in Algorithm-1 below:

The computation of Intent Value is explained in the previous section. The Intent Value is defined in the Wi-Fi Direct specification as “desire” of the P2P device to become GO. For instance, when a P2P device wants to connect to another P2P device it will more likely form an autonomous P2P group.

Algorithm 3.1: Intent Value Computation.

```
Inputs:      RSSI, RSSI_T, RSSI_W, BAT, BAT_T, BAT_W, NBR, NBR_T,
             NBR_W // _T represent Threshold, _W represent Weight parameter.
Outputs: Intent Value
IF      RSSI < RSSI_T:
        RSSI = 0;
        ELSE
                RSSI = RSSI * RSSI_W;
ENDIF.
IF      BAT < BAT_T:
        BAT = 0;
        ELSE
                BAT = BAT * BAT_W;
ENDIF.
IF      NBR < NBR_T:
        NBR = 0;
        ELSE
                NBR = NBR * NBR_W;
ENDIF.
Intent Value = RSSI + Battery + Neighbors
```

However, in several applications where more than two devices are in a shared wireless range and group formation is intended, then the role of GO would be negotiated automatically by the application, and not by the end-user. In this case, the P2P device that becomes GO would be compromising on its resources including battery power, processor, memory and overall performance of the applications using the particular service for which the P2P group is formed. It is discussed earlier, that choosing the Intent Value randomly is not a good approach and it can lead to the poor performance of the applications. In the previous section, we proposed a solution to compute the Intent Value based on the device's overall capabilities.

### 3.1.2 GO Selection

The next step after Intent Value computation is the GO negotiation procedure in which two devices will decide on the role of GO-based on their Intent Value (standard group formation). The Wi-Fi Direct specification restricts the GO negotiation procedure to two devices i.e. only two interested devices can form a P2P group where one become GO and then the GO will announce its presence by sending beacons like an access point. Other P2P devices and legacy Wi-Fi stations can join the group later as clients. This limitation has also several implications on the performance. Let say, a set of N devices intend to form a group for a particular service. The group formation decision is fully automatic and shall be managed by the application. Theoretically, the probability of each device to become a group owner is $p = 1/N$ , where, however, in the standard group formation, the GO negotiation takes place between two devices only. Thus, the two devices which enter into the GO negotiation phase will have increased probability to become GO, each one has $p = 0.5$. If the GO negotiation completes before the other devices enter the GO negotiation phase, it is more probable that the rest (N-2) devices will receive beacons from the GO and will join the existing P2P group. Thus, the standard group formation increases the probability of some nodes and decreases or even eliminates the probability of other nodes to become GO.

To improve the performance of the protocol, it is crucial to assign equal probability to each node. However, to do so the standard protocol functions shall be altered. The GO Negotiation is a three-way handshake between two devices, which should be re-structured as an election procedure between all participating nodes in a common wireless range. All nodes must have equal probability in the election if the Intent

Value is equal. If devices compute the Intent Value using Algorithm-1 proposed in the previous section, the probability distribution is according to the Intent Value.

---

Algorithm 3.2: GO Election Process.

---

```
Inputs:        Number of Nodes, Node's Intent Values
Outputs: GO Index
FOR   i = 1 to Number of Nodes:
        Do:
          Node[i] sends GO Negotiation Request to Node[i+1]
          Node[i+1] sends GO Negotiation Response to Node[i]
          IF    Intent Value[i] > intent_value[i+1]:
                Node[i+1] is disqualified.
                ELSE IF:
                        Intent Value[i+1] > intent_value[i]:
                        Node[i] is disqualified.
          END IF
          i = i + 1;
END FOR
```

---

The proposed GO Election process provided an intuition to illustrate the benefits of electing the most capable GO, instead of the randomly chosen intent value parameter. Section 3.3 provides an optimal scheme to perform the GO selection in Wi-Fi Direct.

### 3.2 Enhanced P2P Group Formation

In opportunistic networks and collaborative networking, wireless peers have to discover each other in a short time and then discover what kind of services are provided by each peer. If peers are interested in a published service by a discovered peer, then they can be aggregated into groups, and share/consume the advertised service (video streaming, software updates, etc.). Using Wi-Fi Direct technology, devices can dynamically organize themselves to form a P2P group. In order to establish the P2P group, P2P devices have to first discover each other and then negotiate the role that each device shall assume. We propose and evaluate a new method to set a GO Intent that best describes the P2P device capabilities. In this thesis, we first provide an overview of the Wi-Fi Direct technology and we describe in detail its GO negotiation and group formation procedures. In addition, we propose a new approach to accelerate the group formation procedure in Wi-Fi Direct technology.

As mentioned earlier, the standard group formation procedure requires a 3-way handshake for the GO negotiation and other messages exchanges in order to form a group within two devices discovering each other. In addition, the GO negotiation is limited to two devices, which can lead to the election of a GO that is not necessarily the best candidate within its neighbours. To overcome these limitations, we propose a new group formation procedure.

### 3.2.1 Proposed Solution

The new procedure consists of eliminating the 3-way handshake of the GO negotiation, and including all required information, to form a group, in the already defined Wi-Fi Direct frames: Probe Request and Probe Response frames. Our method consists in inserting the device GO Intent and the list of already discovered devices (and their corresponding GO Intent) in the P2P Information Element (IE) attributes available in the Probe Request and Probe Response frames. Therefore, when a device receives the Probe Request or the Probe Response frame from a second device, it can easily determine which of the device is more capable of being a GO without a need for a GO negotiation. The device with the highest GO Intent can start an autonomous group formation and invite all discovered devices to join its group. Figure 1 is a state diagram that describes the proposed P2P group procedure.

This method offers P2P devices the ability to have an idea about discovered neighbours' capabilities. In addition, by using the Probe Request and Probe Response frames, the proposed method will be backwards compatible with P2P devices that do not implement the proposed method. By eliminating the GO negotiation, the group formation between two devices can be accelerated. One of the most interesting features provided by the proposed method is the ability to select the best GO from more than two neighbour devices, which is not possible with the current state of the Wi-Fi Direct specification. Another important feature of the proposed method is that each device can build a list of neighbour devices with their corresponding Intent. In such way, when the actual GO leaves the group or does not have the highest Intent anymore, all peers have already a prior knowledge of which device will be elected as a replacement of the actual GO. The description of this backup GO is detailed in the following section.

### 3.2.2 Backup Group Owner (BGO)

In the current Wi-Fi Direct specification, when a GO device leaves a P2P group, then the P2P group is broken, and a new P2P GO negotiation has to be made. There are two cases where the actual GO of a P2P group have to be replaced by another device: i) the GO leaves the P2P group or ii) the GO's Intent value is no more the highest within its neighbours (due to the joining of a device, with a higher GO Intent, to the already created P2P group). Making a new (conventional) P2P group formation is time-consuming and does not necessarily elect the device with the highest Intent value.

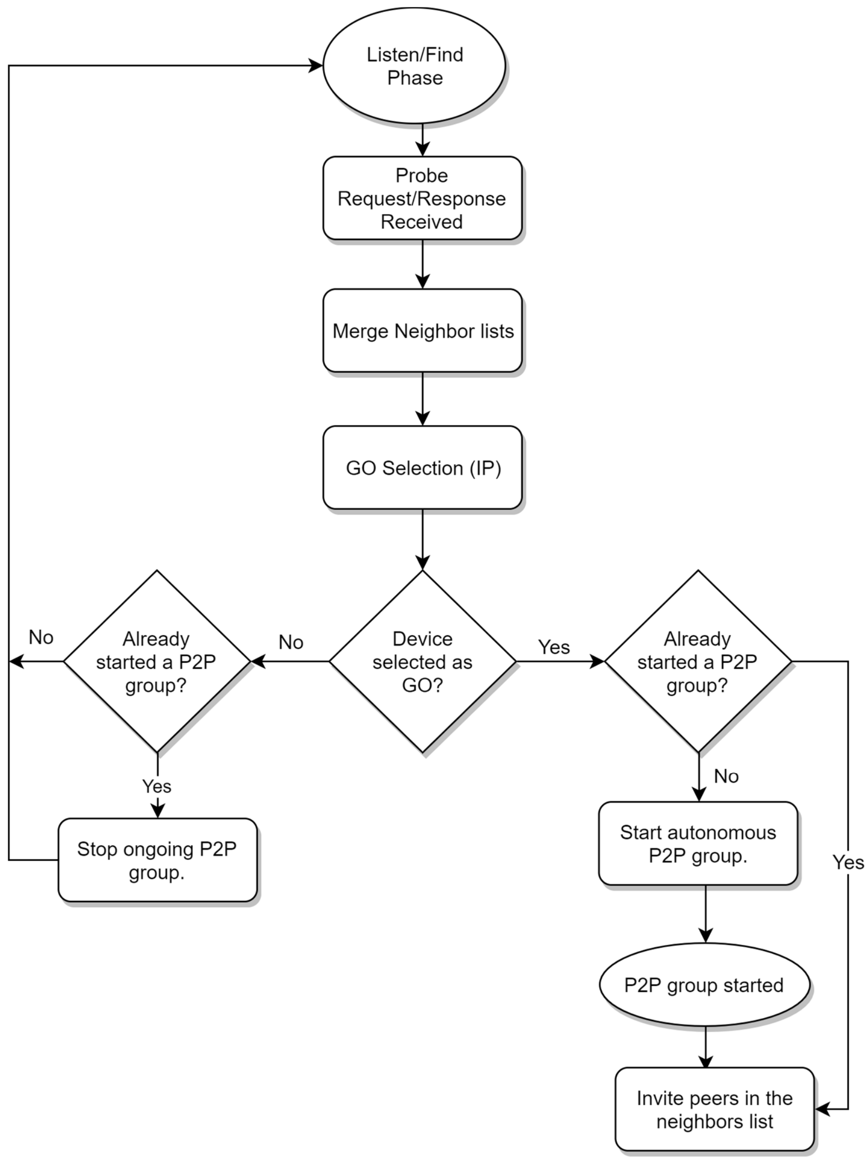


*Figure 3.1* Device state diagram.

Our proposed P2P group formation method addresses this issue. In fact, all devices have a list of all discovered devices and their Intent values. Thus, all devices have already knowledge about the device with the second highest Intent value within their neighbours. We call the second highest Intent value device as a backup GO.

When clients of a P2P group notice that the actual GO is no more reachable or does not have the highest GO Intent value any more, they update their discovered list and start a new P2P group formation procedure. The backup GO becomes the device with the highest Intent value and thus elected as new GO, as described in *Figure 3.2*. The newly elected GO starts a new (autonomous) P2P group and invites all peers in its discovered devices list.

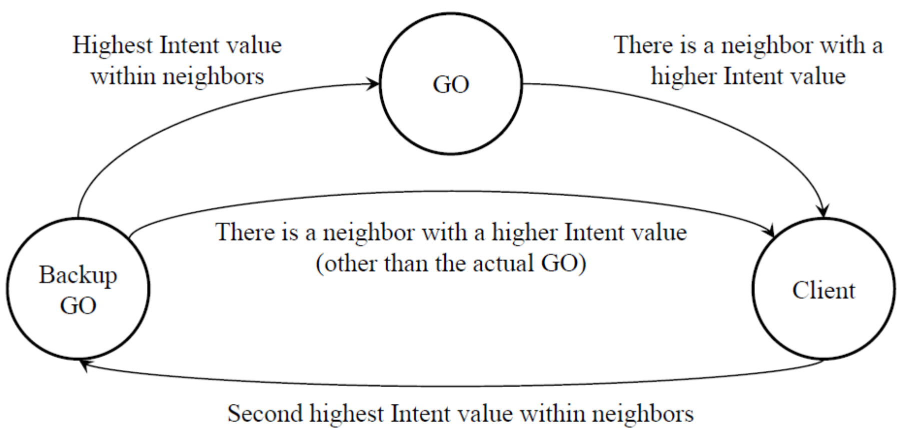


*Figure 3.2* Device state diagram for BGO selection.

### 3.2.3 Experimental Evaluation

This section portrays the performance of our proposed P2P group formation procedure, and the efficiency of the introduction of the backup GO.

The test-bed consists of an Ubuntu-server virtual machine with several virtual wireless interfaces. Each virtual wireless interface is attached to a different P2P node. We created virtual network interfaces using mac80211_hwsim [106]. The mac80211_hwsim driver is a Linux kernel module and is used for testing MAC functionality and userspace tools such as wpa_supplicant/hostapd. The wpa_supplicant module is an implementation of the WPA Supplicant component. It is used for controlling the wireless connection and it allows the use of Wi-Fi Direct [107]. Throughout our experiments, we assume that all devices have identical capabilities (but different Intent values) and we do not take into account the improvement/drop of the per-device throughput/battery. In addition, we presume that all devices are discoverable by each other. Furthermore, in order to automatize the test execution, we always pre-provision devices with a Wi-Fi Protected Setup (WPS) PIN.

We analyze the required time to establish a P2P group in the standard scheme. The group formation procedure consists of several steps. First, devices (A and B) need to discover each other. The device discovery time is random as specified by the Wi-Fi Direct specification. Once device A discovers device B, they start a GO negotiation. Device A sends a GO negotiation request to device B, and device B replies with a GO negotiation response (with success status). Device A replies with a GO negotiation confirmation with a success status. The device with the highest GO Intent (device A for example) starts the group formation by activating the AP-mode. Device B tries then to connect to device A (the GO). *Figure 3.3* shows examples of delays when two devices try to form a group and connect.

*Figure 3.3* depicts the elapsed time in each phase (discovery/negotiation) of a device (elected as a client). Time zero is the start of the finding phase. dev_found bars represents the moment when it discovers another device (during the finding phase). go_neg_success is the moment when the device receives a GO negotiation response, and the negotiation is successful. grp_started represents the moment when the group is successfully formed, and the client is connected to the GO.

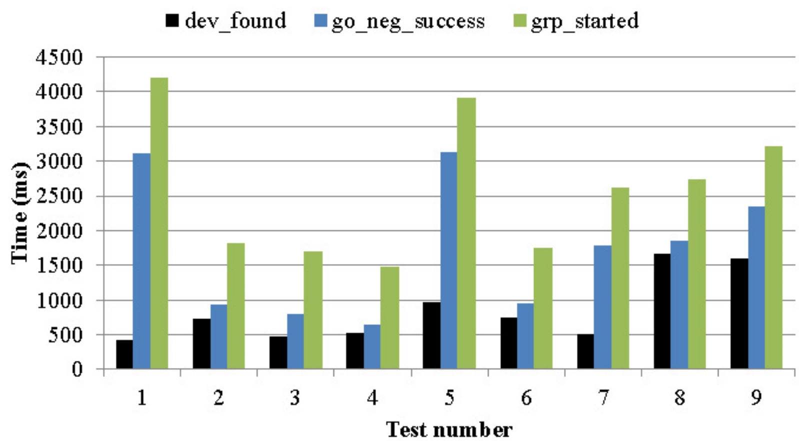


*Figure 3.3* Device discovery and group formation time.

Seventy (70) tests were performed to measure the discovery/group formation procedures. For the sake of clarity, only 9 of these tests are shown in *Figure 3.3*. The Cumulative Distribution Function (CDF) of delay in each P2P group formation phase is depicted in *Figure 3.4*.

*Figure 3.3* and *Figure 3.4* show the randomness resulted from the Wi-Fi Direct discovery algorithm. In average, the device discovery time requires 1070ms. The time elapsed to negotiate the GO and form a group can vary from 850ms to 9000ms and is in average equal to 2198ms (the median is equal to 1958ms). The time required to form a group once the GO negotiation is finished successfully is in average equal to 903ms (the median is equal to 873ms).

As depicted in *Figure 3.3* and *Figure 3.4*, devices spent more than 50% of the time during the GO negotiation phase once they discovered another device. The evaluation shows that there is room for improvement if the procedure of the GO negotiation is combined with the device discovery phase as described earlier. The next section is an evaluation of the proposed method for the P2P group formation.

As already explained in the studies [108], with the current state of Wi-Fi Direct specification, it is hard to manage a variable number of nodes joining the same group. P2P group formation delays can increase rapidly when the number of neighbour devices increases. In the next sections, we evaluate our proposed P2P group formation for the following number of devices: two devices, and five devices.

- **Two Devices:** To evaluate the proposed P2P group formation procedure, we start by measuring the delay performance of P2P group formation between two devices. *Figure 3.6* shows the CDF of the required time to form a P2P group between two devices. Dashed-lines represent the conventional P2P group formation (using a P2P GO negotiation). Solid lines represent our proposed P2P group formation. The results confirm the fact that the proposed method is faster than the conventional P2P group formation between two devices. The median P2P grouping time is improved by 20% when the proposed P2P group formation procedure is used.
- **Five Devices:** The evaluation of the P2P group formation in the case of five devices is a complex task due to the randomness of the device discovery algorithm. Several combinations can be obtained when devices have to make a

GO negotiation with the first discovered device. Most of the time, two P2P groups are formed. The formed group that contains three (or more) devices has a high probability that its GO is not actually the device with the highest GO Intent. As an example, if we consider three devices A, B and C, with respective GO Intent equal to 1, 2 and 3. If devices A and B discover each other and form a P2P group before discovering device C, then the GO will be device B (with an Intent equal to 2). Device C will join later the created P2P group. In this case, device C will have a higher GO Intent (equal to 3) than the GO (device B with a GO Intent equal to 2). The complexity of Wi-Fi Direct to manage a variable number of nodes is well-detailed in [109]. In our proposed P2P group formation, discovered devices (and their GO Intent) are shared between neighbours during each Probe Request/Response frames exchange. If a device within an already created P2P group discovers another device (out of the group) with a higher GO Intent than the current GO, then it will notify all other peers of the group and switch to the new P2P group created by the discovered device. To test the proposed method, each device will proceed as described in the case of two P2P devices. Once the GO is elected, the latter has to invite all discovered devices to join him. For this purpose, in our experiments, the GO will sequentially invite discovered devices so that it does not cause any joining failure, i.e. the next device will be invited just when the already invited device has successfully joined the P2P group. *Figure 3.6* shows the CDF of the elapsed time of each device trying to associate with the created P2P group. The solid line with no marker represents the moment when a first device is discovered. Device dev0 was selected as a group owner (with the highest GO Intent equal to 7). The other devices have a smaller GO Intent than dev0.

Obtained results show how the proposed P2P group formation method can be very efficient to accelerate the grouping of multiple devices. The elapsed time to form a P2P group with 5 devices is equal on average to 8000ms. 8s to form a P2P group, using our proposed method with 5 devices, is almost three times faster than the conventional Wi-Fi Direct P2P group formation procedure.

- **Evaluation of BGO:** In this section, we evaluate the latency of re-grouping a broken P2P group. We assume that the GO of a P2P group formation has left (or turned off). The backup GO takes the lead, becomes a GO (autonomous P2P group formation) and invites all other peers to join him. *Figure 3.7* shows the CDF of the elapsed time regrouping all devices. The red solid line, with no marker, is the time elapsed creating a new P2P group since the backup GO has been disconnected from the former GO. Dashed lines represent the moment when a device has received an invitation from the GO (former backup GO) to join the newly formed P2P group. The experiment shows that having a backup GO is very useful when the P2P group is broken. Short times are required to regroup the devices of a broken P2P group. Contrary to the conventional P2P group formation of Wi-Fi Direct, regrouping devices of a broken P2P group requires a new GO negotiation, and the newly elected GO is not necessarily the best amongst its neighbours.

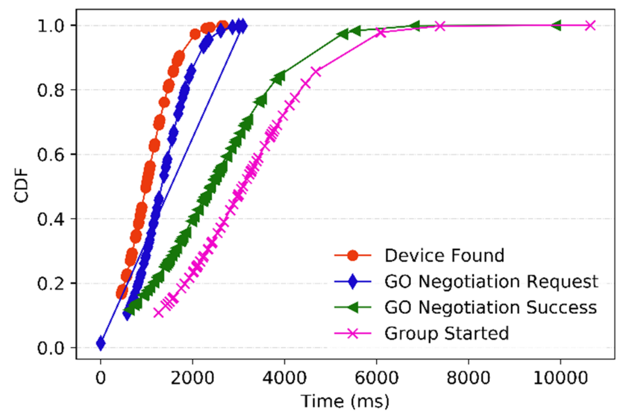


*Figure 3.4* P2P group formation phases.

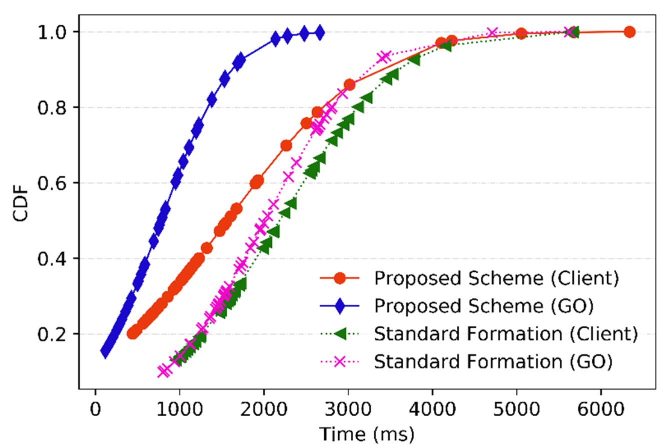


*Figure 3.5* Group formation delay (two P2P devices).

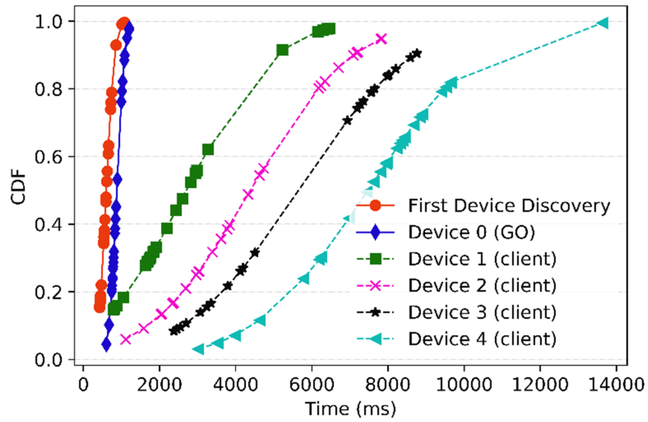


*Figure 3.6* Group formation delay (five P2P devices).

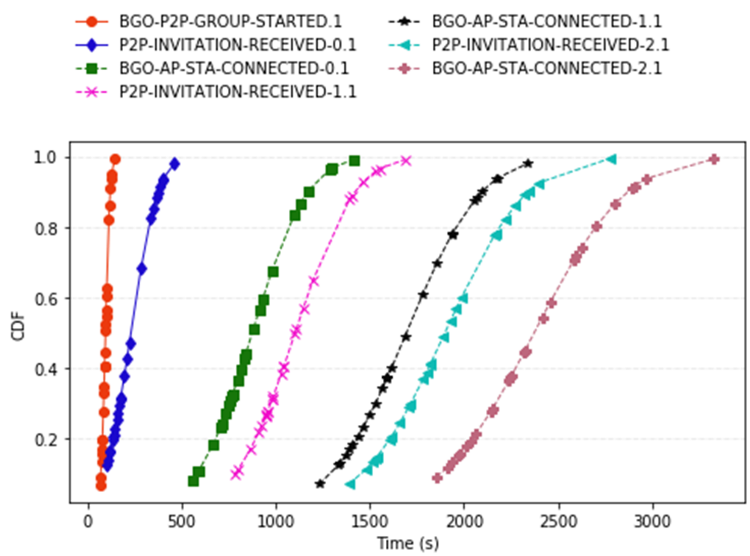


*Figure 3.7* Group formation using BGO.

## 3.3 Optimal Clustering Scheme

Earlier works on Wi-Fi Direct clustering and group formation are typically based on heuristics, which do not guarantee optimum performance. Furthermore, the selection of multiple GOs (in dense networks) has not been rigorously investigated in the literature. In this section, a modified group formation scheme is proposed which formulates the GO selection problem as an optimization problem which is solved using Mixed Integer Programming (MIP) [110]. The GOs are selected based on link capacities with the objective to maximize the overall network throughput. In multicast applications, the proposed scheme is implemented such that the total packet loss ratio of the network is reduced.

### 3.3.1 Proposed Scheme

In a given set of STAs randomly located in a shared wireless range and an AP that has a limitation on the maximum number of associated STAs, and hence can only connect a small number of STAs. It is readily possible to use Wi-Fi Direct to select one or more number of STAs as intermediate devices and connect the remaining STAs to these intermediate devices.

The proposed scheme eliminates the 3-way handshake in the GO negotiation, which takes place between two P2P devices only. The proposed scheme preserves the intent Value attribute defined in the Wi-Fi Direct specifications [13] to select the GO, however, the highest intent Value is now selected by the device selected by the proposed scheme. We propose to modify the standard functionality of the P2P devices as illustrated in Figure 3. In the proposed state diagram of the P2P device, each P2P device when receives a Beacon frame from the AP, it records the SNR of the link to the AP. Each P2P device also sends P2P Request frames that are received by other P2P devices in its range. A P2P device on receiving the P2P Request frame records the MAC address and the SNR to the sender of the P2P Request frame. All the P2P devices, which receive the P2P Request frames, reply with the P2P Response frames. The sender of the P2P Request frame after receiving the P2P Response frames from all its neighbours, record the MAC addresses with their respective SNR values. This device then sends a second P2P Request frame and insert its complete neighbours' list (i.e. MAC IDs and SNR values). By this way, all P2P devices share their complete neighbours' lists. A P2P device on receiving neighbours lists from its neighbours, combine these lists into a master adjacency matrix. The master adjacency matrix contains a list of SNR values from each P2P device to every other P2P device in the network. Every device then runs the GO selection algorithm to determine the best GO. If a device determines itself as the best GO, it sets its intent Value to 15, otherwise zero. The device with the highest GO intent then starts an autonomous group formation and invites all the discovered devices to join the newly created P2P group.

*3.3.1.1 Assumptions:*

The implementation of the proposed scheme assumes the following listed conditions to be always true.

- Each device shall always enable the "PROBING" feature, i.e. each STA constantly sends Probe Request frames and Probe Response frames (in response to Probe Request frames).
- In the proposed scheme, the Probe Request and Probe Response frames are sent with the maximum achievable transmit rates in order to calculate the link data rates used in the proposed scheme.

The proposed scheme aims to select a subset of STAs to act as relays between the AP and GO thus creating one or more clusters called as P2P groups. A P2P GO for each P2P group is selected to connect the STAs in the P2P group to the AP. We discuss two cases for the selection of candidate GOs:

- Optimal selection in which the selection is based on the link quality of both links (AP-GO and GO-STAs links), and
- Sub-optimal selection in which the selection of GO is based on the link quality of first hop (AP-GO) only.

For comparison purpose, we also consider a third case involving the worst selection of GO in which the GO have poorest link quality over both hops (AP-GO and GO-STAs). In the subsequent parts of this section, the GO selection schemes are presented.

### 3.3.2 System Model

Consider a Wi-Fi network where C and G denote the set of Wi-Fi clients (or STAs) and candidate GOs respectively. Let $n = |C|$ and $m = |G|$ denote the total number of STAs and candidate GOs respectively. It is assumed that STAs are randomly placed around an AP. Each STA in the network computes the SNR to all the discovered devices using P2P Request and Response frames, in an array $N_j$, where $j$ is the index of the node.

$$Nj = \begin{bmatrix} id_0 & S_{(0)} \\ id_1 & S_{(1)} \\ id_2 & S_{(2)} \\ . & \\ . & \end{bmatrix} \tag{1}$$

Where, $id_0, id_1, ...$ are the MAC addresses of the devices and $S_0, S_1,..$ are the respective SNR values to these nodes. The first value in the array ($S_0$) denotes the SNR to the AP. Furthermore, the length of the array $N_j$ is different for each node, as each node has a different number of neighbours. Each Node shares this array using the Probe Request to all its neighbours. Each node on receiving the Probe Request frame reply with the Probe Response frame, in which he sends his own neighbours list. Once the discovery phase is completed and all nodes have shared their neighbours' lists, the next step is to transform the neighbour's lists in the appropriate form required in the MIP. Each node creates two arrays, a 1D array $S_i$ and an $n \times n$ array $S_{ij}$. The $S_i$ array contains the Signal-to-Noise Ratio (SNR) of each link between the AP and STAs.

$$S_i = \begin{bmatrix} S_{(0)} \\ S_{(1)} \\ S_{(2)} \\ . \\ . \end{bmatrix} \tag{2}$$

The $S_{ij}$ array contains the SNR values of each link between the STAs.

$$S_{ij} = \begin{bmatrix} S_{(1,1)} & S_{(1,2)} & S_{(1,3)} & \dots & S_{(1,n)} \\ S_{(2,1)} & S_{(2,2)} & S_{(2,3)} & \dots & S_{(2,n)} \\ . & & & & \\ . & & & & \\ S_{(n,1)} & S_{(n,2)} & S_{(n,3)} & \dots & S_{(n,n)} \end{bmatrix} \tag{3}$$

Although the SNR parameter is well known and easily measurable, it is not a good estimate of the actual link data rates in Wi-Fi networks. In practical Wi-Fi implementations, rate adaptation algorithms [111, 112] are used instead of simple rate selection based on SNR. Hence, the $S_i$ and $S_{ij}$ matrices are converted into actual rates i.e. $U_i$ and $U_{ij}$ . The matrices $U_i$ and $U_{ij}$ are used in the optimization problem for GO selection.

### 3.3.3 GO Selection Algorithms

#### *3.3.3.1 Single GO Selection*

Consider the case when the AP has a limit on connecting number of clients denoted as $k$ . If the AP has already connected $(k-1)$ STAs and can connect a maximum of one more STAs, the proposed scheme shall select a single GO from the set of remaining STAs (denoted as n) as illustrated in *Figure 3.8*. The goal of the GO selection is to maximize the total throughput of the network. The network throughput depends upon (i) the application generation rates ($D_j$), (ii) the achievable link rates of STAs to AP ($U_i$) and (iii) the achievable link rates of each STA to its neighbouring STAs ($U_{ij}$).

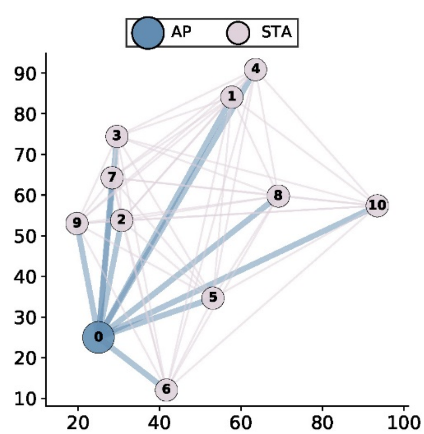


*Figure 3.8* Network topology for GO selection.

In several real-world scenarios' users run different applications such as streaming audio and videos, web browsing, online gaming etc.

- If all STAs are running the same application, the application on each STA transmits at equal rates. STAs has "Equal Demands" i.e. $D_j$ becomes trivial.
- If STAs are running different applications, the data generation rates are unequal i.e. STAs has "Unequal Demands" and $D_j$ shall be incorporated in selecting the optimal GO.

Due to the restriction on the number of GO (only one), the GO selection is formulated as an un-capacitated location problem with the objective to maximize the network throughput. To formulate the problem, two decision variables are defined:

$$X_{ij} = \begin{cases} 1 & if\ STA\ j\ is\ associated\ to\ i^{th}\ GO \\ 0 & otherwise \end{cases} \tag{4}$$

$$Y_i = \begin{cases} 1 & if\ i^{th}\ candidate\ is\ selected\ as\ GO \\ 0 & otherwise \end{cases} \tag{5}$$

Where $X_{ij}$ and $Y_i$ are both binary variables.

The objective function is defined as a function which maximize the total link rates over both hops, i.e. the link rate on AP-GO link ($U_i$) and the sum of link rates of GO-STAs links ($U_{ij}$). It is mathematically formulated as:

$$\max \left\{ \sum_{i=1}^{m} U_i Y_i + \sum_{i=1}^{n} \sum_{j=1}^{m} U_{ij} X_{ij} \right\} \tag{6}$$

Subject to:

$$\sum_{i=1}^{n} Y_i = 1 \quad \forall j \in C \tag{7}$$

$$\sum_{i=1}^{m} X_{ij} = 1 \quad \forall j \in C \tag{8}$$

$$X_{ij} = 0,1 \quad \forall i \in G, j \in C \tag{9}$$

$$Y_i = 0,1 \quad \forall i \in G \tag{10}$$

Constraint (7) ensures that only one GO can be selected. The constraint is explicitly required in the case of single GO selection. Constraint (8) ensures that every STA j can only connect to one GO.

In addition to the aforementioned optimal selection scheme, two other selection schemes are also presented. A sub-optimal selection and worst GO selection: In the suboptimal selection of GO is also considered which maximize the link rates of the AP-GO link ($U_i$) only. It achieves higher data rates on the AP-GO link only. The objective function for sub-optimal selection eliminates the second part of the aforementioned optimization in Equation (6) and limits to the first part $\max \sum_{i=1}^{m} U_i Y_i$ only. This type of sub-optimal selection is applicable to all other schemes in the subsequent sections of this paper. In the worst GO selection, optimization problem always minimizes the Equation (6). The worst GO selection scheme is used for comparison to assess the maximum possible benefit of the optimal selection. The three GO selection schemes, sub-optimal, optimal and worst GO selection are illustrated in *Figure 3.9*.

The MIP produces a full adjacency matrix $X_{ij}^*$ and matrix $Y_i^*$. The $X_{ij}^*$ and $Y_i^*$ matrices are of the same shapes as $X_{ij}$ and 1D matrix $Y_i$. Each element in $Y_i^*$ equal to 1 indicates the index of the node which is selected as GO.

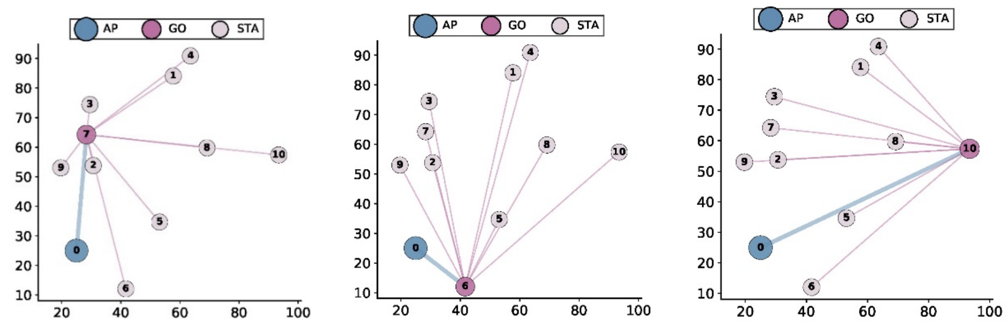


(a) (b) (c)

*Figure 3.9* Single GO selection (a) sub-optimal GO (b) optimal GO (c) worst GO.

*3.3.3.2 Multiple GO Selection*

For a large set of STAs, a single GO may not be capable to meet the demands of all STAs; hence, multiple GOs need to be selected to form several P2P groups. The multiple GO selection problem is illustrated in *Figure 3.10*. In multiple GO selection problem, the achievable link data rates between GO and AP impose an Upper bound on the amount of data that it can serve without delay or losses. Hence, this upper bound shall be applied as a constraint to formulate a constrained optimization problem for multiple GO selection. In a P2P group that connect N P2P clients to the GO, each device can roughly utilize 1=N of total transmission time and hence the channel capacity. Given the channel capacity for a single user *j* to GO $i$ is $U_{ij}$, the total GO throughput can be calculated as:

$$U_i^{DL} = \sum_{n=1}^{N} U_{ij}^{DL} \quad (11)$$

The objective of the optimization problem is a function that maximize the achievable channel capacity (or achievable data rates) over two hops i.e. AP-GO links ($U_i$) and GO-STA links ($U_{ij}$). The problem can be exactly formulated as:

$$\max\left\{\sum_{i=1}^{m} U_i Y_i + \sum_{i=1}^{n} \sum_{j=1}^{m} U_{ij} X_{ij}\right\} \tag{12}$$

Subject to:

$$\sum_{i=1}^{m} X_{ij} = 1 \quad \forall j \in C \tag{13}$$

$$\sum_{j=1}^{m} X_{ij} D'_j U_{ij} \leq (U_i Y_i - D'_i Y_i) \quad \forall i \in G, \forall j \in C \tag{14}$$

$$X_{ij} = 0,1 \quad \forall i \in G, \forall j \in C \tag{15}$$

$$Y_i = 0,1 \quad \forall i \in G \tag{16}$$

Constraint (13) ensures that each STA can only connect to a single GO. Constraint (14) ensures that the sum of effective throughput of STAs connected to a GO i shall be equal or less than the GO effective throughput to AP.

*3.3.3.3 GOs Selection for Multicast Applications:*

In typical Wi-Fi implementation, multicast traffic is sent at the lowest available rates in the AP. The lowest rate is chosen to ensure the reliability of the transmission as the multicast traffic is not acknowledged by the recipients. This leads to severe degradation of the achievable network throughput. In a classic downstream content distribution scenario, which involves contents delivery to a number of STAs, let denote the lowest link rate of an STA $j$ to a candidate GO $i$ by a new variable $r$.

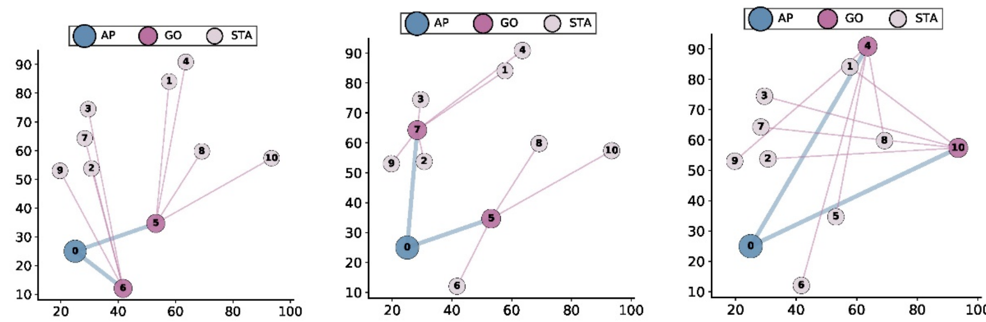


(a) (b) (c)

*Figure 3.10* Multiple GOs selection (a) sub-optimal (b) optimal (c) worst GO.

The proposed scheme aims to maximize the minimum transmit rate between the GO and STAs. The optimization problem is known as "Max-Min" problem. The modified Max-Min objective function is defined as:

$$\max(r) \tag{17}$$

Subject to:

$$\sum_{i=1}^{m} X_{ij} = 1 \quad \forall j \tag{18}$$

$$X_{ij} \le y_i \quad \forall i \in G, \forall j \in C \tag{19}$$

$$X_{ij} = 0,1 \quad \forall i \in G, \forall j \in G \tag{20}$$

$$Y_i = 0,1 \quad \forall i \in G \tag{21}$$

Constraint (19) specifies that each STA can connect to only one GO. Constraint (20) forces that every GO must connect at least one STA. The data rate to send multicast traffic over AP-GO link is selected based on the SNR of the link, whereas the constant multicast rate is used at the GO to send multicast traffic to the clients. The multicast rate is selected as the minimum rate supported by an STA, which is connected to the GO.

### 3.3.4 Simulation Results

To implement the proposed scheme, we deployed a single access point (AP) and $n =$ 10 Wi-Fi stations (STAs). Each node in the simulation model is identified by its $node\_id$. The AP ($node\_id = 0$) is positioned at (25, 25, 10), whereas the STAs ( $node\_id = i$; where $i = 1, 2, ...$) are randomly positioned at ($x_i$, $y_i$, $z_i$). The coordinates of STAs ($x_i$, $y_i$, $z_i$) are randomly chosen from Uniform and Gaussian (Normal) distributions. The positions of the AP and STAs remain fixed throughout the simulation. The optimization problems are solved in the convex optimization tool CVXPY [113, 114]. The proposed scheme explained in the previous section is evaluated using ns-3.

*3.3.4.1 Throughput Performance*

The proposed scheme is first evaluated for improvement in the overall network throughput. A network of 10 STAs is deployed where the STAs are randomly distributed in an area of 50x50 ($m^2$). The AP is located at position (25, 25, 10). In the first scenario, a single STA is selected as GO and the remaining STAs are connected to the GO to form a P2P group. The GO also associate to the AP to cross-connect the STAs to the AP. Three different simulations are performed. In each simulation, GO is selected using the Optimal, Sub-optimal and Worst selection schemes as defined in Section VII-A. In the second scenario, 20 STAs and 2 GOs are selected in each simulation using the Optimal, Sub-optimal and worst selection. The purpose is to evaluate the significance of the proposed scheme in dense networks using a higher number of GOs. Other parameters related to application, MAC and simulation parameters are given in Table 3.1.

The throughput gains for the three GO selection schemes are presented in Figure 3.11 considering single GO. It can be observed that the worst selection of GO can significantly degrade the throughput performance. As the worst GO is the one, which has poorest link quality to the AP as well as to the STAs in the network, it is using lower MCS values for transmissions. The throughput is also more random and varying over time. On the other hand, the proposed optimal selection provides a more stable and higher throughput over time. The sub-optimal selection is relatively higher than the worst case, whereas lower than the optimal selection. The average throughput of the network is 8.97 Mbps, 8.53 Mbps and 7.49 Mbps for optimal, sub-optimal and worst GO respectively.

Thus, the optimal selection of GO has the potential of achieving a throughput gain of 19.8% as compared to the worst selection. The throughput performance of the proposed scheme using multiple GOs is given in *Figure 3.12*. The throughput gain of the proposed scheme is more evident for multiple GOs. In this scenario, the throughput using the optimal and sub-optimal selection is increased by 1:8x and 1:6x as compared to the worst selection respectively.

Table 3.1 *Simulation parameters.*

| Parameter | Single GO | Multiple GOs |
|---|---|---|
| No. of APs | 1 | 1 |
| No. of GOs | 1 | 2, 3 |
| No. of STAs | 5, 10, 15 … 30 | 10, 15, 20 … 50 |
| Position of AP | Fixed | Fixed |
| Distribution of STAs | Random | Random |
| Transmit Power (dbm) | 16 | 16 |
| Transmit gain | 0 | 0 |
| Receive gain | 0 | 0 |
| Channel | 1 | 1, 6, 11 |
| Propagation Model | Lognormal | Lognormal |
| Transmit Antennas | 1 | 1 |
| Receive Antennas | 1 | 1 |
| MAC standard | 802.11n | 802.11n |
| Payload size (Bytes) | 1400 | 1400 |
| Application rate (Mbps) | 1 | 1 |
| Simulation Time (s) | 100 | 100 |

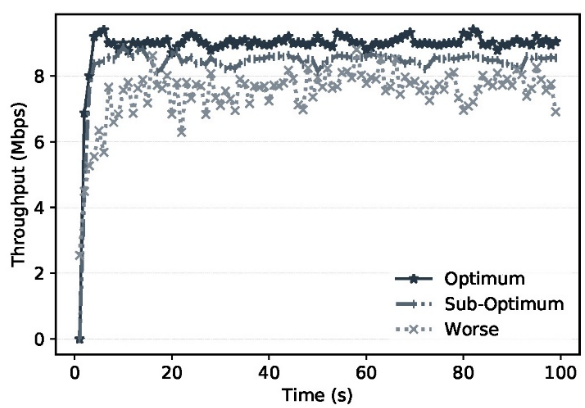


*Figure 3.11* Network throughput (Mbps) using a single GO.

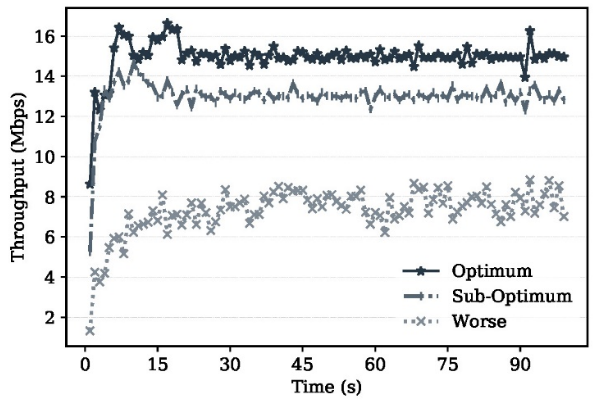


*Figure 3.12* Network throughput (Mbps) using multiple GOs.

*3.3.4.2 Throughput versus Number of STAs*

The performance of the proposed scheme is further investigated by changing the number of users in the network. When the number of STAs in the network is increased, the network performance is impacted in two ways. Firstly, the increase in the number of STAs increases the traffic volume in the network, which will increase the throughput to some extent. However, as the network becomes saturated, the throughput begins to decrease. The point of interest in this evaluation is the time duration of non-saturation. If the GO can maintain better connection qualities over all links, higher data rates are used, and saturation can be avoided for relatively a higher number of STAs.

In *Figure 3.13*, the performance of the proposed optimal and sub-optimal selection is compared against the worst selection of GO. The number of STAs in the network is increased from 5 to 30 and throughput is computed. It can be observed that the throughput decreases in the worst GO case when the network has more than 10 STAs.

The throughput is minimum at 30 STAs, which indicates a congestion state. In comparison, in the sub-optimal GO selection, the throughput increases significantly, until the network has 15 STAs and remains nearly constant until 20 STAs. A slight reduction in throughput is observed after the number of STAs increases from 20 to 30. The performance of the optimal selection provides the highest throughput gain, as expected, for all number of STAs than the sub-optimal and worst cases. For 5 to 15 STAs, the difference in throughput for optimal and sub-optimal selection is little, however, it increases afterwards. The optimal throughput decreases when the number of STAs decreases than 20. The rationale behind the better performance of the optimal selection scheme at a relatively higher number of STAs is the capability of the GO to attain higher data rates for a large subset of STAs connected to it. The capability is relatively less in sub-optimal selection.

The better performance of the optimal GO selection is evident in *Figure 3.13*; however, it is further investigated using more than one GOs. Intuitively, if a single GO optimally selected improve the throughput gain due to the capability to attain higher data rates, then the performance should become much better with an increased number of GOs. More precisely, while increasing the number of STAs, the higher number of GOs shall push the saturation point towards the right in a similar illustration. To verify the impact of the higher number of GOs in the network of different size, the proposed optimal selection scheme is evaluated at 1, 2 and 3 number of GOs, while increasing the number of STA from 10 to 50. The results are presented in *Figure 3.14*. It can be observed that the higher number of GOs not only increases the throughput but also pushes the saturation point towards a higher number of STAs.

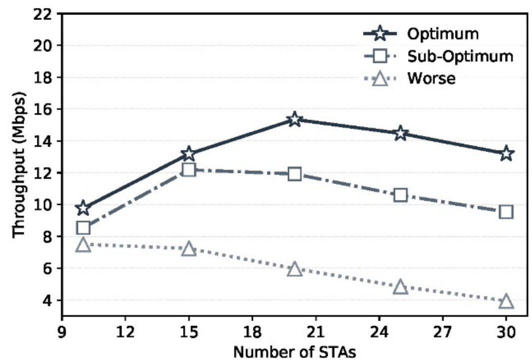


*Figure 3.13* Average network throughput versus the number of stations.

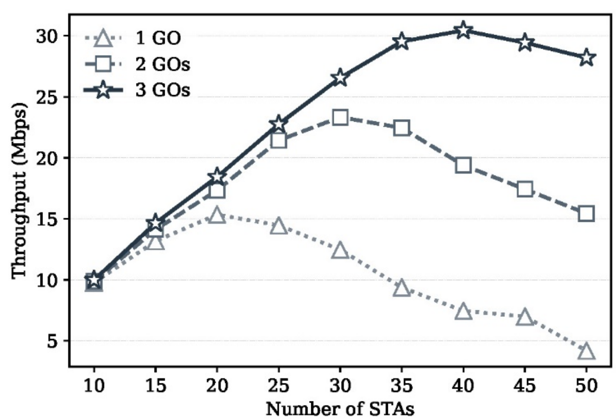


*Figure 3.14* Average network throughput versus the number of stations.

*3.3.4.3 Throughput versus STAs Distribution*

In real Wi-Fi deployments, user's distribution varies in different scenarios. To show the impact of user distribution on the performance of the proposed scheme, the three GO selection schemes are first evaluated with STAs positions following a uniform random distribution. Furthermore, three independent scenarios with area sizes of 50x50, 70x70 and 100x100 ($m^2$) are simulated and throughput is computed to validate the performance of the proposed scheme. The results are presented in *Figure 3.15*.

It can be observed that the proposed scheme using optimal selection produces the highest throughput gains in all scenarios as compared to the sub-optimal and worst selection schemes. This validates the benefit of the proposed scheme. Another observation is that the throughput gains decreases with increasing the area size. The reason behind this is that, by increasing the size of the area, the inter-STAs distances increases and consequently the attained data rates are decreased. To further quantify the results, the average throughput gains in all scenarios are computed. The results report the optimal selection achieves average throughput gains of 6.5% and 17.5% as compared to the sub-optimal and worst selection respectively. Similarly, the sub-optimal selection scheme achieves 10.3% higher throughput gain as compared to the worst selection scheme. The proposed scheme is then evaluated with STAs positions distributed as a Gaussian random variable. Thus, a higher number of STAs are located closer to the AP. Three scenarios with different values of the Scale-parameter i.e. 50, 70 and 100 are deployed. The simulation results are presented in *Figure 3.16*. The analysis of results shows that the optimal selection achieves average throughput gains of 7.9% and 19.8% as compared to the sub-optimal and worst selection respectively. Similarly, the sub-optimal selection achieves 11.1% higher throughput gain as compared to the worst selection of GO.

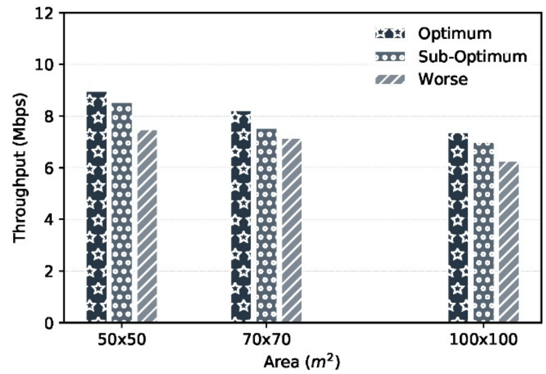


*Figure 3.15* Network throughput using the uniform distribution of STAs.

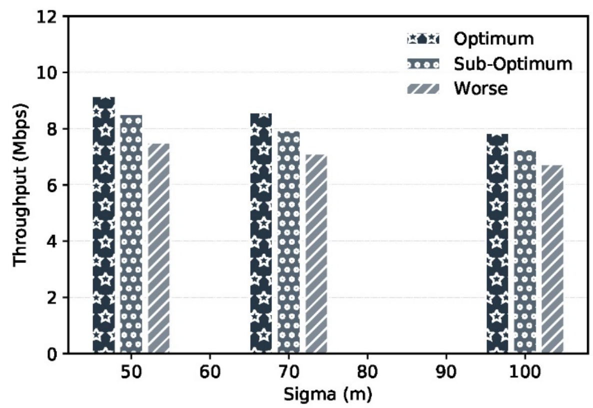


*Figure 3.16* Network throughput using the normal distribution of STAs.

*3.3.4.4 Throughput versus Packet Loss using Multicasting*

The proposed scheme for GO selection using multicast traffic is explained earlier. Multicasting can increase throughput dramatically, however at the cost of packet loss. The proposed scheme aims to benefit from the multicasting to achieve a higher throughput without compromising packet loss. The performance of the proposed scheme is first evaluated by computing the throughput gains for a single GO using unicast and multicast traffic in two different scenarios. In the first scenario, the positions of STAs are distributed as a uniform random variable, whereas in the second scenario, the positions of STAs are following Gaussian distributions. The throughput gains are computed for a different number of STAs and results are presented in *Figure 3.17* and *Figure 3.18*. The dramatic throughput for multicast traffic as compared to unicast traffic is evident in both figures. It is a very likely result as multicasting can achieve a similar throughput performance since all STAs in the multicast group receive the same data. The relative benefit of the proposed scheme using multicast traffic increases as the number of STAs increases in the network. The only reduction in the throughput is the packets lost at some STAs which shall reflect in the figures. The analysis of throughput gains in *Figure 3.17* shows that the proposed scheme with multicast can increase throughput by 8% as compared to unicast.

The throughput gain increases by 2.1x when the number of STAs increases to 30 STAs. Similarly, *Figure 3.18* show throughput gain of 1.97x for 30 STAs, when the positions are Gaussian distributed.

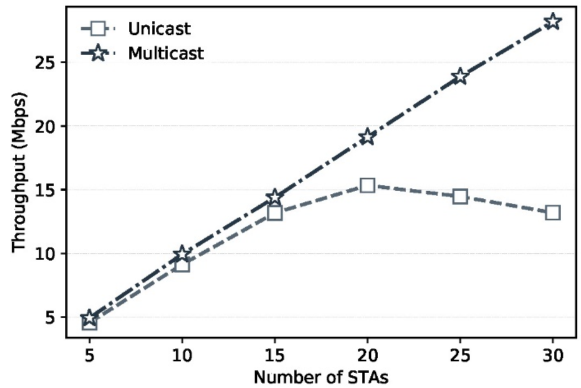


*Figure 3.17* Network throughput with multicast (STAs uniformly distributed).

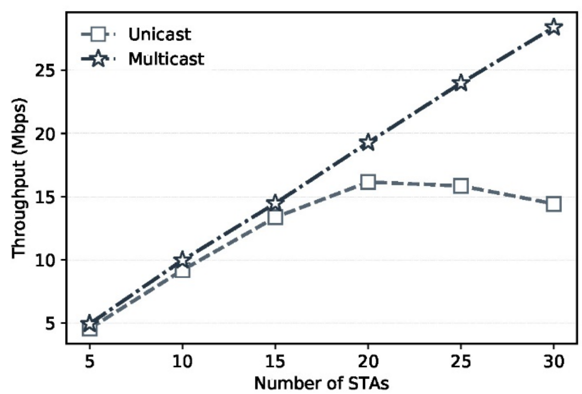


*Figure 3.18* Network throughput with multicast (STAs normally distributed).

In Figures 14 and 15, the packet loss ratio (PLR) of the proposed scheme using unicast and multicast traffic is evaluated using positions of STAs as uniformly and Gaussian distributions respectively. The figures show an incredibly higher PLR (%) for multicast traffic as compared to unicast traffic. The rationale behind high packet loss is well known in the literature, which is caused by lack of acknowledgements in multicasting. However, the packet loss ratio is significantly controlled for a lower number of STAs (i.e. 2.8% and 2.3% for uniform and Gaussian distributions respectively).

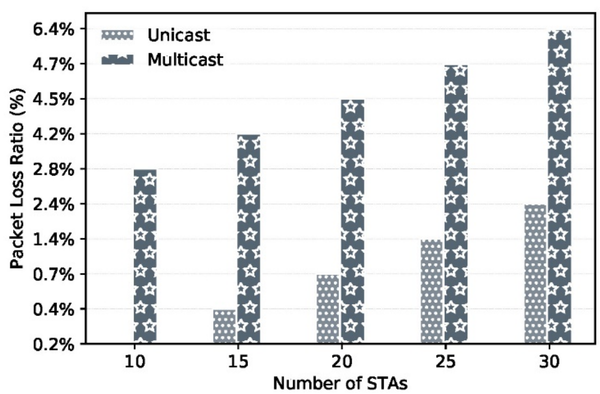


*Figure 3.19* PLR using unicast and multicast traffic (STAs uniformly distributed).

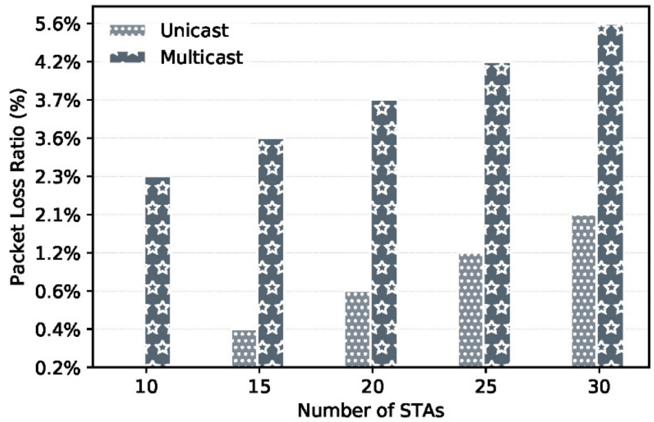


*Figure 3.20* PLR using unicast and multicast traffic (STAs normally distributed).

# CHAPTER 4 : UAV-AIDED WI-FI NETWORKS

The use of unmanned aerial vehicles (UAVs) in future wireless networks is gaining attention due to their quick deployment without requiring existing infrastructure. Earlier studies on UAV-aided communication consider generic scenarios and very few studies exist on the evaluation of UAV-aided communication in practical networks. The existing studies also have several limitations and hence an extensive evaluation of the benefits of UAV communication in practical networks is needed.

In this chapter, we propose a UAV-aided Wi-Fi Direct network architecture. In the proposed architecture, a UAV equipped with a Wi-Fi Direct Group Owner (GO) device, the so-called Soft-AP is deployed in the network to serve a set of Wi-Fi stations. We propose to use a simpler yet efficient algorithm for the optimal placement of the UAV.

Wi-Fi Direct lack efficient group formation mechanism in the standard Wi-Fi Direct to quickly deploy a Wi-Fi Direct network [108, 115-117]. The efficient group formation involves the selection of the most capable device in the network as the Group owner (GO) or Soft-AP to improve the network throughput which extends the coverage by connecting more devices and increase network lifetime. The selection of the best candidate device as GO and enhancement of group formation scheme is proposed in [118] and [108] respectively.

These and other state-of-the-art proposals which focus on the efficient group formation and intra-group communication aim to select the best device from a pool of Wi-Fi Direct enabled devices as the P2P GO. However, although the selected GO is instantly capable to meet the requirements of the network, it is a user-owned device

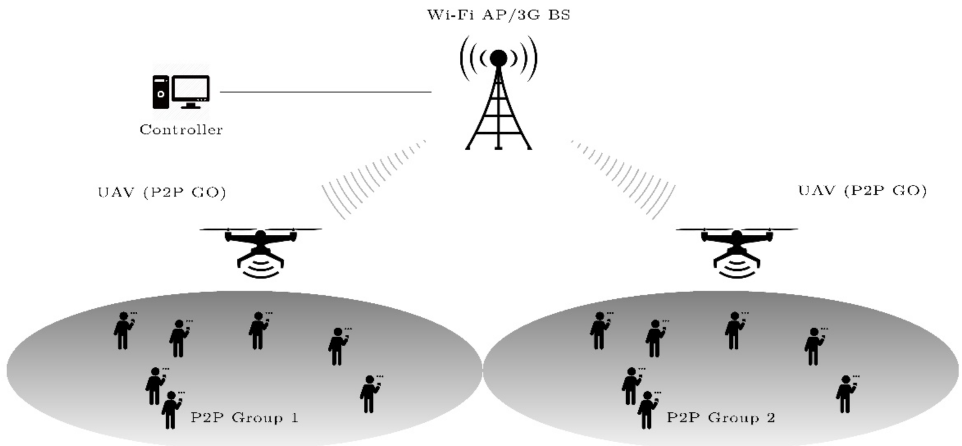


*Figure 4.1* UAV-aided Wi-Fi direct network architecture.

and subject to mobility. The mobility of the user handling the GO device can cause significant disruption of the group connections, achieve poor throughput if it moves to low SNR regions and has battery constraints. Hence, a logical desire is that the GO device shall be owned and fully controlled by the network to cope with these challenges.

Recently, researchers have proposed the use of UAVs (Unmanned Aerial Vehicles) in future communication networks [54], [119]. UAVs in communication networks are favoured for their advantages such as reduced cost due to on-demand operation, more swift and flexible deployments, and controlled mobility [120]. The use of UAVs as network relay has been proposed in [54, 55, 121]. Similarly, UAVs as a means to extend network coverage has been proposed in [119, 122]. Earlier studies on UAV-aided communication focus on the UAV placement and trajectory optimization problems in generic network scenarios. Very few studies are found in the literature that study the UAV-aided communication in practical networks such as Wi-Fi, cellular and IoT networks. The existing studies on UAV-aided Wi-Fi networks have several limitations. Hence, it motivates us to further investigate the potential benefits of UAV aided communication in Wi-Fi and other short-range (SR) communication networks.

### 4.1 UAV-Aided Wi-Fi Direct Architecture

Consider the case where a P2P GO is installed over a UAV that connects several Wi-Fi clients (STAs) to form a single P2P Group. All the STAs are mobile and hence they randomly move in the network. The random movement of the STAs tends to increase the distance between the UAV and the STAs large enough so that to cause de-association of the STAs from the network. To avoid STA's de-associations and maintain a relatively strong network connection to all nodes, it is desired that the P2P GO shall be placed in a location, which reduces the distances to all Wi-Fi stations. Furthermore, when the STAs move around and change their relative positions, the UAV shall automatically re-calculate the new optimum location and relocate immediately. Two distinct cases are discussed:

#### 4.1.1 UAV Moving in 3D Space

Consider the scenario in *Figure 4.2*; a number of STAs are deployed randomly in the Euclidean plane. A UAV initially located at the position $C_{(x,y,z)}$ can move freely in 3D space. This scenario is common and can be applied in several applications i.e. Internet connectivity and content distribution in large conference halls and exhibitions centres.

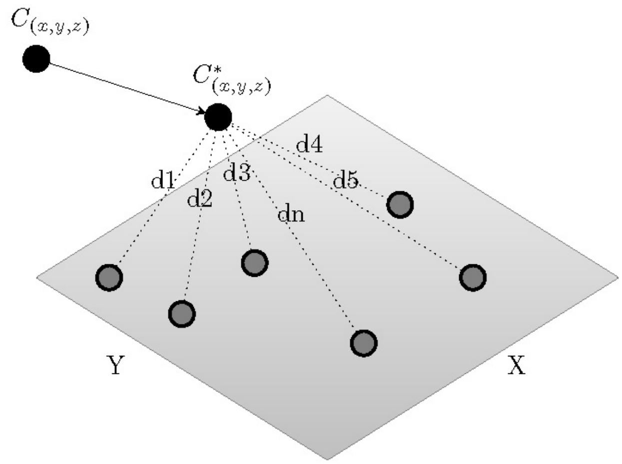


*Figure 4.2* Placement of UAV in 3D space.

The optimal placement of the UAV which involves the minimization of the sum of distances to a set of points is a classical problem in operational research and location theory known as Weber Problem [123]. In the proposed model, initially, all the STA's are randomly placed at locations $p_i = (x_i, y_i, z_i)$, where $i$ is the index of STA. The initial position of the P2P GO is $C_{(x,y,z)}$. Our goal is to find an optimal position $C^*_{(x,y,z)}$ in space for the P2P GO to maintain a fair connection with all STA's and achieve higher aggregate throughput at the cost of less energy consumption. The Euclidean distance between the UAV and each STA is calculated in Equation (22) [124]:

$$d(C,p) = \sqrt{(C_x - P_x)^2 + (C_y - P_y)^2 + (C_z - P_z)^2} \tag{22}$$

Where, $C_x$ , $C_y$ and $C_z$ are the coordinates of the P2P GO, and $P_x$, $P_y$ and $P_z$ are the coordinates of an STA $P_i$ in 3D space. The Euclidean distance in Equation (22) can be modified to compute the weighted Euclidean distance in Equation (23) [125] to address the axis scales.

$$d'(C,p) = \sqrt{w[(C_x - P_x)^2 + (C_y - P_y)^2 + (C_z - P_z)^2]} \tag{23}$$

The equation (23) is also referred to as "weighted l2-norm" or more generally "klp-norm" in [126] where $k$ refers to the weight $w_i$ . A minisum location model using weighted Euclidean distances between P2P GO and each station is given in Equation (24) [127]:

$$f(C) = \sum_{i=1}^{n} w_i d_i(C, p_i) \tag{24}$$

Where, $W_i$ is the weight assigned with each station. For more distant stations, the weights $W_i$ can be assigned higher values so that the UAV can be moved closer to serve better these stations. The equation (24) is known as the Weber Equation. To find the optimum location for the UAV is the same as to reduce the sum of distances to all STAs. The optimum location finding implies the minimization of the Weber Equation (24) and this distance minimization problem is called the Weber problem (also known as the Fermat-Weber problem). Weber problem is an unconstrained optimization problem which can be written as in Equation (25) [125]:

$$\begin{aligned} &\min f(C) = \sum_{i=1}^{n} w_i d_{i(C,p_i)} \\ &s.t. \\ &\qquad \{x, y, z\} \in \mathbb{R}^n \end{aligned} \tag{25}$$

A well-known approach to solve this optimization problem in Equation (25) is known as Weiszfeld algorithm, presented in Algorithm (1). The Weiszfeld algorithm is an iterative approach based on the first-order necessary conditions for a stationary point of the objective function. The convergence of the Weiszfeld algorithm has been proved in [128]. It is worth mentioning that the Weiszfeld algorithm has a serious implication, if any of the $P_i$ accidentally lands in a vertex C. However, it can be solved with a simpler modification as proposed in [129].

### 4.1.2 UAV Moving along a Straight Path

In the last section, we assumed that the UAV can move freely in space along any direction and we aimed to find a point (C*) in 3D space which has the minimum sum of distances to all Wi-Fi stations. In this section, we consider a special case, where the UAV cannot move freely. Instead, the movement of UAV is restricted to only a straight path. The straight path represents a line in Euclidean space and is illustrated in *Figure 4.3*. A practical application of UAV mobility restricted to a fixed straight path can be UAV deployments in large indoor exhibition centres, conference halls and sports arena. The UAVs movement is usually restricted due to several barriers and hence these can be safely deployed to move along hazard-free straight paths to avoid collisions with other objects.

The optimal placement of UAVs with path barriers in the aforementioned example can be formulated as a special case of the unconstrained optimization problem in Equation (25), which is referred to as an optimization problem with distance constraints i.e. with a barrier or forbidden region. Constrained optimization problems

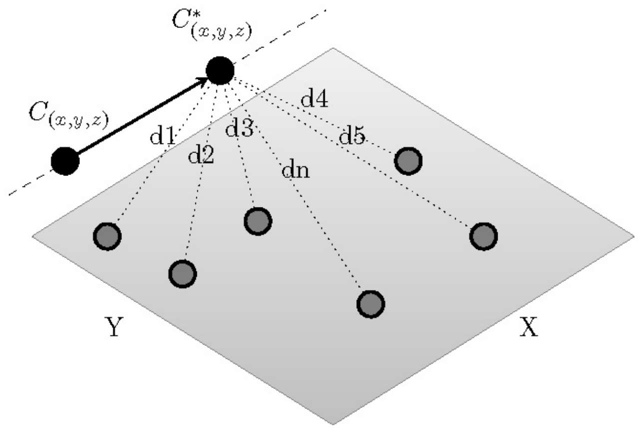


*Figure 4.3* Placement of UAV along a straight path.

with barriers are studied in [130, 131]. To find the optimal point over the straight path that minimizes the sum of distances to all points in the networks, we are using the modified Weiszfeld algorithm proposed in [128].

The proposed method uses "Weighted Euclidean distance" between STAs, which is slightly different from Equation (23). The weights assigned to each axis is set equal to the inverse of the variance or the allowed scale to move along the respective axis as given in Equation (26) [125].

$$d'(C,p) = \sqrt{w_x(C_x - P_x)^2 + w_y(C_y - P_y)^2 + w_z(C_z - P_z)^2} \tag{26}$$

### 4.1.3 Multiple UAVs Placement

In Sections 4.1.1 and 4.1.2, we discussed the problem of finding an optimum location for a single UAV. However, in most practical scenarios, such as dense networks in sports stadiums and large exhibition centres, multiple UAVs have to be deployed to form several network clusters. In this section, we discuss the case of multiple Wi-Fi

Direct networks (called as P2P groups) as shown in *Figure 4.1* using UAVs each equipped with a P2P GO device. We keep the same assumption as in the case of single UAV, that the Wi-Fi stations are initially associated with the GO. However, due to the mobile nature of the stations, the deployed UAVs have to frequently move to the optimum locations to maintain strong connections. This problem is primarily studied as "multiple facility location" problem in location theory [132], and most recently known as clustering [96, 97] in machine learning. The multiple UAVs placement problems can be solved using two different approaches. Firstly, by considering each P2P group independently and placing a UAV in each P2P group, using the single facility location problem as discussed in Section III-A and III-B. This approach is significant if the requirement is to avoid connection loss for the stations. However, if the temporary network connection loss is not a problem; a more useful approach is to use a combined approach to place multiple UAVs at optimum locations. The logical benefit of the second approach is that each STA is independently allocated to the closest UAV than to the rest of the UAVs in the network.

The problem of placing k UAVs in optimum locations is similar to forming $k$ clusters or P2P groups. Given $P = p_1, p_2, .. p_n$ Wi-Fi stations and $k$ k UAVs, the multiple facility location problems are to determine the locations $C^* = C^*{}_1, C^*{}_2, .. C^*{}_k$ for the UAVs and the allocations of $X = X_1, X_2, ..X_n$ stations to each UAV, such that the total sum of distances of each station to its assigned UAV is minimized. It can be represented mathematically [133]:

$$\min_{C_1, C_2, .. C_k} \min_{X_1, X_2, .. X_k} \sum_{j=1}^{k} \sum_{p_i \in X_k} w_i \left\| C_j - X_j \right\| \tag{27}$$

The optimization problem given in Equation (27) can be solved using k-median clustering [134]. The k-median clustering algorithm can be used to partition the set of Wi-Fi stations into k clusters and finding the optimal locations for the UAVs in each cluster. The k-median clustering process is given in Algorithm 4.1.

### 4.2 System Model

To evaluate the performance of the proposed scheme, four distinct scenarios are created. In *Figure 4.2* and *Figure 4.3*, the placement of single UAV is controlled in 3D and 1D space respectively using Algorithm 1. The proposed placement of the UAV in both cases is expected to improve network throughput and coverage while simultaneously achieve energy efficiency. To evaluate the performance of the proposed scheme, two other typical use cases are modelled. In the first case, the P2P GO is kept fixed, which is equivalent to a fixed access point (AP) in legacy Wi-Fi. In the second case, the P2P GO is implemented as a randomly moving device in a 3D space equivalent to a user-owned P2P GO device offering network connections. The four distinguished cases: (i) fixed mobility, (ii) random mobility, (iii) controlled mobility in 3D space and (iv) controlled mobility along a straight path (1D) are modelled. The performance of the proposed scheme is further investigated with the increasing number of UAVs (1, 2 and 3) with their optimal placements in 3D space and 1D space respectively using Algorithm 1.

Algorithm 4.1: UAVs Placement in 3D/1D Space.

Inputs : $\sum_{i=0}^{n} \mathrm{p_i}[\mathrm{x,y,z}], \sum_{k=0}^{K} \mathrm{C_i}(\mathrm{x,y,z})$

Outputs : $\mathrm{C_1}^*, \mathrm{C_2}^*, ...\mathrm{C_k}^*, \mathrm{X_1}, \mathrm{X_2}, ..\mathrm{X_k} \longleftarrow X$ is devices assigned to C

SWITCH j do

case j=1

initialize cluster centroids at $\mathrm{C_j}(\mathrm{x_j}, \mathrm{y_j}, \mathrm{z_j})$

while

error is too small do{

$$\mathrm{d}_i^t = \left\| p_i - C^t \right\|^2$$

$$C^{t+1} = \frac{\sum_{i=1}^{n} w_i a_i / d(p_i, C)}{\sum_{i=1}^{n} w_i / d(p_i, C)}$$

$$error = \left\| C^{t+1} - C^t \right\|^2$$

*end while*

*return* $C^*_{(x,y,z)}$ $\leftarrow$ Single Location

*case* $j \geq 2$

Repeat untill Convergence: {

FOR EACH $i$, *set*:

$$C^{*(i)} = \arg\min \left\| p^{(i)} - C_i \right\|^2$$

### 4.2.1 Single UAV

In this scenario, thirty (30) Wi-Fi STAs are placed in the 300 x 300 ($m^2$) grid. The UAV is initially placed at position (100, 100, 15) and then it is allowed to move or remain fixed according to the mobility model. In the fixed UAV scenario, the UAV remained fixed throughout the simulation at position (100, 100, 15). This is identical to the fixed access point in legacy Wi-Fi networks. In the random mobility (unrestricted) UAV scenario, the UAV is allowed to move freely in the network during the simulation. This is identical to the P2P GO being a user-owned device.

In the controlled mobility (3D) case, the UAV is allowed to move in 3-dimensional space; however, the mobility is controlled i.e. after each time T, the UAV is moved towards the new position computed using Algorithm 1.

Lastly, in the controlled mobility (1D) case, the movement of the UAV is restricted to a single dimension (X-axis) i.e., movement along a straight path (X, 100, 15). Furthermore, the movement along the X-axis is controlled using Algorithm 1.

### 4.2.2 Multiple UAVs

Two distinct scenarios are considered with two UAVs and three UAVs. In both cases, thirty (30) Wi-Fi stations are placed in the 300 x 300 $m^2$ grid. In the first scenarios, the two UAVs are initially placed at positions (100, 100, 15) and (150, 101, 15) whereas, in the second scenarios, a third UAV is placed in the network at (200, 102, 15) and then their positions are updated using the proposed scheme. Similar to the single UAV case, the placement of all UAVs is controlled using Algorithm 1.

## 4.3 Simulation Results

The system model described in Section 4.2 is evaluated in network simulator-3 (ns-3) [135]. We choose ns-3 for several reasons. Firstly, ns-3 is a well known and de-facto standard for performing networks simulations. Secondly, ns-3 is open-source software and it provides full access to the protocol stack. It is enriched with trace sources, which provide access to low-level protocols and network parameters that are usually not accessible in other network simulators. Additionally, ns-3 based simulations are more realistic due to its Linux-like protocol stacks.

We used the Minstrel rate control algorithm [111] which is the default rate control algorithm in the Linux kernel. The minstrel rate control algorithm is originated from MadWifi project [136]. The project was initiated to develop Linux drivers for Wireless LAN cards based on Atheros chipsets. The Minstrel algorithm keeps track of the probability of successfully sending a frame of each available rate. Minstrel then calculates the expected throughput by multiplying the probability with the rate. This approach is chosen to make sure that lower rates are not selected in favour of the higher rates (since lower rates are more likely to have higher probability).

In Minstrel, roughly 10 percent of transmissions are sent at the so-called look-around rate. The purpose of using the look-around rate is to force the algorithm to try a higher rate than the currently used rate, thus automatically selecting higher data rates when the SNR increases. To evaluate the energy performance of the network, we use the "Wi-Fi Radio Energy Model" of ns-3 which computes the energy consumption of a Wi-Fi interface in each state of the PHY layer (*Idle*, *Busy*, *Transmit*, *Receive*, *Channel Switching*, *Sleep, Off*). The default values of these parameters are defined in [137]. The simulation configurations listed in Table 4.1. We used three performance metrics over which the performance of the proposed scheme is evaluated, i.e. the number of associated stations, network throughput and energy efficiency. The performance over these metrics is evaluated and separately presented in the subsequent subsections.

### 4.3.1 Number of Associated Stations

A primary benefit of the proposed scheme is to increase the number of associated stations and maintain fair connections to all clients by moving the UAV to the optimal location.

Table 4.1 *Simulation parameters.*

| **Parameter** | **Value** |
|---|---|
| Area ($m^2$) | 300 x 300 |
| No. of UAVs | 1, 2, 3 |
| No. of STAs | 30 |
| STAs mobility Model | Random waypoint |
| UAVs mobility model | Fixed, Random, Proposed Algorithm |
| WLAN standard | 802.11n (5GHz) |
| Propagation Model | Log-distance propagation loss model |
| Application Type | CBR |
| Payload size | 1462 Bytes |
| Application data rate | 1024 Kbps |
| Battery model | Wifi Radio Energy Model of ns-3 |
| Simulation duration | 600 seconds |

As the network consists of mobile nodes, the network topology, as well as the parameters, are always changing. The quality of the wireless signal (i.e. SNR) degrades as the stations move away from the GO. However, the GO constantly moves to the optimal location determined by the proposed scheme. When the UAV moves to the new optimum location, the distance to each STA is reduced, thus avoiding stations to de-associate from the GO. The proposed scheme does not guarantee 100% STAs association; however, the association ratio can be much improved using the proposed scheme.

The performance of the proposed scheme is evaluated to investigate the STAs association as shown in *Figure 4.4*.

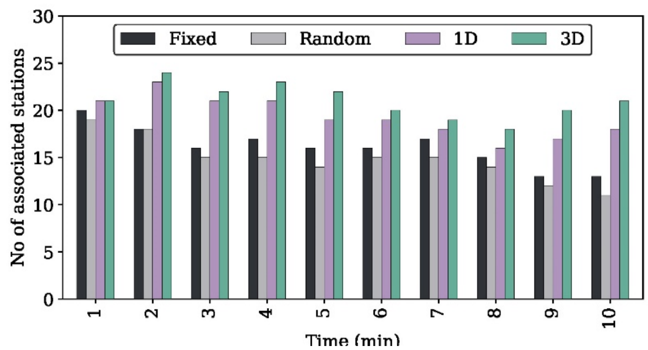


*Figure 4.4* Number of associated stations (single UAV).

Fig. 5 shows that the number of stations associated with a single GO. The STAs are initially placed randomly following a uniform distribution whereas the UAV is placed at (100, 100, 15). The STAs in the communication range connects to the GO whereas some of the STAs outside the coverage of UAV are not associated. The STAs in all cases are randomly moving which changes the network topology at different instants of time. In the case of fixed GO, the STAs are frequently de-associated when they move far away from the GO, reducing the number of associated stations. At the same time, other distant STAs, initially not associated with the GO, may come closer and connect to the GO. The frequent movement of STAs is causing unpredictable association of STAs. A similar behaviour can be observed in the case of randomly moving GO where both the GO and the STAs are moving. On the other hand, the proposed scheme controls the movement of the UAV such that it periodically moves the UAV to an optimal location where the distance to all STAs is minimized. As the objective is to minimize the distance to all STAs, the distance to some STAs initially closer may increase. However, the overall STAs association improves. In the case of UAV movement over a straight path (1D), the proposed scheme cannot place the UAV at the optimal location due to mobility constraint; however, it tends to move the UAV to a sub-optimal location to reduce distances to the STAs. It can be observed in *Figure 4.4*, that the STAs association ratio using such proposed scheme with restricted mobility is still better than the fixed and randomly moving GO cases. The analysis of the simulation results shows that on average, the GO moving in 3D space can maintain 13% more connectivity than Fixed GO and 23% more than the randomly moving GO. In the case of GO moving in 1D; the values are reduced to 8% and 18% respectively. The stations association in the network in case of multiple UAVs is investigated by deploying a different number of UAVs (1, 2 and 3) in the network. The aim is to further strengthen the claim of the proposed scheme by investigating the impact of using multiple UAVs.

The simulation results of STAs association with multiple UAVs using the proposed scheme in 3D and 1D mobility are reported in *Figure 4.5* (a) and (b) respectively.

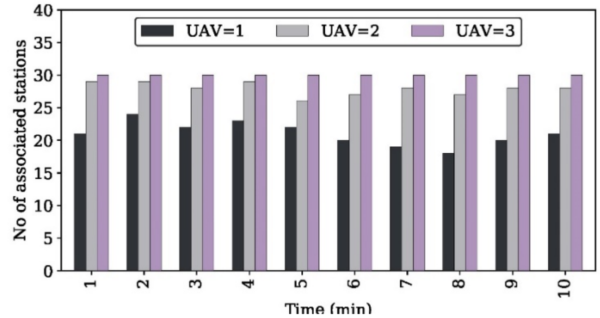


(a)

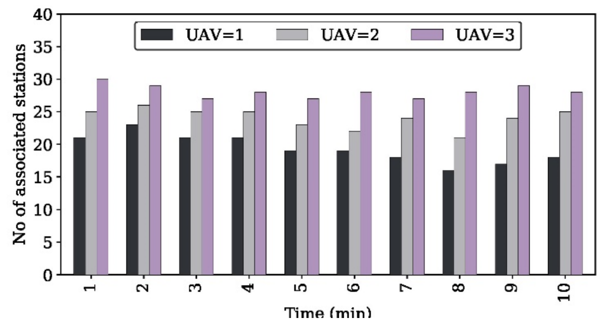


(b)

*Figure 4.5* Number of associated stations using multiple UAVs (a) 3D (b) 1D.

It can be easily observed in *Figure 4.5* that the increasing number of UAVs in the same network can significantly improve the connectivity of network devices. The improvement in UAVs with 3D placement is expectedly greater than with 1D placement. The average association of STAs, using 3D movement is increased by 12% and 28% for increasing number of UAVs to 2 and 3. For 1D movement, the percentage improvement is reduced to 9% and 24% for 2 and 3 UAVs respectively. The presented results were expected, as increasing the number of UAVs can increase the chance of STAs to connect to one of the 2 (or 3) UAVs deployed in the network.

### 4.3.2 Network Throughput

Network throughput is a widely used metric to evaluate network performance. Increasing the received power or more specifically the received SNR directly increases the transmission throughput and consequently improve the application-layer performance [58]. The UAV-aided network is simulated to evaluate the network throughput in Megabits per seconds (Mbps). *Figure 4.6* illustrates the total network throughput using the four distinct scenarios i.e. fixed UAV, randomly moving UAV, proposed scheme with 3D placement and proposed scheme with 1D placement.

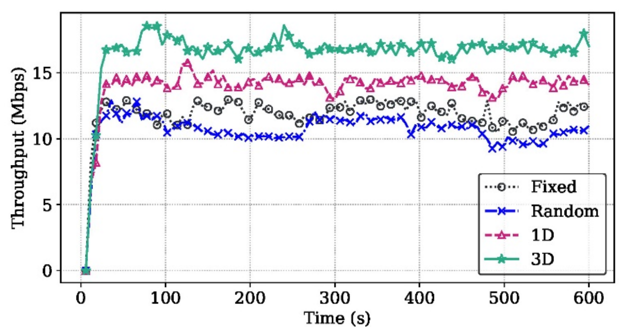


*Figure 4.6* Network throughput (single UAV).

By inspecting *Figure 4.6*, it can be observed for all the four cases that the throughput increases abruptly when the simulation starts in the first couple of seconds. The reason for this increase is that STAs in the coverage of UAV connect in this time and start receiving data. In the case of fixed and randomly moving cases, when all the STAs are connected, the throughput does not increase further. There are slight variations in the instantaneous network throughput that indicates the connection status or the link quality of one or more STAs is changed. When STAs are disconnected, the throughput is decreased and vice versa. Similarly, one or more distant STAs with poor links quality can also vary the throughput. In the case of the proposed scheme (3D and 1D), at time 10 seconds, the UAV has moved to the optimal location in the network that further increases the throughput. The rationale behind the high throughput in the proposed scheme is that by reducing the distance between the UAV and the randomly moving stations, higher SNR values can be achieved, which directly map with the selection of high MCS index, thus increasing higher data rates. Additionally, the selection of higher SNR depicts the quality of the wireless channel that reduces the number of retransmissions to further improve the throughput. It can also be noticed in the graph, that the improvement in throughput is relatively less in the case of UAV moving along a straight path (1D) as compared to the 3D case. The reason is that in the 1D case, the proposed scheme only ensures sub-optimal placement of the UAV. This causes an increase in the throughput relative to fixed and random use cases, but throughput is still less than the 3D case. Another clear observation in *Figure 4.6* is the relatively fewer variations in the network throughput using the proposed scheme (3D and 1D). The reasons for the relatively more constant throughput using the proposed scheme is that STAs association, as well as the link quality, is maintained when the UAV is placed at the optimal location. The retransmissions are also reduced which further smooth the throughput. The analysis of the results obtained shows the significance of the proposed scheme over both 3D and 1D placement of GO. The throughput using the proposed scheme relative to fixed GO is increased by 35% and 15% for 3D and 1D deployments respectively. The throughput relative to randomly moving GO is increased by 54% and 31% using the proposed scheme with 3D and 1D movement of GO respectively.

We further investigated the impact of increasing the number of UAVs on network throughput. We deployed a different number of UAVs (1, 2 and 3) in the network and computed the network throughput with the same simulation parameters. The obtained results were analyzed that show that by increasing the number of UAVs to 2 and 3, the throughput is increased by 21% and 34% in 3D case, and 28% and 35% in 1D case.

It is worthy to note that the throughput gain in the 1D case is greater than the 3D case. However, it should not mislead the reader that the proposed scheme with 1D placement outperforms 3D placement. Instead, the reason for this contrasting behaviour is that the gain is relative to a single UAV case and the increasing number of UAVs with 3D placement does not connect more stations as compared to 1D placement. However, the actual throughput is still higher in the 3D case for an equal number of UAVs as depicted in *Figure 4.7*.

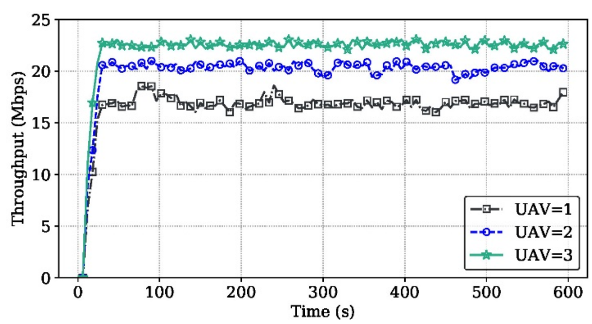


(a)

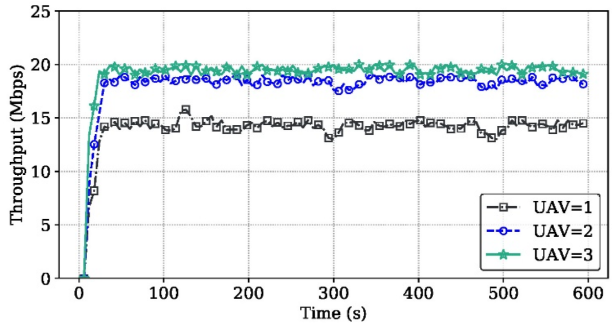


(b)

*Figure 4.7* Throughput versus no. of UAVs (a) 3D (b) 1D.

### 4.3.3 Energy Efficiency

In Wi-Fi networks, energy efficiency can be achieved in several ways: Firstly, by reducing the transmit power of the radio transmitter at the sending station; secondly, by using higher data rates at constant transmit power; and lastly by reducing the number of retransmissions and packet loss. Wi-Fi Direct offers additional algorithms known as OppPS and NoA to further save energy. The proposed scheme in Section III constantly reduces the sum of distances between the GO and the STAs to achieve a higher signal to noise ratios (SNR). With higher SNR, higher transmission rates can be achieved, and the retransmissions of frames are significantly reduced. Ultimately, the energy consumed to transmit the user data can be reduced. To evaluate the energy efficiency of the proposed scheme, we used the metric called "energy consumed per 1 megabit of user data" measured in Joules. The proposed metric precisely calculate the energy consumed in the transmission of the actual user data. A similar metric "energy consumed per frame" is used in [138]. The energy performance of the proposed scheme is evaluated and compared against the fixed and randomly moving GO. The results are shown in *Figure 4.8*.

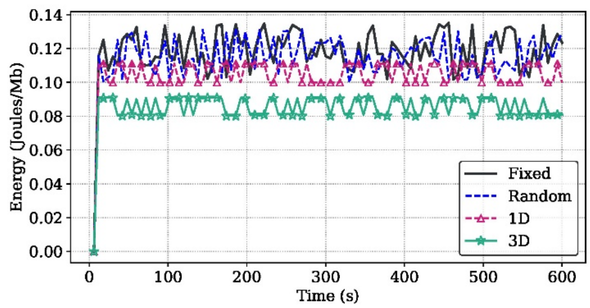


*Figure 4.8* Energy efficiency (single UAV).

The energy consumption increases abruptly in the first few simulation seconds despite the fact that more control frames are communicated in the STAs association phase. However, the cumulative size of the control frames is less, and the impact is negligible in terms of the proposed metric. When all the STAs in coverage associated with the GO, the energy consumption does not vary abruptly, however, variations can be observed throughout the simulation duration. The variations for fixed and randomly moving GOs are higher as compared to that of the proposed scheme. To the best of our understanding, the higher variations in the fixed and random cases are caused by more frequent changes in data rates and the higher number of re-transmissions caused by low links quality. In contrast, relatively fewer variations in energy consumption are observed when the proposed scheme is used. We believe that the Variations can be further reduced if the STAs connected to the GO have similar quality of connections to the GO. It can be logically concluded that the proposed scheme is more efficient in saving energy than fixed GO as well as randomly moving GO. Furthermore, the energy efficiency is more evident in the case of 3D placement of P2P GO, whereas little improvement is achieved for the GO restricted to move along a straight path. The detailed analysis of the obtained results shows that the energy consumption using the proposed scheme as compared to the fixed GO is reduced by 30% and 14% for 3D and 1D deployments respectively. Furthermore, the energy consumption relative to randomly moving GO is reduced by 28% and 12% using the proposed scheme with 3D and 1D movement of GO respectively.

The impact of different number of UAVs in the network is also studied. The energy consumption of the network in case of multiple UAVs is investigated by deploying a different number of UAVs (1, 2 and 3) in the network. The results are plotted in *Figure 4.9*.

A clear observation is that the variations in energy consumption are reduced with an increasing number of UAVs. This strengthens our explanation stated earlier that the possible cause of these variations in the higher variations in fixed and random UAV placement are frequently varying data rates and re-transmissions in the network. With an increasing number of UAVs, the impact of both these parameters is reduced. The analysis of the results obtained shows that by increasing the number of UAVs to 2 and 3, the energy consumption of the network is reduced by 14% and 33% in 3D case, and 10% and 27% in 1D case. Our understanding is that the energy consumption of the network is highly impacted by the distance between the UAV and clients, which reduces more when we placed three (3) UAVs in the network.

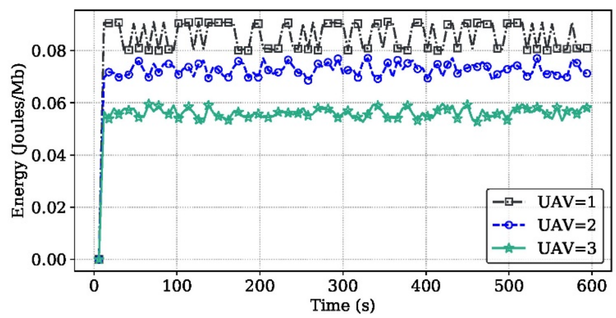


(a)

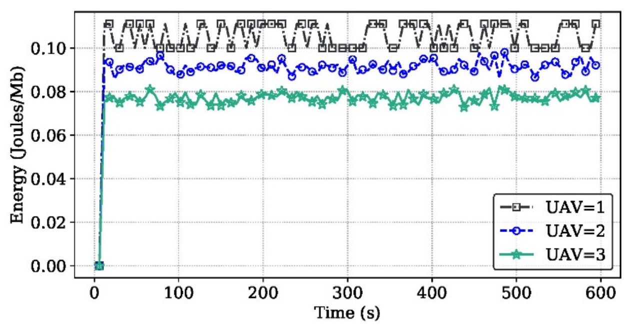


(b)

*Figure 4.9* Energy efficiency versus the number of UAVs. (a) 3D (b) 1D.

### 4.3.4 Comparison with the State-of-the-Art

To further support the benefit of the proposed scheme, we performed a simulation-based comparison of our proposed scheme with two similar solutions proposed in [139] and [63]. In [139], the authors proposed to use a constrained K-means algorithm proposed in [140] for UAV placement and then assign devices to the UAVs. The K-means based algorithm divides the set of network devices into small clusters and optimally place the UAVs at the centres of each cluster. The authors argued that by placing the UAV at the centre of the cluster, the sum of squared distances between

UAVs and its assigned devices is minimized which would reduce the total energy consumption. In [63], the authors proposed a solution to place UAVs such that the total network throughput is maximized. The authors proposed an algorithm that is based on Tabu search to position UAV such that all associated STAs are within the transmission range of the UAV. To ensure that no STA lose the coverage, the UAV is restricted to move only in a fixed circular region called “containing region" of the UAV. The authors further restrict the movement of the UAV to a grid of points inside the containing region called “candidate UAV positions". To search for the optimal UAV position (i.e. grid point) inside the containing region, the authors used a Tabu search method [141]. The algorithm starts with a random initial solution and iteratively improves it by changing its position to a new grid point inside the containing region. A number of positions are evaluated, and the best is chosen to place UAV. To avoid the previously searched non-optimal grid points, the algorithm maintains a list of previously visited positions. We simulated the above two algorithms in ns-3 using the aforementioned system model to compare the performance of our proposed scheme. For a fair comparison, we used the same set of parameters (e.g. number and positions of STAs, mobility model of STAs, transmit power, propagation model, application type, and packet size parameters etc.). *Figure 4.10*, *Figure 4.11* and *Figure 4.12* illustrate the performance comparison of the proposed scheme against the two algorithms. In *Figure 4.10*, the three schemes are evaluated to maintain STAs association.

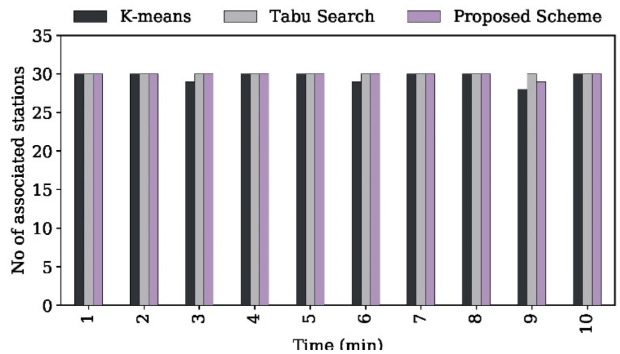


*Figure 4.10* Comparison of STAs association.

It can be observed that all the three schemes maintain connectivity of the STAs throughout the simulation, however, [63] outperform (i.e. maintains 100% connectivity of its associated STAs). It is because the algorithm in [63] is designed to restrict the movement of UAVs to the containing circle so that all the associated STAs remain in the coverage. Furthermore, the proposed scheme outperforms [139] at some instants in the simulation due to the constrained distance used in the algorithm (Eq. 3). In *Figure 4.11*, the three schemes are compared for the throughput gain of the overall network. Both instantaneous (left) and cumulative throughput (right) values are plotted. The figure (left) shows that the proposed scheme outperforms [139] and [63]. One possible reason for this improved performance of the proposed scheme is that it inherently considers the distant STAs in calculating the optimal location of the UAV. This minimize the distance fairly to all STAs, which results in improved quality of all the links. Similar to the proposed scheme. the algorithm in [139] using K-means, also moves the UAV to the centre of the cluster periodically, thus achieves almost equal throughput gain. On the contrary, [63] uses Tabu search to move the UAV in a grid and takes relatively longer time to find the optimal location, which degrades the performance.

Furthermore, as the STAs are constantly moving around, the algorithm [63] rarely achieves optimum performance. The impact of STAs mobility over throughput performance is also highlighted by the authors in [63]. The analysis of the average throughput gain of the three schemes shows that the proposed scheme achieves 5% and 31% more throughput gain as compared to [139] and [63] respectively. A comparison of the energy efficiency of the three scheme is then presented in *Figure 4.12*.

The Tabu search based scheme [63] show poor performance in terms of energy efficiency. It was expected because the UAV in this scheme search all the grid points including several non-optimal grid points before it reaches the optimal location. In such non-optimal locations, the achievable data rate of the UAV is dropped, and the number of retransmissions increases in the network, which consume extra energy to transmit the same data several times. Unlike, the proposed scheme as well as the algorithm in [139] constantly move the UAV only to the optimal location (without searching through the non-optimal space) when the STAs change their positions.

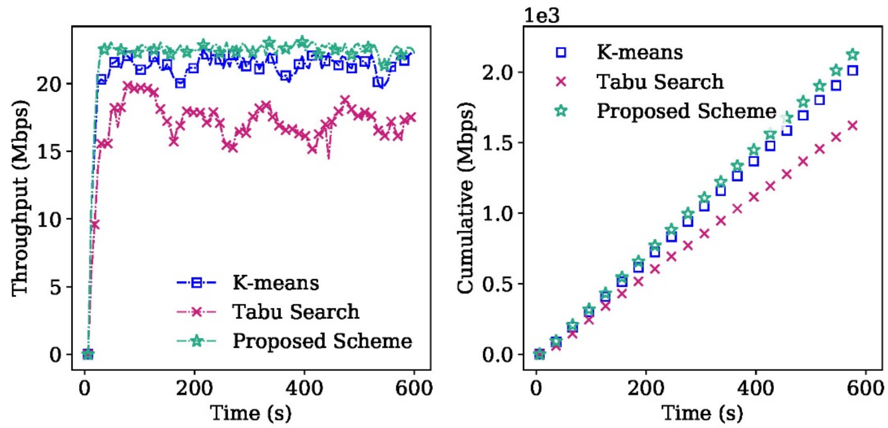


*Figure 4.11* Comparison of network throughput.

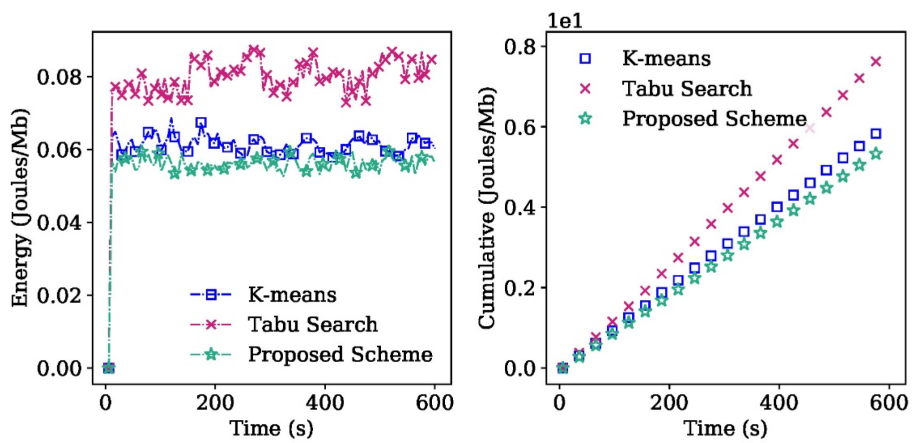


*Figure 4.12* Comparison of energy efficiency.

The analysis of results shows that the proposed scheme achieves the maximum energy efficiency. The average energy consumption of the proposed scheme is 9% less than [139] and 29% less than [63]. Although, the proposed scheme provides a simpler solution to UAV-aided communication in Wi-Fi networks. However, some challenges in terms of practical implementation are worthy to discuss. In order to optimally place

UAV, the UAV requires the current location of devices. The location information i.e. GPS coordinates of the client devices can be acquired at the application layer, which will require user agreement. Alternatively, location estimation algorithms such as RSSI and Angle-of-Arrival (AoA) based location estimation can be applied. Another challenge is the communication between the UAV and the controller. For instance, using only Wi-Fi interfaces, the UAV might leave out of the communication range of the controller. However, this problem can be addressed if the UAV and the controller are equipped with a cellular interface. The dual interfaces can leave a negative impact on the battery life of the UAV. Alternatively, highly directional antennas can be used to enable nearly LOS communication between the UAV and controller at large distances.

# CHAPTER 5 : COGNITIVE WI-FI NETWORKS

In this chapter, we propose data-driven, machine learning based cognitive Wi-Fi networks to dynamically design efficient topologies. In cognitive networks, the network responds to network changes and reconfigure itself to improve the overall performance. Section 5.4.3 proposes a novel handover prediction scheme, which accurately and timely predicts inter-BSS handover using Received Signal Strength (RSS) to avoid unnecessary connection disruption in overlapping regions. In Section 5.4.4, ML-based algorithms are first employed to accurately predict the transmission throughput in Wi-Fi networks. The predicted throughput information is then used to perform intelligent decision making in several network function such as access point selection.

## 5.1 Handover Selection Problem

Handover prediction refers to the problem of anticipating about the connection state of a mobile device associated with an AP. Handover prediction can play a key role in providing seamless connectivity in next-generation networks. It brings several potential benefits; Firstly, the accurate prediction of the handover event allows to timely initiate the transfer of connection to a new AP to reduce handover delay. Secondly, it prevents unnecessary handovers (i.e. Ping-Pongs) to avoid connection disruptions in highly dynamic networks. Handover prediction can be challenging in some cases. *Figure 5.1* illustrates different scenarios of inter-BSS handover in Wi-Fi networks.

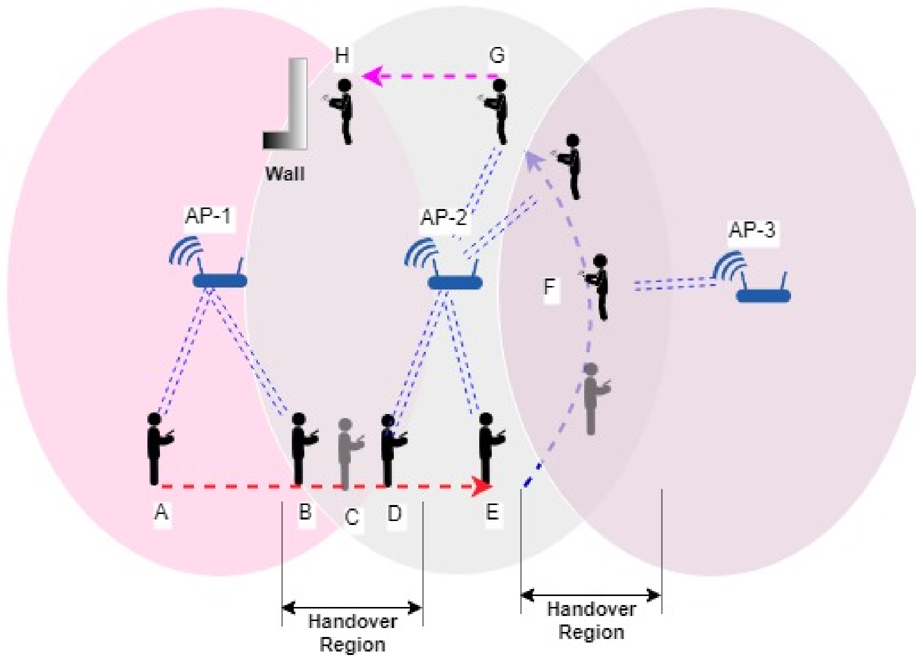


*Figure 5.1* Handover prediction scenarios.

A Wi-Fi user travels from point A to point E (follows the trajectory shown as red, dashed line). When it passes through the region where the radio coverage of AP-1 and AP-2 overlaps, the received signal strength (RSS) drops below the threshold value and it starts scanning for an alternate connection. In the meanwhile, as it moves a bit further to point D, it discovers AP-2 with a stronger signal. It de-associates from AP-1 and associates to AP-2. The user continues to move and follows the trajectory from point E to G (dashed blue line) and thus again passes through an overlapping region of AP-2 and AP-3. At point F, the user changes the association to AP-3 and back to AP-2 when it moves a little further. The user moves ahead and follows the third trajectory from point G to H, and changes the association to AP-1 when it approaches to point H. At Point H, the user cannot move further towards AP-1 due to hindrance and the signal form AP-2 becomes stronger with a slight movement in any direction.

From the above discussion, it becomes obvious that there are some cases where the handover shall not take place despite the signal strength drops slightly below the threshold level to avoid ping-pong effect.

### 5.2 Access Point Selection Problem

When a Wi-Fi device is located in the transmission range of more than one AP, it can associate with either one as shown in *Figure 5.2*. By default, a station associates to the AP from which it first receives a beacon or a probe response frame. However, in practice, such kind of automatic association of stations can cause performance degradation.

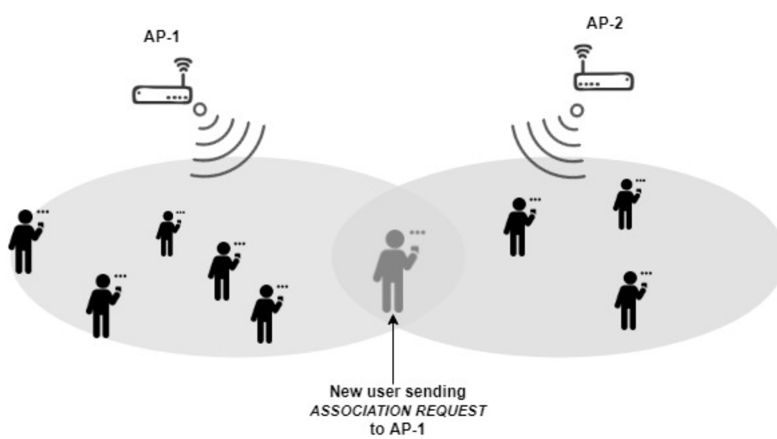


*Figure 5.2* Overlapping BSS.

The optimal selection of an access point in dense WLAN networks is crucial for network performance. The legacy methods for user's association are (i) Strongest

Signal First (SSF) and (ii) Least Loaded First (LLF). Both the SSF and LLF association methods have shortcomings. For instance, In SSF scheme, a station associates to the AP from which it receives a stronger radio signal, however, if the AP is over-utilized, the association of more stations can cause congestion and increase packet loss as well as packet end to end delay [142-144]. On the other hand, in LLF scheme, the selection of the least loaded AP provides APs load balancing, however, it may force a station to associate with a distant AP, and thus the station suffers from poor connection quality. To address these shortcomings of SSF and LLF schemes, the authors in [145] propose a new metric for AP selection named as "potential bandwidth", and is defined as, "the MAC layer bandwidth that an end-host is likely to receive if it were to affiliate with a given access point". The new metric takes into account the signal strength as well as the AP load and additionally the contention on the wireless medium. However, the technique in [145] may not achieve the desired performance if the APs uses different beacons frequencies. It is, therefore, necessary to devise an AP selection strategy that improves the overall network performance while meeting the demand of the new user.

### 5.3 Cognitive Networking

Recently, new architectures are being proposed in the literature [67-69] based on Software Defined Network (SDN) and Cognitive Networking (CN) paradigms. SDN [146, 147] refers to the type of networks in which the control and data forwarding functions are separated. In these architectures, the network devices such as switches, routers and access points act as non-intelligent data forwarding devices while the intelligent functions such as data routing are implemented in a central controller also called as the SDN Controller. On the other hand, cognitive networking [69] refers to the network paradigm in which the networks automatically learn and respond to network changes by actively taking decisions and planning network resources to achieve an end to end performance. Cognitive networks can be realized using both distributed and centralized architectures. A novel approach to realize cognitive networks is to adapt data-driven machine learning (ML) algorithms to address challenges in future ultra-dense and dynamic networks [72-74]. ML algorithms can be used for both network design [75-77] and network performance evaluation [78-81].

This chapter proposes a centralized network architecture using an SDN controller that uses machine-learning algorithms to solve the two aforementioned network problems. Firstly, it anticipates the handover event that is likely to occur and to decide whether the handover is actually required. The proposed scheme reduces the likelihood of unnecessary handover decisions in Overlapping BSS (OBSS) in ultra-dense deployment. Secondly, it solves the AP selection problem by predicting the post-selection network throughput to choose the best AP. Throughput is a significant metric to measure user experience. The prior knowledge of future throughput can help the network to avoid network congestion and thus plays a vital role in AP selection. The proposed scheme can be used to develop large frameworks and testbeds for real-time monitoring and network diagnostic to boost the QoS in Wi-Fi networks.

## 5.4 Proposed Scheme

### 5.4.1 Architecture

The proposed scheme consists of four components: SDN controller, feature extraction module, datasets, and machine learning module. *Figure 5.3* illustrates the functional architecture of the proposed scheme.

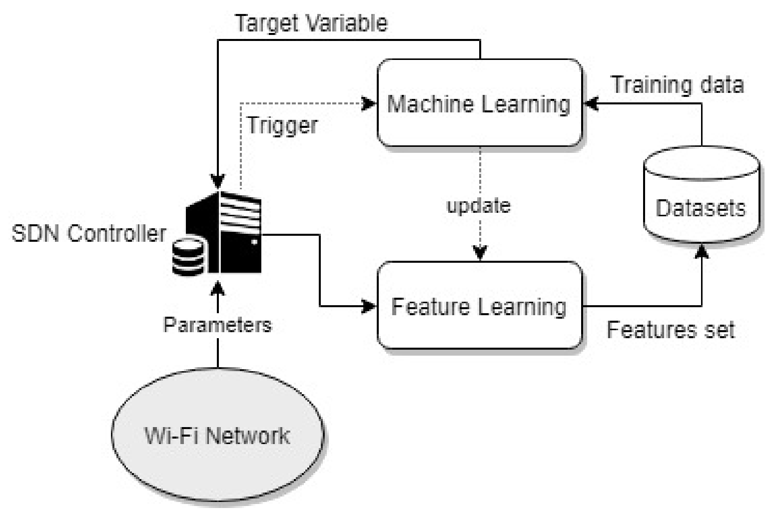


*Figure 5.3* Proposed scheme.

The SDN controller constantly collects network data consisting of several parameters of interest such as device's capability, supporting rates, battery status, position and speed information, Wi-Fi channel being used, packet arrival rates, average throughput and frames retransmission ratios. The network attributes constitute raw data that is then processed to extract useful features. In the feature extraction module, some attributes are directly used as features, whereas some new features are also created from the raw data. For instance, the number of associated clients to an AP is directly used as a feature, whereas the inter-arrival time of the packets is a feature that is computed from the packet-arrival times of two consecutive packets. The features are then combined to form ML-ready datasets that are used by ML algorithms to implement end-to-end learning. Two types of datasets are created namely design datasets and evaluation datasets. The design datasets are used to predict a design parameter e.g. the AP for the association. Other examples include the maximum number of nodes served by AP, transmit power of access points and the optimum channel to be used etc. The evaluation datasets are used for evaluating the network performance in the current conditions e.g. transmission throughput. Other examples include average packet end-to-end delay, packet inter-arrival rates, network congestion and channel access delay.

### 5.4.2 Functional Overview

The SDN controller continuously monitors the network triggers. Three types of triggers are used by the controller i.e. (i) topology change, (ii) performance degradation and (iii) periodic triggers. A new user sending association request to an AP corresponds to the first type of trigger. The lower network throughput or increase in the packet end-to-end delay than a pre-defined threshold level corresponding to the second type of trigger. Periodic triggers are activated at regular intervals regardless of any change in the network state. The activation of any of these triggers automatically run the appropriate ML model. The ML model at fixed intervals imports the required ML ready dataset from the stored datasets to update itself. When triggered, the ML model can thus generate an accurate output. The output of the ML model is used by the SDN controller to implement a control action. The operation of the proposed scheme to predict handover and AP select the best AP is explained as follow:

### 5.4.3 Handover Prediction Scheme

Handover prediction is solved as a binary classification problem using supervised learning techniques. The raw data for handover prediction consists of time series of RSS values of beacon frames received from APs. To be used in supervised learning, the time series are transformed into a dataset that can be readily used in supervised learning. *Figure 5.4* illustrates the proposed handover prediction scheme.

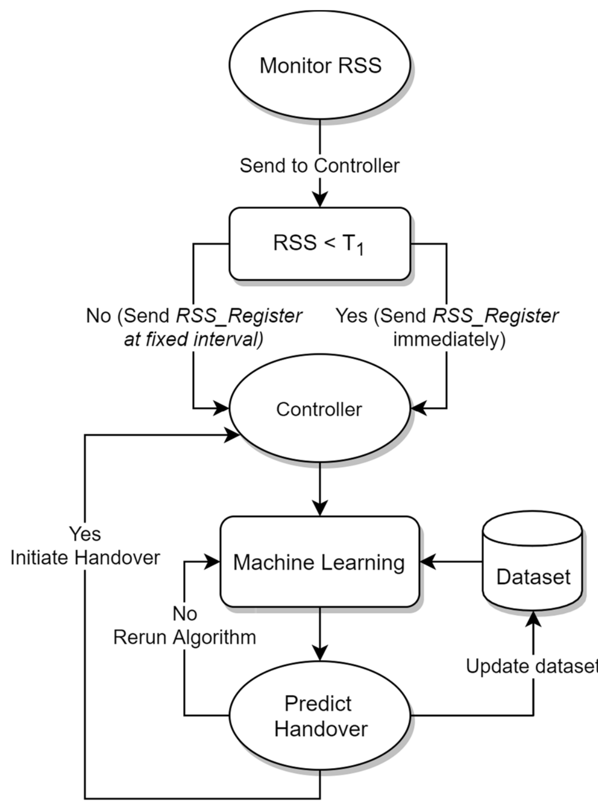


*Figure 5.4* Handover prediction scheme

Each device constantly monitors received signal strengths and records the RSS values in beacon frames in an RSS REGISTER. The RSS REGISTER is then shared with the controller every second. The controller copies the values from the RSS REGISTER into a database of raw data. Each time an RSS REGISTER is received, it is appended to the previous data. The raw data is then accessed by the feature extraction module, which transforms the raw data into ML-ready dataset.

The ML-ready dataset consists of several features as depicted in Table 5.1. Each row in the dataset consists of 13 columns. Columns 1 to 10 contains per-second average RSS values for 10 seconds. Column 11-13 contain the statistics calculated based on the first 10 columns i.e. mean, minimum and maximum. Each row in the dataset is calculated by applying a unit (1 second) shift to the previous column. The controller constantly monitors the current association of the device.

Table 5.1 *Dataset for handover prediction.*

| **Features** | | | | **Class** |
|---|---|---|---|---|
| Columns 1-10 | 11 | 12 | 13 | 1 |
| RSS0, RSS1, … RSS9 | Min RSS | Max RSS | Mean RSS | 1 = Handover<br>0 = No Handover |

The method defines two RSS thresholds denoted as $T_1$ and $T^2$. $T_1$ refers to the RSS level that is significantly low but still supports an ongoing connection despite if RSS drops below it. Whereas, $T_2$ refers to the RSS level which is the minimum level to support a connection. If RSS drops slightly below the threshold, the connection will be terminated. The controller sends the first trigger when the received signal strength of the device drops below the threshold $T_1$. The first trigger indicates the possibility of a handover in the next couple of seconds and hence a proactive measure is necessary. The trigger activates the machine-learning module to run the algorithm at each time step to predict the probability of handover in the next time step. It is worth noticing that the first trigger is significant to reduce unnecessary processing by continuously running the ML algorithms when the device lies in good coverage. Once the trigger is generated, the ML module runs the trained model to predict whether handover should take place or not? The ML module periodically imports the most recent feature vector from the dataset, run the model and predict the handover. The dataset is updated by appending the prediction decision for the given feature vector to improve the future learning process and prediction accuracy. When the handover is detected for a given feature vector, the handover process is initiated. After completing the handover, when the RSS from the new AP is increased and becomes higher than $T_1$, the controller sends another trigger to the machine-learning module to stop running the prediction process. If at any time, the RSS drops below the second threshold $T_2$, a handover is initiated without running the ML model, and the dataset is updated by appending the handover decision to the given feature vector.

### 5.4.4 Access Point Selection Scheme

The AP selection problem is addressed by the proposed scheme using a multi-criteria online learning technique as illustrated in *Figure 5.5*.

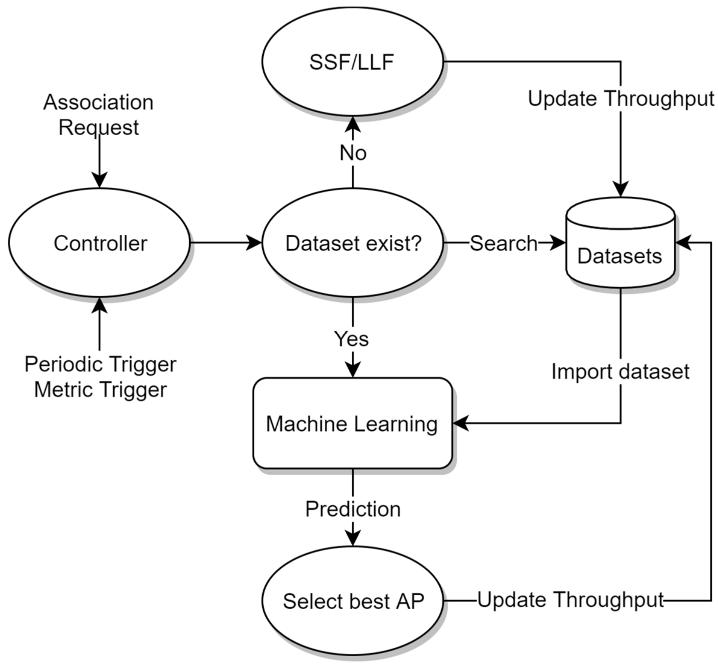


*Figure 5.5* AP selection scheme.

When an AP receives an association request from a Wi-Fi station (STA), it forwards this request to the SDN controller. The SDN controller checks if the dataset is available to use a machine-learning algorithm to choose the best AP to offer connection to the new user. Initially, when the network is first deployed, the dataset is not available. Hence, the controller uses the default algorithm (i.e. SSF or LLF) to select the AP. The controller computes the per BSS throughput for the given network parameters. Once, the dataset is populated with sufficient data points, any new association request is handled by the machine-learning model. The proposed scheme predicts the throughput for each AP in the overlapping BSS and returns the estimated throughput for each AP (if the new STA would be associated with this AP) to the controller. The controller then selects the AP that provides higher estimated throughput, for connecting the requesting client. To create the dataset for throughput estimation, the controller constantly records the information such as the number of associated clients and packet information (e.g. timestamps, arrival time, packet size and signal to noise ratio etc.). A new feature, Inter-Arrival Time (IAT) is calculated from the timestamp and arrival time of each packet. The two features, Inter-arrival time and the number of clients connected to the access point are primarily selected to use in throughput estimation. Furthermore, new features are derived from the IAT values, using the statistics such as Minimum, Maximum, Mean, Variance, Skew and Kurtosis. The features are collected over a time window of fixed duration for the whole network. The structure of ML-ready dataset for throughput estimation is given in Table 5.2.

Table 5.2 *Dataset for throughput prediction.*

| **Parameters** | **Features/Target Variable** | **Derived Features** | **Data-Type** |
|---|---|---|---|
| Associated STAs | n_clients | - | Integer |
| Timestamp<br>Arrival Time | IAT | Mean, min, max,<br>skew, kurtosis | Float |
| Arrival time<br>Packet Size | Throughput | - | Float |

For AP selection, the controller simultaneously collects other parameters to compute features to create a dataset. The structure of dataset used for AP selection is listed in Table 5.3.

Table 5.3 *Dataset for AP selection.*

| Parameters | Features/Target Variable | Derived Features | Data-Type |
|---|---|---|---|
| Associated STAs | n_clients | - | Integer |
| RSSI<br>Noise Level | SNR | Mean, min, max, skew, kurtosis | Float |
| Queue Length<br>Timestamp | Contention delay | Mean, min, max, skew, kurtosis | Float |
| Packet Arrival time<br>Packet Size | Throughput | - | Float |

### 5.5 Evaluation

The proposed scheme is implemented using ns-3 simulator [135] and Linux-based Mininet network emulator [148]. Mininet provides a sufficient level of flexibility and control over the network to dynamically implement new configurations. Additionally, it allows interactive simulation and user can add traffic and applications on devices as well as apply some topological changes during the simulation runtime, thus enabling users to create more dynamic scenarios. On the other hand, ns-3 is a de-facto standard for simulating wireless networks. It provides accurate models of the wireless channel. The recent version of ns-3 also supports indoor models where users can model buildings, floors, rooms and other parameters of the real world. To implement the proposed scheme for handover prediction, we performed extensive simulations in ns-3 to acquire raw network data. Both indoors and outdoors, devices are deployed in the simulation. The raw data acquired is transformed into the dataset as given in Table

5.1. The datasets are then used in Mininet-based simulation to predict handovers using Random Forest (RF) algorithm. Random Forest (RF) [149] is a supervised learning algorithm employed in classification problems. It randomly selects features to build several decision trees and then averages the results. It is a relatively simpler algorithm and requires less time to build models.

To implement the proposed scheme for AP selection, the controller is configured to simulate the two user association algorithms i.e. SSF and LLF in Mininet. The simulations include 3 APs and 50 STAs, randomly moving in the network and changing association controlled by these algorithms. The network traces are collected, and the dataset is created according to Table 5.3. The previously collected datasets are used to train the ML model to estimate network throughput. The STA-AP association with higher estimated aggregate throughput is then selected.

The AP selection dataset involves the use of estimated throughput and hence it is necessary to evaluate the accuracy of the algorithms that estimate the throughput. To evaluate the accuracy of estimated throughput, we used two algorithms i.e. MLP and SVR due to their capability to better predict such metrics [83]. The raw traces, form the simulated network, are collected and transformed into useful features as listed in Table III to create the ML-ready dataset. The dataset is divided into training-validation (70-30 %) splits. The two algorithms are trained with the training data and are then tested by applying to the unseen validation data. To further validate the statistical significance of the model, 10-fold cross-validation is used to avoid over-fitting.

## 5.6 Results and Discussion

The performance of the proposed handover prediction scheme primarily depends on the accuracy of the machine-learning model. Firstly, the prediction accuracy of the RF algorithm used for handover prediction is evaluated using the confusion matrix. A confusion matrix shows the percentage of correct and wrong predictions on data points of both classes in the dataset. The confusion matrix shown in Table 5.4 shows the accuracy of the RF algorithm.

Table 5.4 *Confusion matrix.*

| | Predicted Handover | Predicted No Handover |
|---|---|---|
| Actual Handover | 92% | 8% |
| Actual No Handover | 11% | 89% |

It can be seen that the RF algorithm provides high accuracy to correctly predict the handover events. In the next step, the performance of the proposed handover prediction scheme is compared to other methods stated earlier to assess the overall performance. *Figure 5.6* shows the performance of the proposed scheme versus two other handover prediction methods based on RSS forecasting method and travelling distance method [150].

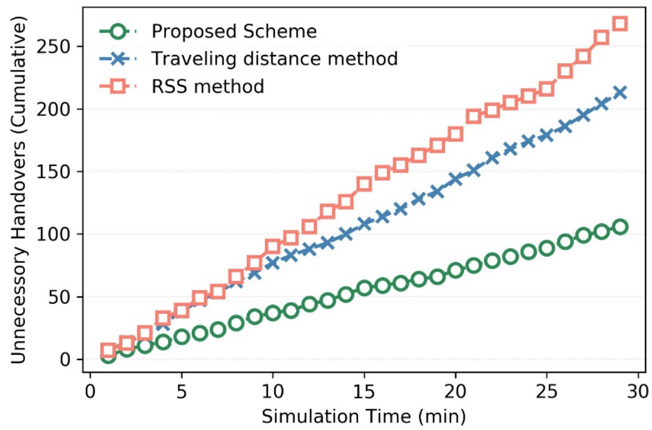


*Figure 5.6* Unnecessary handovers using the proposed scheme.

The figure shows the number of unnecessary handovers (cumulative) overtime computed for the three methods. It can be seen that the proposed scheme outperforms the two methods by reducing the overall numbers of unnecessary handover. The analysis of results shows that the proposed scheme reduces the number of unnecessary handovers by approximately 60% and 50% as compared to the RSS method and travelling distance method respectively.

The proposed scheme for AP selection problem is then evaluated which is based on the accuracy of throughput estimation. Hence, the accuracy of the machine learning algorithms i.e. MLP and SVR for throughput estimation are first evaluated. The predicted throughput versus actual throughput is plotted for both algorithms as given in Fig. V and V. It can be observed that the MLP model provides better accuracy (i.e. predicted values are much closer to the actual values) as compared to the SVR model.

To further quantify the performance of both models, three performance metrics i.e. training time, Mean Squared Error (MSE) and R-squared are computed and the results are listed in Table VII. The MLP based model requires long training time (1.59 second) than the SVR model (0.211 seconds), however it provides better accuracy (i.e. less MSE for MLP = 0.067 as compared to SVR = 0.211) and better generalization to future predictions (i.e. higher R-squared for MLP = 0.974 as compared to SVR = 0.916). The better learning capabilities of MLP costs longer training time due to its complex design (hundreds of neurons arranged in several layers).

Table 5.5 *Complexity analysis.*

| **Parameter** | **MLP** | **SVR** |
|---|---|---|
| Training Time | 1.59 | 0.211 |
| R-Squared | 0.974 | 0.916 |
| MSE | 0.067 | 0.156 |

The MLP-based throughput estimation is then used in the AP selection problem. In AP selection, two performance metrics i.e. average BSS throughput and per-STA throughput are used to compare the throughput gain of the proposed scheme versus conventional AP selection schemes (i.e. SSF and LLF). The results are shown in *Figure 5.7* (average BSS throughput) and

*Figure 5.8* (per-STA throughput).

It can be observed that the proposed scheme improves the average BSS throughput as well as per-STA throughput. The analysis of throughput gains reports an average improvement of 9.2% and 8% as compared to the SSF and LLF schemes respectively.

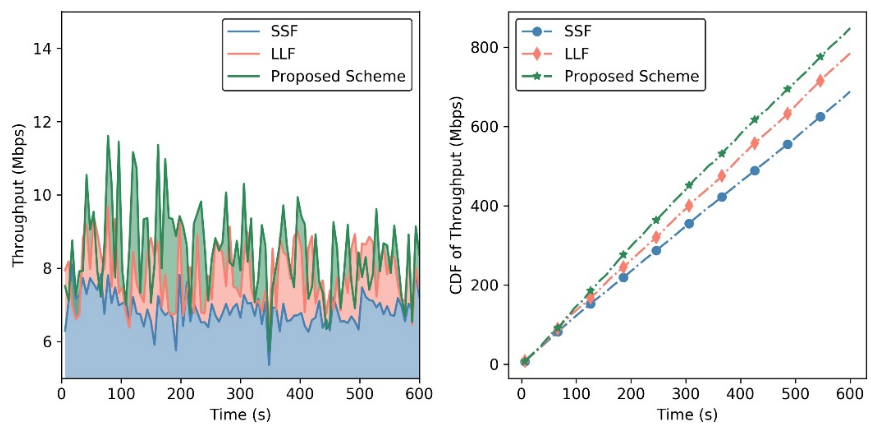


*Figure 5.7* Performance improvement using the proposed scheme

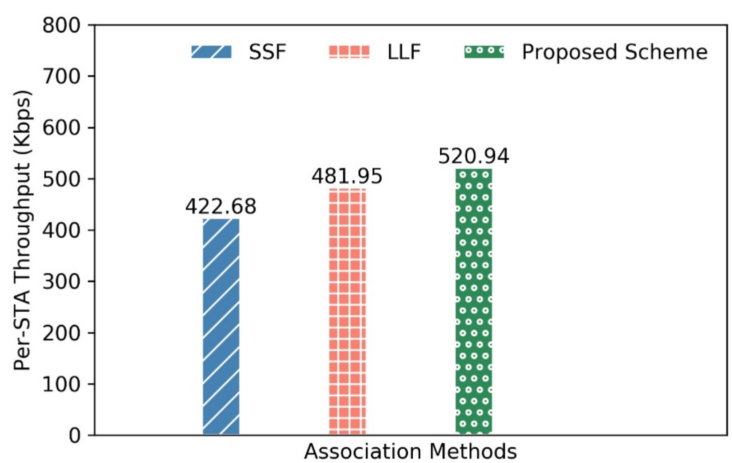


*Figure 5.8* Per STA throughput improvement.

# CHAPTER 6 : CONCLUSIONS AND FUTURE WORKS

In this dissertation, we investigated the current state of the Wi-Fi networks including the Wi-Fi Direct technology. The literature review in CHAPTER 2 reveals several areas of research to improve the performance of Wi-Fi networks in future communication scenarios. The Wi-Fi Direct technology has been recognized as a candidate technology to deploy in dense D2D communication networks. However, the study of Wi-Fi Direct specifications and the state-of-the-art has found several shortcomings in the standard specifications. The inherent limitations of Wi-Fi Direct technology have been discussed in Section 2.4. The first limitation of Wi-Fi Direct is the group formation schemes that do not allow more than two devices to simultaneously participate in the group formation procedure. We proposed a modified group formation scheme in Section 3.2 that is backwards compatible with the standard group formation scheme. The modified group formation scheme ensures that every P2P device in the network participates in the group formation. The benefit of this scheme is to provide equal chances to all devices to become the Group Owner (GO). To further ensure, that only the most capable devices are selected as GO, a device's capability-based GO selection scheme is proposed in Section 3.1. In case of non-availability of the GO device, a back-up GO (BGO) is also preselected in the enhanced group formation.

The proposed group formation scheme in Section 3.2 is defined to create a single P2P group. In large networks, a single GO cannot serve all the devices. Hence, multiple P2P groups are to be created. To create multiple P2P groups in large networks, the problem becomes two-fold: firstly, the clustering of devices into multiple P2P groups, and secondly the selection of GO for each cluster. The problem is solved using Mixed Integer Programming (MIP) in Section 3.3.

The problems mentioned earlier in this section are related to fixed networks with limited or no device mobility. In dynamic networks, where the devices including the selected GOs might move away from the network frequently, the group formation procedure shall be reinstated so frequently. This leads to severe connection disruptions and longer delays that usually cannot be afforded in several applications. To cope with user mobility, a novel UAV-aided network architecture is proposed in Section 4.1. In the proposed network architecture, the GO device is deployed over a UAV while the mobility of the UAV is controlled. A modified Weiszfeld algorithm is used for controlling the mobility of single UAV whereas modified K-median algorithm is employed for multiple UAVs. It was shown that by minimizing the distance between the network device and the UAV, higher network throughput gains, higher number of device's association and energy efficiency is achieved.

Nevertheless, the aforementioned schemes in Section 3.3 and 4.1 offer a significant improvement in network performance, there are other challenges related to future Wi-Fi networks. For instance, dynamic nature of the wireless channel, users running different applications, switching frequently between different services, frequent movement of users in overlapping coverage regions, interference between Wi-Fi users, and many other issues that exist are major challenges for network owners. The existing solutions for network management and optimizations do not guarantee the QoS delivered to the end-users. To cope with challenges, cognitive Wi-Fi network design is proposed in Section 5.4. The proposed scheme uses data-driven, machine-learning algorithms to implement network monitoring and control functions. The proposed scheme has been implemented to solve two known problems in dense networks i.e. handover prediction and access point selection. The algorithm not only looks at the current network stats but also learns from the past data to accurately decide precise action, thus enabling self-organizing networks.

The findings of this study make significant contributions to current knowledge. However, further research work is needed for further investigation. Some possible extensions of the presented works are listed:

- The selection of device parameters and the associated weights for the selection of GO need further investigation for different applications.
- The proposed UAV-aided architecture is evaluated in ns-3. A further study to investigate the proposed architecture in real testbed would be an interesting contribution.
- The cognitive network implemented and evaluated in this study uses small datasets created using network simulations. An excellent contribution will be the deployment of this and other similar schemes in real dense networks to acquire large datasets.

REFERENCES

[1] *IEEE Standard for Wireless LAN Medium Access Control (MAC) and Physical Layer (PHY) specifications*, 1997.

[2] *IEEE Standard for Telecommunications and Information Exchange Between Systems - LAN/MAN Specific Requirements - Part 11: Wireless Medium Access Control (MAC) and physical layer (PHY) specifications: High Speed Physical Layer in the 5 GHz band*, 1999.

[3] *IEEE Standard for Information technology-- Local and metropolitan area networks-- Specific requirements-- Part 11: Wireless LAN Medium Access Control (MAC) and Physical Layer (PHY) Specifications: Further Higher Data Rate Extension in the 2.4 GHz Band*, 2003.

[4] *IEEE Standard for Information technology--Local and metropolitan area networks--Specific requirements--Part 11: Wireless LAN Medium Access Control (MAC) and Physical Layer (PHY) Specifications - Amendment 8: Medium Access Control (MAC) Quality of Service Enhancements*, 2005.

[5] *IEEE Standard for Information Technology - Telecommunications and Information Exchange Between Systems - Local and Metropolitan Area Networks - Specific Requirements - Part 11: Wireless LAN Medium Access Control (MAC) and Physical Layer (PHY) Specifications*, 2007.

[6] *IEEE Standard for Information technology-- Local and metropolitan area networks-- Specific requirements-- Part 11: Wireless LAN Medium Access Control (MAC)and Physical Layer (PHY) Specifications Amendment 5: Enhancements for Higher Throughput*, 2009.

[7] *IEEE Standard for Information technology--Telecommunications and information exchange between systems Local and metropolitan area networks--Specific requirements Part 11: Wireless LAN Medium Access Control (MAC) and Physical Layer (PHY) Specifications*, 2012.

[8] *IEEE Standard for Information technology--Telecommunications and information exchange between systems Local and metropolitan area networks--Specific requirements Part 11: Wireless LAN Medium Access Control (MAC) and Physical Layer (PHY) Specifications Amendment 2: MAC Enhancements for Robust Audio Video Streaming*, 2012.

[9] *IEEE Standard for Information technology-- Telecommunications and information exchange between systemsLocal and metropolitan area networks-- Specific requirements--Part 11: Wireless LAN Medium Access Control (MAC) and Physical Layer (PHY) Specifications--Amendment 4: Enhancements for Very High Throughput for Operation in Bands below 6 GHz*, 2013.

[10] *IEEE Standard for Information technology—Telecommunications and information exchange between systems Local and metropolitan area networks—Specific requirements - Part 11: Wireless LAN Medium Access Control (MAC) and Physical Layer (PHY) Specifications*, 2016.

[11] *IEEE Standard for Information technology-- Local and metropolitan area networks-- Specific requirements-- Part 11: wireless LAN medium access control (MAC) and physical layer (PHY) specifications: higher-speed physical layer extension in the 2.4 GHz band*, 1999.

[12] Cisco, "Cisco Visual Networking Index: Global Mobile Data Traffic Forecast Update, 2017–2022," US., Whitepaper February, 2019 2019, Available: https://www.cisco.com/c/m/en_us/solutions/service-provider/visual-networking-index.html, Accessed on: 22 August 2019.

[13] *Wi-Fi peer-to-peer (p2p) technical specification, version 1.7*, 2016.

[14] S. C. Perez, H. A. Facchini, L. A. Bisaro, and J. Campos, "Tuning Mechanism For IEEE 802.11e EDCA Optimization," *IEEE Latin America Transactions,* vol. 11, no. 4, pp. 1134-1142, 2013.

[15] I. A. T. Group, "IEEE 802.1 Audio/Video Bridging (AVB)," ed.

[16] I. W. Group, "Part 11: wireless LAN medium access control (MAC) and physical layer (PHY) specifications: higher-speed physical layer extension in the 2.4 GHz band," *ANSI/IEEE Std 802.11,* 1999.

[17] *P802.11ax - IEEE Draft Standard for Information Technology -- Telecommunications and Information Exchange Between Systems Local and Metropolitan Area Networks -- Specific Requirements Part 11: Wireless LAN Medium Access Control (MAC) and Physical Layer (PHY) Specifications Amendment Enhancements for High Efficiency WLAN*, 2017.

[18] K. J. Yoon and Y. Y. Kim, "Relayed Multicast Scheme in IEEE 802.11 Wireless LAN Systems," in *Proceedings IEEE INFOCOM 2006. 25TH IEEE International Conference on Computer Communications*, Barcelona, 2006, pp. 1-2.

[19] O. Alay, T. Korakis, Y. Wang, and S. Panwar, "Layered wireless video multicast using directional relays," in *15th IEEE International Conference on Image Processing*, San Diego, CA, pp. 2020-2023: IEEE.

[20] E. E. O . Alay, T. Korakis, S. Panwar, and Y. Wang, "Video multicast, such as layered video multicast for example, using relay devices defined by a channel quality parameter hierarchy," US, Jun. 11, 2009.

[21] K. J. Yoon and Y. Y. Kim, "Relayed multicast scheme in IEEE 802.11 wireless LAN systems," in *Proceedings IEEE INFOCOM 2006. 25TH IEEE International Conference on Computer Communications*, Barcelona, pp. 1-2: IEEE.

[22] B. Rong and A. Hafid, "Cooperative multicast for mobile IPTV over wireless mesh networks: the relay-selection study," *IEEE transactions on Vehicular Technology,* vol. 59, no. 5, pp. 2207-2218, 2010.

[23] O. Alay, T. Korakis, Y. Wang, E. Erkip, and S. Panwar, "Layered wireless video multicast using omni-directional relays," in *2008 IEEE International Conference on Acoustics, Speech and Signal Processing*, Las Vegas, NV, 2008, pp. 2149-2152: IEEE.

[24] O. Alay, K. Guan, Y. Wang, E. Erkip, S. Panwar, and R. Ghanadan, "Wireless video multicast in tactical environments," in *MILCOM 2008 - 2008 IEEE Military Communications Conference*, San Diego, CA, 2008, pp. 1-7: IEEE.

[25] Ö. Alay, P. Liu, Y. Wang, E. Erkip, and S. S. Panwar, "Cooperative layered video multicast using randomized distributed space time codes," *IEEE Transactions on Multimedia,* vol. 13, no. 5, pp. 1127-1140, 2011.

[26] O. Alay, R. Ding, E. Erkip, Y. Wang, and A. Scaglione, "Layered randomized cooperation for multicast," in *2008 42nd Asilomar Conference on Signals, Systems and Computers*, Pacific Grove, CA, 2008, pp. 1484-1488: IEEE.

[27] O. Alay, X. Pan, E. Erkip, and Y. Wang, "Layered randomized cooperative multicast for lossy data: a superposition approach," in *2009 43rd Annual Conference on Information Sciences and Systems*, Baltimore, MD, 2009, pp. 330-335: IEEE.

[28] Ö. Alay, Z. Guo, Y. Wang, E. Erkip, and S. Panwar, "Enhanced parity packet transmission for video multicast using R-DSTC," in *21st Annual IEEE International Symposium on Personal, Indoor and Mobile Radio Communications*, Instanbul, 2010, pp. 2210-2215: IEEE.

[29] M. O. Hasna and M. S. Alouini, "A performance study of dual-hop transmissions with fixed gain relays," *IEEE transactions on wireless communications,* vol. 3, no. 6, pp. 1963-1968, 2004.

[30] L. Yang, M. O. Hasna, and M. S. Alouini, "Average outage duration of multihop communication systems with regenerative relays," *IEEE Transactions on Wireless Communications,* vol. 4, no. 4, pp. 1366-1371, 2005.

[31] K. K. Gurrala and S. Das, "Impact of relay location on the performance of multi-relay cooperative communication," *International Journal of Computer Networks and Wireless Communications,* vol. 2, no. 2, pp. 226-231, 2012.

[32] D. Gesbert and M. Alouini, "Selective multi-user diversity," in *Proceedings of the 3rd IEEE International Symposium on Signal Processing and Information Technology (IEEE Cat. No.03EX795)*, 2003, pp. 162-165.

[33] M. O. Hasna and M. S. Alouini, "Optimal power allocation for relayed transmissions over Rayleigh fading channels," *IEEE Transactions on Wireless Communications,* vol. 3, no. 6, pp. 2461-2465, Nov. 2004 2004.

[34] F. Benkhelifa, A. Tall, Z. Rezki, and M. Alouini, "On the Low SNR Capacity of MIMO Fading Channels With Imperfect Channel State Information," *IEEE Transactions on Communications,* vol. 62, no. 6, pp. 1921-1930, 2014.

[35] M. Abouelseoud and A. Nosratinia, "Heterogeneous relay selection," *IEEE Transactions on Wireless Communications,* vol. 12, no. 4, pp. 1735-1743, 2013.

[36] V. N. Q. Bao, N. Linh-Trung, and M. Debbah, "Relay selection schemes for dual-hop networks under security constraints with multiple eavesdroppers," *IEEE transactions on wireless communications,* vol. 12, no. 12, pp. 6076-6085, 2013.

[37] N. Yang, M. Elkashlan, and J. Yuan, "Outage probability of multiuser relay networks in Nakagami-$ m $ fading channels," *IEEE Transactions on Vehicular Technology,* vol. 59, no. 5, pp. 2120-2132, 2010.

[38] M. Khafagy, A. Ismail, M.-S. Alouini, and S. Aissa, "On the outage performance of full-duplex selective decode-and-forward relaying," *IEEE Communications Letters,* vol. 17, no. 6, pp. 1180-1183, 2013.

[39] E. Bjornson, M. Matthaiou, and M. Debbah, "A new look at dual-hop relaying: Performance limits with hardware impairments," *IEEE Transactions on Communications,* vol. 61, no. 11, pp. 4512-4525, 2013.

[40] G. Chen, Z. Tian, Y. Gong, and J. Chambers, "Decode-and-forward buffer-aided relay selection in cognitive relay networks," *IEEE transactions on vehicular technology,* vol. 63, no. 9, pp. 4723-4728, 2014.

[41] W.-F. Alliance, "Wi-Fi Protected Access: Strong, standards-based, interoperable security for today's Wi-Fi networks," *White paper, University of Cape Town,* pp. 492-495, 2003.

[42] W.-F. Alliance, "Wi-fi protected setup specification," *WiFi Alliance Document,* vol. 23, 2007.

[43] I. Jabri, N. Krommenacker, T. Divoux, and A. Soudani, "IEEE 802.11 Load balancing: an approach for QoS Enhancement," *International Journal of Wireless Information Networks,* vol. 15, no. 1, pp. 16-30, 2008.

[44] L.-H. Yen, T.-T. Yeh, and K.-H. Chi, "Load balancing in IEEE 802.11 networks," *IEEE Internet Computing,* vol. 13, no. 1, pp. 56-64, 2009.

[45] H. Velayos, V. Aleo, and G. Karlsson, "Load balancing in overlapping wireless LAN cells," in *2004 IEEE International Conference on Communications*, Paris, France, 2004, vol. 7, pp. 3833-3836: IEEE.

[46] J. Kim and H. Lee, "VADA: Wi-Fi direct based voluntary advertisement dissemination algorithm for social commerce service," in *2015 IEEE 81st Vehicular Technology Conference (VTC Spring)*, Glasgow, 2015, pp. 1-6: IEEE.

[47] A. A. Shahin and M. Younis, "Alert dissemination protocol using service discovery in Wi-Fi direct," in *2015 IEEE International Conference on Communications (ICC)*, London, 2015, pp. 7018-7023: IEEE.

[48] R. Rajadurai, K. S. Gopalan, M. Patil, and S. Chitturi, "Enhanced interworking of LTE and wi-fi direct for public safety," *IEEE Communications Magazine,* vol. 54, no. 4, pp. 40-46, 2016.

[49] M. Mozaffari, W. Saad, M. Bennis, Y. H. Nam, and M. Debbah, "A tutorial on UAVs for wireless networks: Applications, challenges, and open problems. arXiv 2018," *arXiv preprint arXiv:1803.00680*.

[50] M. Mozaffari, W. Saad, M. Bennis, and M. Debbah, "Efficient Deployment of Multiple Unmanned Aerial Vehicles for Optimal Wireless Coverage," *IEEE Communications Letters,* vol. 20, no. 8, pp. 1647-1650, 2016.

[51] R. I. Bor-Yaliniz, A. El-Keyi, and H. Yanikomeroglu, "Efficient 3-D placement of an aerial base station in next generation cellular networks," in *2016 IEEE International Conference on Communications (ICC)*, 2016, pp. 1-5.

[52] P. Series, "Propagation data and prediction methods required for the design of terrestrial broadband radio access systems operating in a frequency range from 3 to 60 GHz," *Recommendation ITU-R,* pp. 1410-1415, 2013.

[53] R. Ghanavi, E. Kalantari, M. Sabbaghian, H. Yanikomeroglu, and A. Yongacoglu, "Efficient 3D aerial base station placement considering users mobility by reinforcement learning," in *2018 IEEE Wireless Communications and Networking Conference (WCNC)*, 2018, pp. 1-6.

[54] Y. Chen, W. Feng, and G. Zheng, "Optimum Placement of UAV as Relays," *IEEE Communications Letters,* vol. 22, no. 2, pp. 248-251, 2018.

[55] Y. Zeng, R. Zhang, and T. J. Lim, "Throughput Maximization for Mobile Relaying Systems," in *2016 IEEE Globecom Workshops (GC Wkshps)*, 2016, pp. 1-6.

[56] D. Ashutosh, G. Mahanth, and C. Romit Roy, "Extending Cell Tower Coverage through Drones," in *Proceedings of the 18th International Workshop on Mobile Computing Systems and Applications*, 2017.

[57] A. Guillen-Perez, R. Sanchez-Iborra, M. Cano, J. C. Sanchez-Aarnoutse, and J. Garcia-Haro, "WiFi networks on drones," in *2016 ITU Kaleidoscope: ICTs for a Sustainable World (ITU WT)*, 2016, pp. 1-8.

[58] A. Al-Fuqaha, M. Guizani, M. Mohammadi, M. Aledhari, and M. Ayyash, "Internet of Things: A Survey on Enabling Technologies, Protocols, and Applications," *IEEE Communications Surveys & Tutorials,* vol. 17, no. 4, pp. 2347-2376, 2015.

[59] G. Ding, Q. Wu, L. Zhang, Y. Lin, T. A. Tsiftsis, and Y. Yao, "An Amateur Drone Surveillance System Based on the Cognitive Internet of Things," *IEEE Communications Magazine,* vol. 56, no. 1, pp. 29-35, 2018.

[60] A. Mahdi, G. Domenico, H. Karin Anna, and H. Simon, "Characterizing 802.11n aerial communication," in *Proceedings of the second ACM MobiHoc workshop on Airborne networks and communications*, 2013.

[61] S. Hayat, E. Yanmaz, and C. Bettstetter, "Experimental analysis of multipoint-to-point UAV communications with IEEE 802.11n and 802.11ac," in *2015 IEEE 26th Annual International Symposium on Personal, Indoor, and Mobile Radio Communications (PIMRC)*, 2015, pp. 1991-1996.

[62] Q. Wu and R. Zhang, "Common Throughput Maximization in UAV-Enabled OFDMA Systems With Delay Consideration," *IEEE Transactions on Communications,* vol. 66, no. 12, pp. 6614-6627, 2018.

[63] S. u. Rahman, G. Kim, Y. Cho, and A. Khan, "Positioning of UAVs for throughput maximization in software-defined disaster area UAV communication networks," *Journal of Communications and Networks,* vol. 20, no. 5, pp. 452-463, 2018.

[64] Z. Dawy, W. Saad, A. Ghosh, J. G. Andrews, and E. Yaacoub, "Toward Massive Machine Type Cellular Communications," *IEEE Wireless Communications,* vol. 24, no. 1, pp. 120-128, 2017.

[65] Y. Zeng, R. Zhang, and T. J. Lim, "Wireless communications with unmanned aerial vehicles: opportunities and challenges," *IEEE Communications Magazine,* vol. 54, no. 5, pp. 36-42, 2016.

[66] M. Mozaffari, W. Saad, M. Bennis, and M. Debbah, "Mobile Unmanned Aerial Vehicles (UAVs) for Energy-Efficient Internet of Things Communications," *IEEE Transactions on Wireless Communications,* vol. 16, no. 11, pp. 7574-7589, 2017.

[67] H. Ali-Ahmad *et al.*, "An SDN-based network architecture for extremely dense wireless networks," in *2013 IEEE SDN for Future Networks and Services (SDN4FNS)*, Trento, 2013, pp. 1-7: IEEE.

[68] M. Danieletto, G. Quer, R. R. Rao, and M. Zorzi, "CARMEN: a cognitive networking testbed on android OS devices," *IEEE Communications Magazine,* vol. 52, no. 9, pp. 98-107, 2014.

[69] M. Slavik, I. Mahgoub, and A. Badi, "Cross-layer design for wireless networks with cognitive controllers," in *2008 Wireless Telecommunications Symposium*, Pomona, CA, 2008, pp. 273-277: IEEE.

[70] D. Kreutz, F. Ramos, P. Verissimo, C. E. Rothenberg, S. Azodolmolky, and S. Uhlig, "Software-defined networking: A comprehensive survey," *arXiv preprint arXiv:1406.0440,* 2014.

[71] R. W. Thomas, D. H. Friend, L. A. DaSilva, and A. B. MacKenzie, "Cognitive networks," in *Cognitive radio, software defined radio, and adaptive wireless systems*: Springer, 2007, pp. 17-41.

[72] C. Jiang, H. Zhang, Y. Ren, Z. Han, K.-C. Chen, and L. Hanzo, "Machine learning paradigms for next-generation wireless networks," *IEEE Wireless Communications,* vol. 24, no. 2, pp. 98-105, 2016.

[73] N. Kato *et al.*, "The deep learning vision for heterogeneous network traffic control: Proposal, challenges, and future perspective," *IEEE wireless communications,* vol. 24, no. 3, pp. 146-153, 2016.

[74] A. Omri, R. Bouallegue, R. Hamila, and M. Hasna, "Channel estimation for LTE uplink system by perceptron neural network," *International Journal of Wireless & Mobile Networks (IJWMN),* vol. 2, no. 3, pp. 155-165, 2010.

[75] F. Cadger, K. Curran, J. Santos, and S. Moffet, "Opportunistic neighbour prediction using an Artificial Neural Network," in *Artificial Intelligence: Concepts, Methodologies, Tools, and Applications*: IGI Global, 2017, pp. 1674-1686.

[76] D. Del Testa, M. Danieletto, G. M. Di Nunzio, and M. Zorzi, "Estimating the number of receiving nodes in 802.11 networks via machine learning techniques," in *2016 IEEE Global Communications Conference (GLOBECOM)*, Washington, DC, 2016, pp. 1-7: IEEE.

[77] S. Kajita *et al.*, "A channel selection strategy for WLAN in urban areas by regression analysis," in *2014 IEEE 10th International Conference on Wireless and Mobile Computing, Networking and Communications (WiMob)*, Larnaca, 2014, pp. 642-647: IEEE.

[78] M. O. Khan and L. Qiu, "Accurate WiFi packet delivery rate estimation and applications," in *IEEE INFOCOM 2016 - The 35th Annual IEEE International Conference on Computer Communications*, San Francisco, CA, 2016, pp. 1-9: IEEE.

[79] L. Kriara, M. K. Marina, and A. Farshad, "Characterization of 802.11 n wireless LAN performance via testbed measurements and statistical analysis," in *2013 IEEE International Conference on Sensing, Communications and Networking (SECON)*, New Orleans, LA, 2013, pp. 158-166: IEEE.

[80] T. Phit and K. Abe, "Packet inter-arrival time estimation using neural network models," Citeseer.

[81] S. Chinchali and S. Tandon, "Deep Learning for Wireless Interference Segmentation and Prediction," ed, 2012.

[82] M. Mirza, J. Sommers, P. Barford, and X. Zhu, "A machine learning approach to TCP throughput prediction," *IEEE/ACM Transactions on Networking,* vol. 18, no. 4, p. 13, 2010 2010.

[83] S. Ayoubi *et al.*, "Machine learning for cognitive network management," *IEEE Communications Magazine,* vol. 56, no. 1, pp. 158-165, 2018.

[84] P. Lin and T. Lin, "Machine-learning-based adaptive approach for frame-size optimization in wireless LAN environments," *IEEE transactions on vehicular technology,* vol. 58, no. 9, pp. 5060-5073, 2009.

[85] N. R. Draper and H. Smith, *Applied regression analysis*. John Wiley & Sons, 1998.

[86] L. E. Peterson, "K-nearest neighbor," *Scholarpedia,* vol. 4, no. 2, p. 1883, 2009.

[87] J. A. K. Suykens and J. Vandewalle, "Least squares support vector machine classifiers," *Neural processing letters,* vol. 9, no. 3, pp. 293-300, 1999.

[88] A. J. Smola and B. Schölkopf, "A tutorial on support vector regression," *Statistics and computing,* vol. 14, no. 3, pp. 199-222, 2004.

[89] V.-s. Feng and S. Y. Chang, "Determination of wireless networks parameters through parallel hierarchical support vector machines," *IEEE Transactions on Parallel and Distributed Systems,* vol. 23, no. 3, pp. 505-512, 2011.

[90] B. K. Donohoo, C. Ohlsen, S. Pasricha, Y. Xiang, and C. Anderson, "Context-aware energy enhancements for smart mobile devices," *IEEE Transactions on Mobile Computing,* vol. 13, no. 8, pp. 1720-1732, 2013.

[91] R. M. Neal, *Bayesian learning for neural networks*. Springer Science & Business Media, 2012.

[92] C.-K. Wen, S. Jin, K.-K. Wong, J.-C. Chen, and P. Ting, "Channel estimation for massive MIMO using Gaussian-mixture Bayesian learning," *IEEE Transactions on Wireless Communications,* vol. 14, no. 3, pp. 1356-1368, 2014.

[93] D. Reynolds, "Gaussian mixture models," *Encyclopedia of biometrics,* pp. 827-832, 2015.

[94] T. K. Moon, "The expectation-maximization algorithm," *IEEE Signal processing magazine,* vol. 13, no. 6, pp. 47-60, 1996.

[95] S. Fine, Y. Singer, and N. Tishby, "The hierarchical hidden Markov model: Analysis and applications," *Machine learning,* vol. 32, no. 1, pp. 41-62, 1998.

[96] A. K. Jain, "Data clustering: 50 years beyond K-means," *Pattern recognition letters,* vol. 31, no. 8, pp. 651-666, 2010.

[97] A. Likas, N. Vlassis, and J. J. Verbeek, "The global k-means clustering algorithm," *Pattern recognition,* vol. 36, no. 2, pp. 451-461, 2003.

[98] M. Xia, Y. Owada, M. Inoue, and H. Harai, "Optical and wireless hybrid access networks: Design and optimization," *Journal of Optical Communications and Networking,* vol. 4, no. 10, pp. 749-759, 2012.

[99] I. Jolliffe, *Principal component analysis*. Springer, 2011.

[100] P. Comon, "Independent component analysis, a new concept?," *Signal processing,* vol. 36, no. 3, pp. 287-314, 1994.

[101] A. Pinkus, "Approximation theory of the MLP model in neural networks," *Acta numerica,* vol. 8, pp. 143-195, 1999.

[102] H. Ramchoun, M. A. J. Idrissi, Y. Ghanou, and M. Ettaouil, "Multilayer Perceptron: Architecture Optimization and Training," *IJIMAI,* vol. 4, no. 1, pp. 26-30, 2016.

[103] M. R. Ackermann, J. Blömer, and C. Sohler, "Clustering for metric and nonmetric distance measures," *ACM Transactions on Algorithms (TALG),* vol. 6, no. 4, p. 59, 2010.

[104] U. Botrel Menegato, L. Souza Cimino, S. E. Delabrida Silva, F. A. Medeiros Silva, J. Castro Lima, and R. A. R. Oliveira, "Dynamic clustering in wifi direct technology," in *Proceedings of the 12th ACM international symposium*

*on Mobility management and wireless access (MobiWac '14 )*, Montreal, QC, Canada, 2014, pp. 25-29: ACM.

[105] S. Har-Peled and S. Mazumdar, "On coresets for k-means and k-median clustering," in *Proceedings of the thirty-sixth annual ACM symposium on Theory of computing (STOC '04)*, Chicago, IL, USA, 2004, pp. 291-300: ACM.

[106] J. Malinen, "mac8011 hwsim," ed, 2008.

[107] (30 August 2019). *Linux Wireless How to P2P*. Available: https://wireless.wiki.kernel.org/en/developers/p2p/howto

[108] M. A. Khan, W. Cherif, and F. Filali, "Group owner election in Wi-Fi direct," in *2016 IEEE 7th Annual Ubiquitous Computing, Electronics & Mobile Communication Conference (UEMCON)*, 2016, pp. 1-9.

[109] M. Conti, F. Delmastro, G. Minutiello, and R. Paris, "Experimenting opportunistic networks with WiFi Direct," in *2013 IFIP Wireless Days (WD)*, Valencia, 2013, pp. 1-6: IEEE.

[110] A. Schrijver, *Theory of linear and integer programming*. John Wiley & Sons, 1998.

[111] D. Smithies and F. Fietkau, "Minstrel rate control algorithm," *Online. Disponıvel em http://linuxwireless. org/en/developers/Documentation/mac80211/RateControl/minstrel. Ultimo acesso em,* vol. 16, no. 11, p. 2009, 2005.

[112] S. H. Y. Wong, H. Yang, S. Lu, and V. Bharghavan, "Robust rate adaptation for 802.11 wireless networks," in *Proceedings of the 12th annual international*

*conference on Mobile computing and networking (MobiCom '06)*, Los Angeles, CA, USA, 2006, pp. 146-157: ACM.

[113] S. Diamond, E. Chu, and S. Boyd, "CVXPY: A Python-embedded modeling language for convex optimization, version 0.2," ed: May, 2014.

[114] S. Diamond and S. Boyd, "CVXPY: A Python-embedded modeling language for convex optimization," *The Journal of Machine Learning Research,* vol. 17, no. 1, pp. 2909-2913, 2016.

[115] M. A. Khan, W. Cherif, F. Filali, and R. Hamila, "Wi-Fi Direct Research - Current Status and Future Perspectives," *Journal of Network and Computer Applications,* vol. 93, pp. 245-258, 2017/09/01/ 2017.

[116] A. A. Shahin and M. Younis, "Efficient multi-group formation and communication protocol for Wi-Fi Direct," in *2015 IEEE 40th Conference on Local Computer Networks (LCN)*, Clearwater Beach, FL, 2015, pp. 233-236: IEEE.

[117] Z. Hongxu, W. Yufeng, and C. T. Chiu, "WD2: an improved wifi-direct group formation protocol," in *Proceedings of the 9th ACM MobiCom workshop on Challenged networks*, 2014.

[118] W. Cherif, M. A. Khan, F. Filali, S. Sharafeddine, and Z. Dawy, "P2P Group Formation Enhancement for Opportunistic Networks with Wi-Fi Direct," in *2017 IEEE Wireless Communications and Networking Conference (WCNC)*, 2017, pp. 1-6.

[119] M. Alzenad, A. El-Keyi, F. Lagum, and H. Yanikomeroglu, "3-D Placement of an Unmanned Aerial Vehicle Base Station (UAV-BS) for Energy-Efficient

Maximal Coverage," *IEEE Wireless Communications Letters,* vol. 6, no. 4, pp. 434-437, 2017.

[120] Y. Zeng and R. Zhang, "Energy-Efficient UAV Communication With Trajectory Optimization," *IEEE Transactions on Wireless Communications,* vol. 16, no. 6, pp. 3747-3760, 2017.

[121] P. Zhan, K. Yu, and A. L. Swindlehurst, "Wireless Relay Communications with Unmanned Aerial Vehicles: Performance and Optimization," *IEEE Transactions on Aerospace and Electronic Systems,* vol. 47, no. 3, pp. 2068-2085, 2011.

[122] Y. Li and L. Cai, "UAV-Assisted Dynamic Coverage in a Heterogeneous Cellular System," *IEEE Network,* vol. 31, no. 4, pp. 56-61, 2017.

[123] J. Brimberg, "The Fermat—Weber location problem revisited," *Mathematical Programming,* vol. 71, no. 1, pp. 71-76, 1995.

[124] L. R. Foulds and H. W. Hamacher, "Optimal bin location and sequencing in printed circuit board assembly," *European Journal of Operational Research,* vol. 66, no. 3, pp. 279-290, 1993.

[125] J. Brimberg and R. F. Love, "Properties of ordinary and weighted sums of order $ p $ used for distance estimation," *RAIRO-Operations Research-Recherche Opérationnelle,* vol. 29, no. 1, pp. 59-72, 1995.

[126] H. Üster and R. F. Love, "Application of a weighted sum of order p to distance estimation," *IIE Transactions,* vol. 33, no. 8, pp. 675-684, 2001.

[127] L. Cánovas, R. Cañavate, and A. Marín, "On the convergence of the Weiszfeld algorithm," *Mathematical programming,* vol. 93, no. 2, pp. 327-330, 2002.

[128] H. W. Kuhn, "A note on Fermat's problem," *Mathematical programming,* vol. 4, no. 1, pp. 98-107, 1973.

[129] Y. Vardi and C.-H. Zhang, "A modified Weiszfeld algorithm for the Fermat-Weber location problem," *Mathematical Programming,* vol. 90, no. 3, pp. 559-566, 2001.

[130] Y. P. Aneja and M. Parlar, "Algorithms for Weber facility location in the presence of forbidden regions and/or barriers to travel," *Transportation Science,* vol. 28, no. 1, pp. 70-76, 1994.

[131] M. Bischoff and K. Klamroth, "An efficient solution method for Weber problems with barriers based on genetic algorithms," *European Journal of Operational Research,* vol. 177, no. 1, pp. 22-41, 2007.

[132] R. Z. Farahani, M. SteadieSeifi, and N. Asgari, "Multiple criteria facility location problems: A survey," *Applied Mathematical Modelling,* vol. 34, no. 7, pp. 1689-1709, 2010.

[133] A. Klose and A. Drexl, "Facility location models for distribution system design," *European Journal of Operational Research,* vol. 162, no. 1, pp. 4-29, 2005/04/01/ 2005.

[134] C. Whelan, G. Harrell, and J. Wang, "Understanding the K-Medians Problem," 2015, p. 219: The Steering Committee of The World Congress in Computer Science, Computer ….

[135] T. R. Henderson, M. Lacage, G. F. Riley, C. Dowell, and J. Kopena, "Network simulations with the ns-3 simulator," *SIGCOMM demonstration,* vol. 14, no. 14, p. 527, 2008.

[136] S. Leffler, "The MadWifi project," ed, 2009.

[137] D. P. Consumption, D. Halperin, B. Greenstein, A. Sheth, and D. Wetherall, "Demystifying 802.11 n Power Consumption."

[138] P. Serrano, A. Garcia-Saavedra, G. Bianchi, A. Banchs, and A. Azcorra, "Per-Frame Energy Consumption in 802.11 Devices and Its Implication on Modeling and Design," *IEEE/ACM Transactions on Networking,* vol. 23, no. 4, pp. 1243-1256, 2015.

[139] M. Mozaffari, W. Saad, M. Bennis, and M. Debbah, "Mobile Internet of Things: Can UAVs Provide an Energy-Efficient Mobile Architecture?," in *2016 IEEE Global Communications Conference (GLOBECOM)*, 2016, pp. 1-6.

[140] F. Höppner and F. Klawonn, "Clustering with size constraints," in *Computational Intelligence Paradigms*: Springer, 2008, pp. 167-180.

[141] F. Glover and M. Laguna, "Tabu search," in *Handbook of combinatorial optimization*: Springer, 1998, pp. 2093-2229.

[142] A. Balachandran, P. Bahl, and G. M. Voelker, "Hot-spot congestion relief and service guarantees in public-area wireless networks," *ACM SIGCOMM Computer Communication Review,* vol. 32, no. 1, pp. 59-59, 2002.

[143] Y. Bejerano, S.-J. Han, and L. E. Li, "Fairness and load balancing in wireless LANs using association control," *IEEE/ACM Transactions on Networking,* vol. 15, no. 3, pp. 315-329, June 2007 2007.

[144] V. Mhatre and K. Papagiannaki, "Using smart triggers for improved user performance in 802.11 wireless networks," in *Proceedings of the 4th international conference on Mobile systems, applications and services (MobiSys '06)*, Uppsala, Sweden, pp. 246-259: ACM.

[145] S. Vasudevan, K. Papagiannaki, C. Diot, J. Kurose, and D. Towsley, "Facilitating access point selection in IEEE 802.11 wireless networks," pp. 26-26: Usenix Association.

[146] H. Kim and N. Feamster, "Improving network management with software defined networking," *IEEE Communications Magazine,* vol. 51, no. 2, pp. 114-119, 2013.

[147] A. Zahmatkesh and T. Kunz, "Software defined multihop wireless networks: Promises and challenges," *Journal of Communications and Networks,* vol. 19, no. 6, pp. 546-554, 2017.

[148] R. L. S. De Oliveira, C. M. Schweitzer, A. A. Shinoda, and L. R. Prete, "Using mininet for emulation and prototyping software-defined networks," pp. 1-6: IEEE.

[149] A. Liaw and M. Wiener, "Classification and regression by randomForest," *R news,* vol. 2, no. 3, pp. 18-22, 2002.

[150] X. Yan, N. Mani, and Y. A. Sekercioglu, "A traveling distance prediction based method to minimize unnecessary handovers from cellular networks to WLANs," *IEEE communications letters,* vol. 12, no. 1, pp. 14-16, 2008.